NASA/CR—1998-207405

A Method for Generating Reduced-Order Linear Models of Multidimensional Supersonic Inlets

Amy Chicatelli and Tom T. Hartley
University of Akron, Akron, Ohio

Prepared under Grant NCC3–508

National Aeronautics and
Space Administration

Lewis Research Center

May 1998

Available from

NASA Center for Aerospace Information
7121 Standard Drive
Hanover, MD 21076
Price Code: A05

National Technical Information Service
5287 Port Royal Road
Springfield, VA 22100
Price Code: A05

Contents

A Method for Generating Reduced Order Linear Models of Multidimensional Supersonic Inlets

Amy Chicatelli
Tom T. Hartley

The Department of Electrical Engineering
University Of Akron
Akron, OH 44325-3904

Summary

Simulation of high speed propulsion systems may be divided into two categories, nonlinear and linear. The nonlinear simulations are usually based on multidimensional computational fluid dynamics (CFD) methodologies and tend to provide high resolution results that show the fine detail of the flow. Consequently, these simulations are large, numerically intensive, and run much slower than real-time. The linear simulations are usually based on large lumping techniques that are linearized about a steady-state operating condition. These simplistic models often run at or near real-time but do not always capture the detailed dynamics of the plant. Under a grant sponsored by the NASA Lewis Research Center, Cleveland, Ohio, a new method has been developed that can be used to generate improved linear models for control design from multidimensional steady-state CFD results. This CFD-based linear modeling technique provides a small perturbation model that can be used for control applications and real-time simulations. It is important to note the utility of the modeling procedure; all that is needed to obtain a linear model of the propulsion system is the geometry and steady-state operating conditions from a multidimensional CFD simulation or experiment. This research represents a beginning step in establishing a bridge between the controls discipline and the CFD discipline so that the control engineer is able to effectively use multidimensional CFD results in control system design and analysis.

1 Introduction

The development of inlet models for high speed propulsion systems is important because of the current interest in high speed air-breathing propulsion systems. Modeling of these systems is difficult, because the complex physical processes are represented by nonlinear partial differential equations (PDE). An accurate plant model is required to develop a control system for the plant; the more accurate the model, the better the control design. Typically these models are either based on traditional propulsion control models or CFD models.

Traditional propulsion control models typically utilize a large lumping technique for the spatial derivatives so that the propulsion system is represented by a set of nonlinear ordinary differential equations (ODE). These equations are often linearized about a steady-state point so that the control model is linear. Methods based on this linear ODE approach have been developed for propulsion systems, some of which are: the Cole-Willoh model [1], the Martin model [2], the Barry models [3], circuit models [4], and the Laplace transform of the Green's function method [5] [6]. Unfortunately these models are often difficult to implement, do not always capture the nonlinear dynamics of the system, and are not typically used for multidimensional flows.

Accurate nonlinear models of complex flows are usually obtained from CFD codes [7] [8]. These models can to some degree predict the behavior of large perturbations in the flow field, including unstart, buzz, turbulence, boundary layer growth, et cetera. Typically these CFD models are based on a large number of nodes which can then be used in a finite difference method to produce a large system of nonlinear equations. However due to their nonlinearity and large size, these models require large amounts of computational time and therefore are not suitable for controls analysis and design.

An effective propulsion system model for control system design must adequately capture the dynamics of the system but also be of small order. CFD models fulfill the first requirement, and traditional controls models fulfill the second requirement. Therefore, a method that is based on both ideas might provide a reasonable model for controls applications. This concept has already been illustrated for one dimensional CFD models [9]. In that paper, the development of a CFD-based linear modeling method combined with model reduction is used to model the inviscid flow of an axisymmetric one dimensional mixed compression inlet.

In this paper, the CFD-based linear modeling method is applied to the inviscid flow of an axisymmetric *multidimensional* mixed compression inlet. It should be noted that the whole inlet needs to be modeled in order to accurately capture transient behavior. The CFD code PARC is used to obtain the steady-state and transient data. The inflow boundary condition is assumed to be supersonic, the outflow boundary condition is assumed to be subsonic, and the Mach number at the exit is used as the boundary condition input. The next section describes the multidimensional CFD model development which is the basis for the linear model of the inlet; this includes the governing equations, the development of the split flux model, and the development of the boundary conditions. Then in section three, the linear model is derived by implementing linearized methods of the previous section; an input and various outputs are also developed in this section. A summary of the model reduction method and calculation of the associated error bounds follow in sections four and five. In section six, an application of the method is illustrated on a mixed compression inlet, and a conclusion follows in section seven.

2 CFD Model Development

2.1 Governing Equations

The dynamics of an internal flow propulsion system are often represented by the nonviscous multidimensional Euler equations. The conservative form of these equations is defined by Hirsch [10] as:

Conservation of Mass:

$$\frac{\partial(\rho)}{\partial t} + \frac{\partial(\rho u)}{\partial x} + \frac{\partial(\rho v)}{\partial y} + \frac{\partial(\rho w)}{\partial z} = 0 \tag{2.1}$$

Conservation of Momentum:

$$\frac{\partial(\rho u)}{\partial t} + \frac{\partial(\rho u^2 + p)}{\partial x} + \frac{\partial(\rho uv)}{\partial y} + \frac{\partial(\rho uw)}{\partial z} = 0$$

$$\begin{aligned}\frac{\partial(\rho v)}{\partial t}+\frac{\partial(\rho uv)}{\partial x}+\frac{\partial\left(\rho v^2+p\right)}{\partial y}+\frac{\partial(\rho vw)}{\partial z} &= 0 \\ \frac{\partial(\rho w)}{\partial t}+\frac{\partial(\rho uw)}{\partial x}+\frac{\partial(\rho vw)}{\partial y}+\frac{\partial\left(\rho w^2+p\right)}{\partial z} &= 0\end{aligned} \tag{2.2}$$

Conservation of Energy:

$$\frac{\partial(\rho E)}{\partial t}+\frac{\partial[u(\rho E+p)]}{\partial x}+\frac{\partial[v(\rho E+p)]}{\partial y}+\frac{\partial[w(\rho E+p)]}{\partial z}=0 \tag{2.3}$$

The number of equations in the nonlinear system of partial differential equations is $5N_1N_2N_3$ where N_1, N_2, and N_3 are the number of grid points in the x, y, and z-directions. The two dimensional form of the Euler equations is obtained by removing the third momentum equation and the spatial derivatives with respect to z in the remaining equations. Throughout this paper the three dimensional form of the equations will be implemented.

If the partial derivative terms are expanded, the conservative form of the equations can be rewritten as:

$$\frac{\partial\vec{u}}{\partial t}+\frac{\partial\vec{f}(\vec{u})}{\partial x}+\frac{\partial\vec{g}(\vec{u})}{\partial y}+\frac{\partial\vec{h}(\vec{u})}{\partial z}=0 \tag{2.4}$$

where the vector components, $\vec{u}$, $\vec{f}(\vec{u})$, $\vec{g}(\vec{u})$ and $\vec{h}(\vec{u})$, are defined below.

State vector:

$$\vec{u}=\begin{bmatrix}\rho\\ \rho u\\ \rho v\\ \rho w\\ \rho E\end{bmatrix}=\begin{bmatrix}\rho\\ m_1\\ m_2\\ m_3\\ \varepsilon\end{bmatrix} \tag{2.5}$$

The total energy per unit volume, ε, is defined as, $\varepsilon=\rho E=\rho\left(e+\dfrac{u^2+v^2+w^2}{2}\right)$, where e is the internal energy per unit mass.

Flux vectors:

$$\vec{f}(\vec{u})=\begin{bmatrix}\rho u\\ \rho u^2+p\\ \rho uv\\ \rho uw\\ u(\varepsilon+p)\end{bmatrix} \tag{2.6}$$

$$\vec{g}(\vec{u})=\begin{bmatrix}\rho v\\ \rho uv\\ \rho v^2+p\\ \rho vw\\ v(\varepsilon+p)\end{bmatrix} \tag{2.7}$$

$$\vec{h}\left(\vec{u}\right) = \begin{bmatrix} \rho w \\ \rho u w \\ \rho v w \\ \rho w^2 + p \\ w\left(\varepsilon + p\right) \end{bmatrix} \tag{2.8}$$

For a perfect gas the static pressure can be defined as:

$$\begin{aligned} p &= \left(\gamma - 1\right)\left(\varepsilon - \frac{\rho}{2}\vec{v}^2\right) \\ &= \left(\gamma - 1\right)\left(\varepsilon - \frac{\rho}{2}\left(\vec{v}\cdot\vec{v}\right)\right) \\ &= \left(\gamma - 1\right)\left(\varepsilon - \rho\frac{u^2 + v^2 + w^2}{2}\right) \end{aligned} \tag{2.9}$$

where $\vec{v} = u\hat{i} + v\hat{j} + w\hat{k}$, and the flux vectors may be rewritten in terms of the state variables. Since the flux vectors are homogenous functions of degree one in $\vec{u}$, they can be written as:

$$\begin{aligned} \vec{f}\left(\vec{u}\right) &= A\vec{u} \\ \vec{g}\left(\vec{u}\right) &= B\vec{u} \\ \vec{h}\left(\vec{u}\right) &= C\vec{u} \end{aligned} \tag{2.10}$$

Now the derivative of the first flux vector with respect to x can be represented in quasi-linear form by the following,

$$\frac{\partial \vec{f}\left(\vec{u}\right)}{\partial x} = A\frac{\partial \vec{u}}{\partial x} \tag{2.11}$$

where A is the Jacobian of the flux vector,

$$A = \frac{\partial \vec{f}\left(\vec{u}\right)}{\partial \vec{u}} \tag{2.12}$$

The Jacobians of the other flux vectors may be computed in the same manner. The substitution of the Jacobians into equation (2.4) results in the following partial differential equation,

$$\frac{\partial \vec{u}}{\partial t} + A\frac{\partial \vec{u}}{\partial x} + B\frac{\partial \vec{u}}{\partial y} + C\frac{\partial \vec{u}}{\partial z} = 0 \tag{2.13}$$

where the Jacobians are defined as:

$$A = \begin{bmatrix} 0 & 1 & 0 & 0 & 0 \\ -u^2 + \frac{\gamma - 1}{2}\vec{v}^2 & \left(3 - \gamma\right)u & -\left(\gamma - 1\right)v & -\left(\gamma - 1\right)w & \gamma - 1 \\ -uv & v & u & 0 & 0 \\ -uw & w & 0 & u & 0 \\ -u\left[\frac{\gamma\varepsilon}{\rho} - \left(\gamma - 1\right)\vec{v}^2\right] & \frac{\gamma\varepsilon}{\rho} - \frac{\gamma - 1}{2}\left(\vec{v}^2 + 2u^2\right) & -\left(\gamma - 1\right)uv & -\left(\gamma - 1\right)uw & \gamma u \end{bmatrix} \tag{2.14}$$

$$B = \begin{bmatrix} 0 & 0 & 1 & 0 & 0 \\ -uv & v & u & 0 & 0 \\ -v^2 + \frac{\gamma-1}{2}\overrightarrow{v}^2 & -(\gamma-1)\,u & (3-\gamma)\,v & -(\gamma-1)\,w & \gamma-1 \\ -vw & 0 & w & v & 0 \\ -v\left[\frac{\gamma\varepsilon}{\rho} - (\gamma-1)\,\overrightarrow{v}^2\right] & -(\gamma-1)\,uv & \frac{\gamma\varepsilon}{\rho} - \frac{\gamma-1}{2}\left(\overrightarrow{v}^2 + 2v^2\right) & -(\gamma-1)\,vw & \gamma v \end{bmatrix} \tag{2.15}$$

$$C = \begin{bmatrix} 0 & 0 & 0 & 1 & 0 \\ -uw & w & 0 & u & 0 \\ -vw & 0 & w & v & 0 \\ -w^2 + \frac{\gamma-1}{2}\overrightarrow{v}^2 & -(\gamma-1)\,u & -(\gamma-1)\,v & (3-\gamma)\,w & (\gamma-1) \\ -w\left[\frac{\gamma\varepsilon}{\rho} - (\gamma-1)\,\overrightarrow{v}^2\right] & -(\gamma-1)\,uw & -(\gamma-1)\,vw & \frac{\gamma\varepsilon}{\rho} - \frac{\gamma-1}{2}\left(\overrightarrow{v}^2 + 2w^2\right) & \gamma w \end{bmatrix} \tag{2.16}$$

The characteristics, or local eigenvalues, of the first Jacobian are equal to:

$$\begin{aligned} \lambda_{1,2,3} &= u \\ \lambda_4 &= u + c \\ \lambda_5 &= u - c \end{aligned} \tag{2.17}$$

the characteristics of the second Jacobian are equal to:

$$\begin{aligned} \lambda_{1,2,3} &= v \\ \lambda_4 &= v + c \\ \lambda_5 &= v - c \end{aligned} \tag{2.18}$$

and the characteristics of the third Jacobian are equal to:

$$\begin{aligned} \lambda_{1,2,3} &= w \\ \lambda_4 &= w + c \\ \lambda_5 &= w - c \end{aligned} \tag{2.19}$$

Note that c is the speed of sound. A system of ordinary differential equations that approximate equation (2.13) can be obtained by replacing the spatial derivative terms with finite difference expressions; then the system of equations may be integrated numerically to obtain the flow field solution. In order for the overall system to be numerically stable, the direction of the characteristics must be taken into account when the spatial derivatives are replaced. For example in the axial direction when the flow is supersonic, the characteristics are all positive, and one finite difference expression can be used for the $\frac{\partial \overrightarrow{u}}{\partial x}$ term. If the flow is subsonic, the signs of the characteristics are mixed, and a single finite difference expression for $\frac{\partial \overrightarrow{u}}{\partial x}$ will create an unstable set of ordinary differential equations. If the Jacobians of equation (2.13) are split according to the signs of the characteristics, then different finite difference expressions for the spatial derivatives can be used for each of the positive and negative terms. The next section illustrates how to split the system into its positive and negative parts.

2.2 Split Flux Model

The split flux method detailed in references [10] and [11] is summarized in this section. The split flux method separates a flux vector into subvectors which correspond to the positive and negative characteristics of the Jacobian. The split flux model can be written as the following equation,

$$\frac{\partial \vec{u}}{\partial t} + \frac{\partial \vec{f^+}(\vec{u})}{\partial x} + \frac{\partial \vec{f^-}(\vec{u})}{\partial x} + \frac{\partial \vec{g^+}(\vec{u})}{\partial y} + \frac{\partial \vec{g^-}(\vec{u})}{\partial y} + \frac{\partial \vec{h^+}(\vec{u})}{\partial z} + \frac{\partial \vec{h^-}(\vec{u})}{\partial z} = 0 \tag{2.20}$$

and the positive and negative subvectors can be calculated from the following:

$$\begin{aligned} \vec{f^\pm}(\vec{u}) &= A^\pm \vec{u} \\ \vec{g^\pm}(\vec{u}) &= B^\pm \vec{u} \\ \vec{h^\pm}(\vec{u}) &= C^\pm \vec{u} \end{aligned} \tag{2.21}$$

Substitution of equation (2.21) into the split flux model equation (2.20) produces the following result.

$$\frac{\partial \vec{u}}{\partial t} + A^+\frac{\partial \vec{u}}{\partial x} + A^-\frac{\partial \vec{u}}{\partial x} + B^+\frac{\partial \vec{u}}{\partial y} + B^-\frac{\partial \vec{u}}{\partial y} + C^+\frac{\partial \vec{u}}{\partial z} + C^-\frac{\partial \vec{u}}{\partial z} = 0 \tag{2.22}$$

The positive and negative Jacobians satisfy,

$$\begin{aligned} A &= A^+ + A^- \\ B &= B^+ + B^- \\ C &= C^+ + C^- \end{aligned} \tag{2.23}$$

and are calculated from:

$$\begin{aligned} A^\pm &= K_1 \Lambda_1^\pm K_1^{-1} \\ B^\pm &= K_2 \Lambda_2^\pm K_2^{-1} \\ C^\pm &= K_3 \Lambda_3^\pm K_3^{-1} \end{aligned} \tag{2.24}$$

The right eigenvectors of A, B, and C are defined as:

$$K_1 = \begin{bmatrix} 1 & 0 & 0 & \frac{\rho}{2c} & \frac{\rho}{2c} \\ u & 0 & 0 & \frac{\rho}{2c}(u+c) & \frac{\rho}{2c}(u-c) \\ v & 0 & -\rho & \frac{\rho v}{2c} & \frac{\rho v}{2c} \\ w & \rho & 0 & \frac{\rho w}{2c} & \frac{\rho w}{2c} \\ \frac{\vec{v}^2}{2} & \rho w & -\rho v & \frac{\rho}{2c}\left(\frac{\vec{v}^2}{2} + \frac{c^2}{\gamma - 1} + cu\right) & \frac{\rho}{2c}\left(\frac{\vec{v}^2}{2} + \frac{c^2}{\gamma - 1} - cu\right) \end{bmatrix} \tag{2.25}$$

$$K_2 = \begin{bmatrix} 0 & 1 & 0 & \frac{\rho}{2c} & \frac{\rho}{2c} \\ 0 & u & \rho & \frac{\rho u}{2c} & \frac{\rho u}{2c} \\ 0 & v & 0 & \frac{\rho}{2c}(v+c) & \frac{\rho}{2c}(v-c) \\ -\rho & w & 0 & \frac{\rho w}{2c} & \frac{\rho w}{2c} \\ -\rho w & \frac{\overrightarrow{v}^2}{2} & \rho u & \frac{\rho}{2c}\left(\frac{\overrightarrow{v}^2}{2} + \frac{c^2}{\gamma-1} + cv\right) & \frac{\rho}{2c}\left(\frac{\overrightarrow{v}^2}{2} + \frac{c^2}{\gamma-1} - cv\right) \end{bmatrix} \tag{2.26}$$

$$K_3 = \begin{bmatrix} 0 & 0 & 1 & \frac{\rho}{2c} & \frac{\rho}{2c} \\ 0 & -\rho & u & \frac{\rho u}{2c} & \frac{\rho u}{2c} \\ \rho & 0 & v & \frac{\rho v}{2c} & \frac{\rho v}{2c} \\ 0 & 0 & w & \frac{\rho}{2c}(w+c) & \frac{\rho}{2c}(w-c) \\ \rho v & -\rho u & \frac{\overrightarrow{v}^2}{2} & \frac{\rho}{2c}\left(\frac{\overrightarrow{v}^2}{2} + \frac{c^2}{\gamma-1} + cw\right) & \frac{\rho}{2c}\left(\frac{\overrightarrow{v}^2}{2} + \frac{c^2}{\gamma-1} - cw\right) \end{bmatrix} \tag{2.27}$$

and the matrices $\Lambda_1^{\pm}$, $\Lambda_2^{\pm}$, and $\Lambda_3^{\pm}$ can be defined as:

$$\Lambda_1^{\pm} = \begin{bmatrix} \frac{1}{2}(u \pm |u|) & 0 & 0 & 0 & 0 \\ 0 & \frac{1}{2}(u \pm |u|) & 0 & 0 & 0 \\ 0 & 0 & \frac{1}{2}(u \pm |u|) & 0 & 0 \\ 0 & 0 & 0 & \frac{1}{2}(u+c \pm |u+c|) & 0 \\ 0 & 0 & 0 & 0 & \frac{1}{2}(u-c \pm |u-c|) \end{bmatrix} \tag{2.28}$$

$$\Lambda_2^{\pm} = \begin{bmatrix} \frac{1}{2}(v \pm |v|) & 0 & 0 & 0 & 0 \\ 0 & \frac{1}{2}(v \pm |v|) & 0 & 0 & 0 \\ 0 & 0 & \frac{1}{2}(v \pm |v|) & 0 & 0 \\ 0 & 0 & 0 & \frac{1}{2}(v+c \pm |v+c|) & 0 \\ 0 & 0 & 0 & 0 & \frac{1}{2}(v-c \pm |v-c|) \end{bmatrix} \tag{2.29}$$

$$\Lambda_3^{\pm} = \begin{bmatrix} \frac{1}{2}(w \pm |w|) & 0 & 0 & 0 & 0 \\ 0 & \frac{1}{2}(w \pm |w|) & 0 & 0 & 0 \\ 0 & 0 & \frac{1}{2}(w \pm |w|) & 0 & 0 \\ 0 & 0 & 0 & \frac{1}{2}(w+c \pm |w+c|) & 0 \\ 0 & 0 & 0 & 0 & \frac{1}{2}(w-c \pm |w-c|) \end{bmatrix} \tag{2.30}$$

There are a variety of splittings that can be used for Λ. As long as the characteristics of Λ^+ and Λ^- satisfy $\Lambda = \Lambda^+ + \Lambda^-$, the splitting is valid. Once the system, equation (2.22), is split into its positive and negative

Jacobians, a different finite difference expression can be used to approximate the spatial derivatives for each Jacobian. The spatial derivatives associated with the positive Jacobians are discretized with a backward difference operator:

$$\begin{aligned}
\frac{\partial \overrightarrow{u}_{i,j,k}}{\partial x} &= \frac{\overrightarrow{u}_{i,j,k} - \overrightarrow{u}_{i-1,j,k}}{x_{i,j,k} - x_{i-1,j,k}} \\
\frac{\partial \overrightarrow{u}_{i,j,k}}{\partial y} &= \frac{\overrightarrow{u}_{i,j,k} - \overrightarrow{u}_{i,j-1,k}}{y_{i,j,k} - y_{i,j-1,k}} \\
\frac{\partial \overrightarrow{u}_{i,j,k}}{\partial z} &= \frac{\overrightarrow{u}_{i,j,k} - \overrightarrow{u}_{i,j,k-1}}{z_{i,j,k} - z_{i,j,k-1}}
\end{aligned} \tag{2.31}$$

and the spatial derivatives associated with the negative Jacobians are discretized with a forward difference operator:

$$\begin{aligned}
\frac{\partial \overrightarrow{u}_{i,j,k}}{\partial x} &= \frac{\overrightarrow{u}_{i+1,j,k} - \overrightarrow{u}_{i,j,k}}{x_{i+1,j,k} - x_{i,j,k}} \\
\frac{\partial \overrightarrow{u}_{i,j,k}}{\partial y} &= \frac{\overrightarrow{u}_{i,j+1,k} - \overrightarrow{u}_{i,j,k}}{y_{i,j+1,k} - y_{i,j,k}} \\
\frac{\partial \overrightarrow{u}_{i,j,k}}{\partial z} &= \frac{\overrightarrow{u}_{i,j,k+1} - \overrightarrow{u}_{i,j,k}}{z_{i,j,k+1} - z_{i,j,k}}
\end{aligned} \tag{2.32}$$

The grid point is denoted by the subscript i, j, k. The approximations for the spatial derivatives are substituted into equation (2.22) which results in the following equation at each grid point of the system.

$$\begin{aligned}
0 = \frac{\partial \overrightarrow{u}_{i,j,k}}{\partial t} &+ A^+_{i,j,k}\left(\frac{\overrightarrow{u}_{i,j,k} - \overrightarrow{u}_{i-1,j,k}}{x_{i,j,k} - x_{i-1,j,k}}\right) + A^-_{i,j,k}\left(\frac{\overrightarrow{u}_{i+1,j,k} - \overrightarrow{u}_{i,j,k}}{x_{i+1,j,k} - x_{i,j,k}}\right) \\
&+ B^+_{i,j,k}\left(\frac{\overrightarrow{u}_{i,j,k} - \overrightarrow{u}_{i,j-1,k}}{y_{i,j,k} - y_{i,j-1,k}}\right) + B^-_{i,j,k}\left(\frac{\overrightarrow{u}_{i,j+1,k} - \overrightarrow{u}_{i,j,k}}{y_{i,j+1,k} - y_{i,j,k}}\right) \\
&+ C^+_{i,j,k}\left(\frac{\overrightarrow{u}_{i,j,k} - \overrightarrow{u}_{i,j,k-1}}{z_{i,j,k} - z_{i,j,k-1}}\right) + C^-_{i,j,k}\left(\frac{\overrightarrow{u}_{i,j,k+1} - \overrightarrow{u}_{i,j,k}}{z_{i,j,k+1} - z_{i,j,k}}\right)
\end{aligned} \tag{2.33}$$

This can be rewritten as:

$$\begin{aligned}
0 = \frac{\partial \overrightarrow{u}_{i,j,k}}{\partial t} &- \frac{A^+_{i,j,k}}{x_{i,j,k} - x_{i-1,j,k}}\overrightarrow{u}_{i-1,j,k} - \frac{B^+_{i,j,k}}{y_{i,j,k} - y_{i,j-1,k}}\overrightarrow{u}_{i,j-1,k} - \frac{C^+_{i,j,k}}{z_{i,j,k} - z_{i,j,k-1}}\overrightarrow{u}_{i,j,k-1} \\
&+ \left(\frac{A^+_{i,j,k}}{x_{i,j,k} - x_{i-1,j,k}} - \frac{A^-_{i,j,k}}{x_{i+1,j,k} - x_{i,j,k}} + \frac{B^+_{i,j,k}}{y_{i,j,k} - y_{i,j-1,k}}\right. \\
&\left. - \frac{B^-_{i,j,k}}{y_{i,j+1,k} - y_{i,j,k}} + \frac{C^+_{i,j,k}}{z_{i,j,k} - z_{i,j,k-1}} - \frac{C^-_{i,j,k}}{z_{i,j,k+1} - z_{i,j,k}}\right)\overrightarrow{u}_{i,j,k} \\
&+ \frac{A^-_{i,j,k}}{x_{i+1,j,k} - x_{i,j,k}}\overrightarrow{u}_{i+1,j,k} + \frac{B^-_{i,j,k}}{y_{i,j+1,k} - y_{i,j,k}}\overrightarrow{u}_{i,j+1,k} + \frac{C^-_{i,j,k}}{z_{i,j,k+1} - z_{i,j,k}}\overrightarrow{u}_{i,j,k+1}
\end{aligned} \tag{2.34}$$

Equation (2.34) represents the dynamics of the internal grid points of the CFD model; there are still boundary conditions that must be satisfied at the following locations:

$$\begin{aligned}
i &= j = k = 1 \\
i &= N_1 \\
j &= N_2 \\
k &= N_3
\end{aligned}$$

where N_1, N_2, and N_3 are the total number of grid points in the x, y and z-directions. The boundary conditions are developed in the next section.

2.3 Boundary Conditions

Boundary conditions can be categorized as either physical or numerical. Numerical boundary conditions correspond to characteristics leaving the domain; therefore they are determined from the interior grid points. The physical boundary conditions correspond to characteristics entering the domain and cannot be determined from the interior grid points; therefore, they must be specified. The numerical treatment for the boundary conditions follows in the next two sections.

2.3.1 Wall Boundary Conditions

The boundary conditions at the y and z-planes are implemented using the method of non-reflective boundary conditions [10]. When using this method, the physical boundary conditions are set equal to zero, and the numerical boundary conditions are determined from the interior grid points of the computational grid. Since the characteristics at the boundary are propagating in one direction, one finite difference equation can be used to replace the spatial derivative. The following is a general equation that can be used at these boundaries ($j = 1, j = N_2, k = 1,$ and $k = N_3$) for the boundary conditions.

$$\begin{aligned} 0 \;=\; & \frac{\partial \overrightarrow{u}_{i,j,k}}{\partial t} - \frac{A^+_{i,j,k}}{x_{i,j,k} - x_{i-1,j,k}} \overrightarrow{u}_{i-1,j,k} + \left(\frac{A^+_{i,j,k}}{x_{i,j,k} - x_{i-1,j,k}} - \frac{A^-_{i,j,k}}{x_{i+1,j,k} - x_{i,j,k}} \right) \overrightarrow{u}_{i,j,k} \\ & + \frac{A^-_{i,j,k}}{x_{i+1,j,k} - x_{i,j,k}} \overrightarrow{u}_{i+1,j,k} + K_2 \Lambda_{2_{bc}} K_2^{-1} \frac{\partial \overrightarrow{u}_{i,j,k}}{\partial y} + K_3 \Lambda_{3_{bc}} K_3^{-1} \frac{\partial \overrightarrow{u}_{i,j,k}}{\partial z} \end{aligned} \tag{2.35}$$

At the boundaries, $\Lambda_{2_{bc}}$ and $\Lambda_{3_{bc}}$ are determined from the numerical boundary conditions; where as, A^+ and A^- are determined from the positive and negative Jacobians from the split flux method.

For $j = 1$, the spatial derivative $\dfrac{\partial \overrightarrow{u}}{\partial y}$ is replaced with a *forward* finite difference, equation (2.32), hence $\Lambda_{2_{bc}}$ must have all negative characteristics. Therefore, $\dfrac{\partial \overrightarrow{u}}{\partial y}$, $\Lambda_{2_{bc}}$, B^+, and B^- become the following:

$$\frac{\partial \overrightarrow{u}}{\partial y} = \frac{\overrightarrow{u}_{i,j+1,k} - \overrightarrow{u}_{i,j,k}}{y_{i,j+1,k} - y_{i,j,k}}$$

$$\begin{aligned} \Lambda_{2_{bc}} \;=\; & \begin{bmatrix} 0 & 0 & 0 & 0 & 0 \\ 0 & 0 & 0 & 0 & 0 \\ 0 & 0 & 0 & 0 & 0 \\ 0 & 0 & 0 & 0 & 0 \\ 0 & 0 & 0 & 0 & v-c \end{bmatrix}, \; v > 0 \\ \Lambda_{2_{bc}} \;=\; & \begin{bmatrix} v & 0 & 0 & 0 & 0 \\ 0 & v & 0 & 0 & 0 \\ 0 & 0 & v & 0 & 0 \\ 0 & 0 & 0 & 0 & 0 \\ 0 & 0 & 0 & 0 & v-c \end{bmatrix}, \; v < 0 \end{aligned} \tag{2.36}$$

$$
\begin{aligned}
B^{+} &= 0 \\
B^{-} &= K_2 \Lambda_{2_{bc}} K_2^{-1}
\end{aligned}
$$

Likewise, for $k = 1$, $\dfrac{\partial \overrightarrow{u}}{\partial z}$, $\Lambda_{3_{bc}}$, C^{+}, and C^{-} become the following:

$$
\frac{\partial \overrightarrow{u}}{\partial z} = \frac{\overrightarrow{u}_{i,j,k+1} - \overrightarrow{u}_{i,j,k}}{z_{i,j,k+1} - z_{i,j,k}}
$$

$$
\begin{aligned}
\Lambda_{3_{bc}} &= \begin{bmatrix} 0 & 0 & 0 & 0 & 0 \\ 0 & 0 & 0 & 0 & 0 \\ 0 & 0 & 0 & 0 & 0 \\ 0 & 0 & 0 & 0 & 0 \\ 0 & 0 & 0 & 0 & w-c \end{bmatrix}, \; w > 0 \\
\Lambda_{3_{bc}} &= \begin{bmatrix} w & 0 & 0 & 0 & 0 \\ 0 & w & 0 & 0 & 0 \\ 0 & 0 & w & 0 & 0 \\ 0 & 0 & 0 & 0 & 0 \\ 0 & 0 & 0 & 0 & w-c \end{bmatrix}, \; w < 0 \\
C^{+} &= 0 \\
C^{-} &= K_3 \Lambda_{3_{bc}} K_3^{-1}
\end{aligned}
\tag{2.37}
$$

For $j = N_2$, the spatial derivative $\dfrac{\partial \overrightarrow{u}}{\partial y}$ is replaced with a *backward* finite difference, equation (2.31), hence $\Lambda_{2_{bc}}$ must have all positive characteristics. Therefore, $\dfrac{\partial \overrightarrow{u}}{\partial y}$, $\Lambda_{2_{bc}}$, B^{+}, and B^{-} become the following:

$$
\frac{\partial \overrightarrow{u}}{\partial y} = \frac{\overrightarrow{u}_{i,j,k} - \overrightarrow{u}_{i,j-1,k}}{y_{i,j,k} - y_{i,j-1,k}}
$$

$$
\begin{aligned}
\Lambda_{2_{bc}} &= \begin{bmatrix} v & 0 & 0 & 0 & 0 \\ 0 & v & 0 & 0 & 0 \\ 0 & 0 & v & 0 & 0 \\ 0 & 0 & 0 & v+c & 0 \\ 0 & 0 & 0 & 0 & 0 \end{bmatrix}, \; v > 0 \\
\Lambda_{2_{bc}} &= \begin{bmatrix} 0 & 0 & 0 & 0 & 0 \\ 0 & 0 & 0 & 0 & 0 \\ 0 & 0 & 0 & 0 & 0 \\ 0 & 0 & 0 & v+c & 0 \\ 0 & 0 & 0 & 0 & 0 \end{bmatrix}, \; v < 0 \\
B^{+} &= K_2 \Lambda_{2_{bc}} K_2^{-1} \\
B^{-} &= 0
\end{aligned}
\tag{2.38}
$$

and for $k = N_3$, $\frac{\partial \vec{u}}{\partial z}$, $\Lambda_{3_{bc}}$, C^+, and C^- become the following:

$$\frac{\partial \vec{u}}{\partial z} = \frac{\vec{u}_{i,j,k} - \vec{u}_{i,j,k-1}}{z_{i,j,k} - z_{i,j,k-1}}$$

$$\Lambda_{3_{bc}} = \begin{bmatrix} w & 0 & 0 & 0 & 0 \\ 0 & w & 0 & 0 & 0 \\ 0 & 0 & w & 0 & 0 \\ 0 & 0 & 0 & w+c & 0 \\ 0 & 0 & 0 & 0 & 0 \end{bmatrix}, \; w > 0$$

$$\Lambda_{3_{bc}} = \begin{bmatrix} 0 & 0 & 0 & 0 & 0 \\ 0 & 0 & 0 & 0 & 0 \\ 0 & 0 & 0 & 0 & 0 \\ 0 & 0 & 0 & w+c & 0 \\ 0 & 0 & 0 & 0 & 0 \end{bmatrix}, \; w < 0 \tag{2.39}$$

$$C^+ = K_3 \Lambda_{3_{bc}} K_3^{-1}$$
$$C^- = 0$$

The coefficients for the wall boundary condition equations listed in section 3.2 will be computed from the B^+, B^-, C^+, and C^- terms defined in the above equations.

2.3.2 Inflow and Outflow Boundary Conditions

Compatibility relations with time-differenced physical boundary conditions is the method used for the treatment of the inflow and outflow boundary conditions. Using this method, the incoming characteristics are replaced with specific physical boundary conditions so that only information transmitted from the interior is maintained. The general development for the treatment of the boundary conditions as taken from Hirsch [10] and Chakravarthy [12] follows.

If the governing PDE, equation (2.4) from section 2.1,

$$\frac{\partial \vec{u}}{\partial t} + \frac{\partial \vec{f}(\vec{u})}{\partial x} + \frac{\partial \vec{g}(\vec{u})}{\partial y} + \frac{\partial \vec{h}(\vec{u})}{\partial z} = 0$$

is rewritten in terms of the characteristic variables for the time derivative, the characteristic variables can be split into the incoming physical characteristics, $\vec{w^P}$, and the outgoing numerical characteristics, $\vec{w^N}$.

$$\frac{\partial}{\partial t}\begin{bmatrix} \vec{w^N} \\ \vec{w^P} \end{bmatrix} + \begin{bmatrix} (K_1^{-1})^N \\ (K_1^{-1})^P \end{bmatrix} A\frac{\partial \vec{u}}{\partial x} + \begin{bmatrix} (K_1^{-1})^N \\ (K_1^{-1})^P \end{bmatrix} B\frac{\partial \vec{u}}{\partial y} + \begin{bmatrix} (K_1^{-1})^N \\ (K_1^{-1})^P \end{bmatrix} C\frac{\partial \vec{u}}{\partial z} = 0 \tag{2.40}$$

The partitioning of the K_1 matrix shown here will be discussed in detail in section 3.3.1. Note that the position of the physical and numerical characteristics will be different for different types of boundary conditions. With this boundary condition method, information transmitted by the characteristics to the interior is discarded. Therefore, the incoming characteristics are set equal to zero by replacing them with the physical boundary condition, $B_{bc} = 0$, as follows.

$$\frac{\partial}{\partial t}\begin{bmatrix} \vec{w^N} \\ B_{bc} \end{bmatrix} + \begin{bmatrix} (K_1^{-1})^N \\ 0 \end{bmatrix} A\frac{\partial \vec{u}}{\partial x} + \begin{bmatrix} (K_1^{-1})^N \\ 0 \end{bmatrix} B\frac{\partial \vec{u}}{\partial y} + \begin{bmatrix} (K_1^{-1})^N \\ 0 \end{bmatrix} C\frac{\partial \vec{u}}{\partial z} = 0 \tag{2.41}$$

Converting back to conservative variables and replacing $\frac{\partial B_{bc}}{\partial t}$ with $\frac{\partial B_{bc}}{\partial \overrightarrow{u}}\frac{\partial \overrightarrow{u}}{\partial t}$ yields,

$$\begin{bmatrix} \left(K_1^{-1}\right)^N \frac{\partial \overrightarrow{u}}{\partial t} \\ \frac{\partial B_{bc}}{\partial \overrightarrow{u}}\frac{\partial \overrightarrow{u}}{\partial t} \end{bmatrix} + \begin{bmatrix} \left(K_1^{-1}\right)^N \\ 0 \end{bmatrix} A\frac{\partial \overrightarrow{u}}{\partial x} + \begin{bmatrix} \left(K_1^{-1}\right)^N \\ 0 \end{bmatrix} B\frac{\partial \overrightarrow{u}}{\partial y} + \begin{bmatrix} \left(K_1^{-1}\right)^N \\ 0 \end{bmatrix} C\frac{\partial \overrightarrow{u}}{\partial z} = 0 \quad (2.42)$$

Now the implementation of the time-differenced boundary condition is performed. This is done by taking the derivative of B_{bc} with respect to time and replacing the derivative by a finite difference equation.

$$\begin{aligned} \frac{\partial B_{bc}}{\partial t} &= \frac{\partial B_{bc}}{\partial \overrightarrow{u}}\frac{\partial \overrightarrow{u}}{\partial t} \\ B_{bc}\left(\overrightarrow{u}^{n+1}\right) - B_{bc}\left(\overrightarrow{u}^{n}\right) &= \frac{\partial B_{bc}}{\partial \overrightarrow{u}}\left(\overrightarrow{u}^{n+1} - \overrightarrow{u}^{n}\right) \\ B_{bc}\left(\overrightarrow{u}^{n+1}\right) &= B_{bc}\left(\overrightarrow{u}^{n}\right) + \frac{\partial B_{bc}}{\partial \overrightarrow{u}}\left(\overrightarrow{u}^{n+1} - \overrightarrow{u}^{n}\right) \end{aligned} \quad (2.43)$$

Now $B_{bc}\left(\overrightarrow{u}^{n+1}\right)$ is set equal to zero, because it has replaced the incoming characteristic.

$$\begin{aligned} 0 &= B_{bc}\left(\overrightarrow{u}^{n}\right) + \frac{\partial B_{bc}}{\partial \overrightarrow{u}}\left(\overrightarrow{u}^{n+1} - \overrightarrow{u}^{n}\right) \\ -B_{bc}\left(\overrightarrow{u}^{n}\right) &= \frac{\partial B_{bc}}{\partial \overrightarrow{u}}\left(\overrightarrow{u}^{n+1} - \overrightarrow{u}^{n}\right) \\ -B_{bc}\left(\overrightarrow{u}\right) &= \frac{\partial B_{bc}}{\partial \overrightarrow{u}}\frac{\partial \overrightarrow{u}}{\partial t} \end{aligned} \quad (2.44)$$

Substitute the last line of (2.44) into equation (2.42).

$$\begin{bmatrix} \left(K_1^{-1}\right)^N \\ \frac{\partial B_{bc}}{\partial \overrightarrow{u}} \end{bmatrix} \frac{\partial \overrightarrow{u}}{\partial t} + \begin{bmatrix} \left(K_1^{-1}\right)^N \\ 0 \end{bmatrix} A\frac{\partial \overrightarrow{u}}{\partial x} + \begin{bmatrix} \left(K_1^{-1}\right)^N \\ 0 \end{bmatrix} B\frac{\partial \overrightarrow{u}}{\partial y} + \begin{bmatrix} \left(K_1^{-1}\right)^N \\ 0 \end{bmatrix} C\frac{\partial \overrightarrow{u}}{\partial z} = \begin{bmatrix} 0 \\ -B_{bc} \end{bmatrix} \quad (2.45)$$

Let L_1 be defined as:

$$L_1 = \begin{bmatrix} \left(K_1^{-1}\right)^N \\ \frac{\partial B_{bc}}{\partial \overrightarrow{u}} \end{bmatrix} \quad (2.46)$$

and L_2 be defined as:

$$L_2 = \begin{bmatrix} \left(K_1^{-1}\right)^N \\ 0 \end{bmatrix} \quad (2.47)$$

Substitute (2.46) and (2.47) into equation (2.45) and simplify.

$$\begin{aligned} \frac{\partial \overrightarrow{u}}{\partial t} + L_1^{-1}L_2A\frac{\partial \overrightarrow{u}}{\partial x} + L_1^{-1}L_2B\frac{\partial \overrightarrow{u}}{\partial y} + L_1^{-1}L_2C\frac{\partial \overrightarrow{u}}{\partial z} &= L_1^{-1}\begin{bmatrix} 0 \\ -B_{bc} \end{bmatrix} \\ \frac{\partial \overrightarrow{u}}{\partial t} + L_1^{-1}L_2\left(A\frac{\partial \overrightarrow{u}}{\partial x} + B\frac{\partial \overrightarrow{u}}{\partial y} + C\frac{\partial \overrightarrow{u}}{\partial z}\right) &= L_1^{-1}\begin{bmatrix} 0 \\ -B_{bc} \end{bmatrix} \end{aligned} \quad (2.48)$$

Since the incoming characteristics have been zeroed out and replaced with physical boundary conditions, the spatial derivative can be replaced with one finite difference expression. At the cowl lip the spatial derivative with respect to x is replaced with a forward difference equation (2.32), and at the compressor face it is replaced with a backward difference equation (2.31). For the spatial derivatives in the other directions, they are replaced after $B^{\pm}$ and $C^{\pm}$ have been defined either from the boundary conditions or from the split flux method, as shown in the following equations.

Cowl lip boundary condition:

$$\begin{aligned}
&\frac{\partial \vec{u}_{1,j,k}}{\partial t} + L_1^{-1} L_2 \left(\frac{A_{1,j,k}}{x_{2,j,k} - x_{1,j,k}} \vec{u}_{2,j,k} - \frac{A_{1,j,k}}{x_{2,j,k} - x_{1,j,k}} \vec{u}_{1,j,k} - \frac{B^{+}_{1,j,k}}{y_{1,j,k} - y_{1,j-1,k}} \vec{u}_{1,j-1,k} \right. \\
&+ \left(\frac{B^{+}_{1,j,k}}{y_{1,j,k} - y_{1,j-1,k}} - \frac{B^{-}_{1,j,k}}{y_{1,j+1,k} - y_{1,j,k}} \right) \vec{u}_{1,j,k} + \frac{B^{-}_{1,j,k}}{y_{1,j+1,k} - y_{1,j,k}} \vec{u}_{1,j+1,k} \\
&- \frac{C^{+}_{1,j,k}}{z_{1,j,k} - z_{1,j,k-1}} \vec{u}_{1,j,k-1} + \left(\frac{C^{+}_{1,j,k}}{z_{1,j,k} - z_{1,j,k-1}} - \frac{C^{-}_{1,j,k}}{z_{1,j,k+1} - z_{1,j,k}} \right) \vec{u}_{1,j,k} \\
&\left. + \frac{C^{-}_{1,j,k}}{z_{1,j,k+1} - z_{1,j,k}} \vec{u}_{1,j,k+1} \right) = L_1^{-1} \begin{bmatrix} -B_{bc} \\ 0 \end{bmatrix}
\end{aligned} \tag{2.49}$$

Compressor face boundary condition:

$$\begin{aligned}
&\frac{\partial \vec{u}_{N_1,j,k}}{\partial t} + L_1^{-1} L_2 \left(\frac{A_{N_1,j,k}}{x_{N_1,j,k} - x_{N_1-1,j,k}} \vec{u}_{N_1,j,k} - \frac{A_{N_1,j,k}}{x_{N_1,j,k} - x_{N_1-1,j,k}} \vec{u}_{N_1-1,j,k} \right. \\
&- \frac{B^{+}_{N_1,j,k}}{y_{N_1,j,k} - y_{N_1,j-1,k}} \vec{u}_{N_1,j-1,k} + \left(\frac{B^{+}_{N_1,j,k}}{y_{N_1,j,k} - y_{N_1,j-1,k}} - \frac{B^{-}_{N_1,j,k}}{y_{N_1,j+1,k} - y_{N_1,j,k}} \right) \vec{u}_{N_1,j,k} \\
&+ \frac{B^{-}_{N_1,j,k}}{y_{N_1,j+1,k} - y_{N_1,j,k}} \vec{u}_{N_1,j+1,k} - \frac{C^{+}_{N_1,j,k}}{z_{N_1,j,k} - z_{N_1,j,k-1}} \vec{u}_{N_1,j,k-1} + \left(\frac{C^{+}_{N_1,j,k}}{z_{N_1,j,k} - z_{N_1,j,k-1}} \right. \\
&\left. \left. - \frac{C^{-}_{N_1,j,k}}{z_{N_1,j,k+1} - z_{N_1,j,k}} \right) \vec{u}_{N_1,j,k} + \frac{C^{-}_{N_1,j,k}}{z_{N_1,j,k+1} - z_{N_1,j,k}} \vec{u}_{N_1,j,k+1} \right) = L_1^{-1} \begin{bmatrix} 0 \\ -B_{bc} \end{bmatrix}
\end{aligned} \tag{2.50}$$

The next section develops the linear model using the split flux technique from section 2.2 and the boundary condition methods from section 2.3.

3 Linear Model Development

3.1 Small Perturbation Model

For a small perturbation model, the states, inputs, and outputs of a nonlinear system are assumed to be the combination of a steady-state value and a small time dependent perturbation as shown below in equations (3.1) through (3.3).

States:

$$\vec{X} = \vec{X}_{ss} + \delta \vec{X} \tag{3.1}$$

Inputs:

$$\overrightarrow{U} = \overrightarrow{U}_{ss} + \delta\overrightarrow{U} \tag{3.2}$$

Outputs:

$$\overrightarrow{Y} = \overrightarrow{Y}_{ss} + \delta\overrightarrow{Y} \tag{3.3}$$

The small perturbation model is only valid when operating within a small region around the steady-state value; once outside this region, the linear model is no longer an accurate representation of the nonlinear system. In other words, the farther the nonlinear model moves away from the operating point, the less accurate the linear dynamic response.

Because of the large number of equations in the CFD-based model, it is convenient to describe the small perturbation model in state space format; this also facilitates the placement of the inputs and outputs for the system.

$$\begin{aligned} \frac{d}{dt}\delta\overrightarrow{X} &= \mathbf{A}\delta\overrightarrow{X} + \mathbf{B}\delta\overrightarrow{U} \\ \delta\overrightarrow{Y} &= \mathbf{C}\delta\overrightarrow{X} + \mathbf{D}\delta\overrightarrow{U} \end{aligned} \tag{3.4}$$

The **A**, **B**, **C**, and **D** matrices are defined as follows:

$$\begin{aligned} \mathbf{A} &= \textit{system matrix} \\ \mathbf{B} &= \textit{input matrix} \\ \mathbf{C} &= \textit{output matrix} \\ \mathbf{D} &= \textit{input/output matrix} \end{aligned} \tag{3.5}$$

The data needed for the calculation of these matrices is obtained from a steady-state operating point of the propulsion system model. The contents of these matrices are developed in the following sections.

3.2 System Matrix

The system matrix for the small perturbation model is generated by applying equation (2.34) to each grid point of the propulsion system with the Jacobians evaluated at the steady-state operating point. For the interior grid points, equation (2.34) can be rewritten as follows:

$$\begin{aligned} \frac{\partial\delta\overrightarrow{u}_{i,j,k}}{\partial t} &= \mathbf{d}_{i,j,k}\delta\overrightarrow{u}_{i-1,j,k} + \mathbf{b}_{i,j,k}\delta\overrightarrow{u}_{i,j-1,k} + \mathbf{g}_{i,j,k}\delta\overrightarrow{u}_{i,j,k-1} + \mathbf{a}_{i,j,k}\delta\overrightarrow{u}_{i,j,k} \\ &\quad + \mathbf{e}_{i,j,k}\delta\overrightarrow{u}_{i+1,j,k} + \mathbf{c}_{i,j,k}\delta\overrightarrow{u}_{i,j+1,k} + \mathbf{f}_{i,j,k}\delta\overrightarrow{u}_{i,j,k+1} \end{aligned} \tag{3.6}$$

where the coefficients on $\delta\overrightarrow{u}$ are defined as:

$$\begin{aligned} \mathbf{a}_{i,j,k} &= \frac{A^-_{i,j,k}}{x_{i+1,j,k} - x_{i,j,k}} - \frac{A^+_{i,j,k}}{x_{i,j,k} - x_{i-1,j,k}} + \frac{B^-_{i,j,k}}{y_{i,j+1,k} - y_{i,j,k}} \\ &\quad - \frac{B^+_{i,j,k}}{y_{i,j,k} - y_{i,j-1,k}} + \frac{C^-_{i,j,k}}{z_{i,j,k+1} - z_{i,j,k}} - \frac{C^+_{i,j,k}}{z_{i,j,k} - z_{i,j,k-1}} \\ \mathbf{b}_{i,j,k} &= \frac{B^+_{i,j,k}}{y_{i,j,k} - y_{i,j-1,k}} \\ \mathbf{c}_{i,j,k} &= \frac{-B^-_{i,j,k}}{y_{i,j+1,k} - y_{i,j,k}} \end{aligned}$$

$$
\begin{aligned}
\mathbf{d}_{i,j,k} &= \frac{A^{+}_{i,j,k}}{x_{i,j,k} - x_{i-1,j,k}} \\
\mathbf{e}_{i,j,k} &= \frac{-A^{-}_{i,j,k}}{x_{i+1,j,k} - x_{i,j,k}} \\
\mathbf{f}_{i,j,k} &= \frac{-C^{-}_{i,j,k}}{z_{i,j,k+1} - z_{i,j,k}} \\
\mathbf{g}_{i,j,k} &= \frac{C^{+}_{i,j,k}}{z_{i,j,k} - z_{i,j,k-1}}
\end{aligned}
\tag{3.7}
$$

This can be written in the following compact form:

$$
\frac{d}{dt}\delta\overrightarrow{X} = \mathbf{A}\delta\overrightarrow{X} \tag{3.8}
$$

If the i, j, and k indices are incremented in the following manner $(((k = 1, \cdots, N_3)\, j = 1, \cdots, N_2)\, i = 1, \cdots, N_1)$ $\delta\overrightarrow{X}$ is defined as:

$$
\delta\overrightarrow{X} = \begin{bmatrix}
\delta\overrightarrow{u}_{1,1,1} \\
\delta\overrightarrow{u}_{1,1,2} \\
\vdots \\
\delta\overrightarrow{u}_{1,1,N_3} \\
\delta\overrightarrow{u}_{1,2,1} \\
\vdots \\
\delta\overrightarrow{u}_{1,2,N_3} \\
\vdots \\
\delta\overrightarrow{u}_{1,N_2,1} \\
\vdots \\
\delta\overrightarrow{u}_{1,N_2,N_3} \\
\delta\overrightarrow{u}_{2,1,1} \\
\vdots \\
\delta\overrightarrow{u}_{N_1,N_2,N_3}
\end{bmatrix} \tag{3.9}
$$

The banded structure of the $\mathbf{A}$ matrix is shown below:

$$
\mathbf{A} = \begin{bmatrix}
\mathbf{a} & \mathbf{f} & & & \mathbf{c} & & & \mathbf{e} & & \\
\mathbf{g} & \mathbf{a} & \mathbf{f} & & & \mathbf{c} & & & \mathbf{e} & \\
 & \mathbf{g} & \mathbf{a} & \mathbf{f} & & & \mathbf{c} & & & \mathbf{e} \\
 & & \mathbf{g} & \mathbf{a} & \mathbf{f} & & & \mathbf{c} & & \\
\mathbf{b} & & & \mathbf{g} & \mathbf{a} & \mathbf{f} & & & \mathbf{c} & \\
 & \mathbf{b} & & & \mathbf{g} & \mathbf{a} & \mathbf{f} & & & \mathbf{c} \\
 & & \mathbf{b} & & & \mathbf{g} & \mathbf{a} & \mathbf{f} & & \\
\mathbf{d} & & & \mathbf{b} & & & \mathbf{g} & \mathbf{a} & \mathbf{f} & \\
 & \mathbf{d} & & & \mathbf{b} & & & \mathbf{g} & \mathbf{a} & \mathbf{f} \\
 & & \mathbf{d} & & & \mathbf{b} & & & \mathbf{g} & \mathbf{a}
\end{bmatrix} \tag{3.10}
$$

The size of the system matrix is $5N_1N_2N_3$ by $5N_1N_2N_3$. There may be some confusion between the system eigenvalues, which are the eigenvalues of the $\mathbf{A}$ matrix, and the local eigenvalues, which are the characteristics of the Jacobians. The local eigenvalues may be positive or negative depending on the flow conditions, but the eigenvalues of a stable continuous time linear model must have negative real parts. Therefore, all the eigenvalues of $\mathbf{A}$ must have negative real parts. The small perturbation model will be stable when the spatial derivatives of equation (2.22) are properly discretized according to the local eigenvalues.

The procedure for the development of the system matrix must be modified when the boundary conditions are taken into consideration. The linearized equations needed for the wall boundary conditions and inflow boundary conditions will be developed below. The linearized equations for the outflow boundary conditions are listed, but their development is detailed in section 3.3.

3.2.1 Wall Boundary Conditions for the System Matrix

The wall boundary conditions are implemented as modifications to the system matrix following the method developed in section 2.3.1. With $i = 2, \cdots, N_1 - 1$, the equations and coefficients are shown below.

$$\frac{\partial \delta \overrightarrow{u}_{i,1,1}}{\partial t} = \mathbf{d}_{i,1,1}\delta \overrightarrow{u}_{i-1,1,1} + \mathbf{a}_{i,1,1}\delta \overrightarrow{u}_{i,1,1} + \mathbf{e}_{i,1,1}\delta \overrightarrow{u}_{i+1,1,1} + \mathbf{c}_{i,1,1}\delta \overrightarrow{u}_{i,2,1} + \mathbf{f}_{i,1,1}\delta \overrightarrow{u}_{i,1,2} \quad (3.11)$$

$$\mathbf{d}_{i,1,1} = \frac{A^+_{i,1,1}}{x_{i,1,1} - x_{i-1,1,1}}$$

$$\mathbf{a}_{i,1,1} = \frac{A^-_{i,1,1}}{x_{i+1,1,1} - x_{i,1,1}} - \frac{A^+_{i,1,1}}{x_{i,1,1} - x_{i-1,1,1}} + \frac{B^-_{i,1,1}}{y_{i,2,1} - y_{i,1,1}} + \frac{C^-_{i,1,1}}{z_{i,1,2} - z_{i,1,1}}$$

$$\mathbf{e}_{i,1,1} = \frac{-A^-_{i,1,1}}{x_{i+1,1,1} - x_{i,1,1}}$$

$$\mathbf{c}_{i,1,1} = \frac{-B^-_{i,1,1}}{y_{i,2,1} - y_{i,1,1}}$$

$$\mathbf{f}_{i,1,1} = \frac{-C^-_{i,1,1}}{z_{i,1,2} - z_{i,1,1}}$$

$$\frac{\partial \delta \overrightarrow{u}_{i,1,k}}{\partial t} = \mathbf{d}_{i,1,k}\delta \overrightarrow{u}_{i-1,1,k} + \mathbf{g}_{i,1,k}\delta \overrightarrow{u}_{i,1,k-1} + \mathbf{a}_{i,1,k}\delta \overrightarrow{u}_{i,1,k} \quad (3.12)$$
$$+\mathbf{e}_{i,1,k}\delta \overrightarrow{u}_{i+1,1,k} + \mathbf{c}_{i,1,k}\delta \overrightarrow{u}_{i,2,k} + \mathbf{f}_{i,1,k}\delta \overrightarrow{u}_{i,1,k+1}, \; k = 2, \cdots, N_3 - 1$$

$$\mathbf{d}_{i,1,k} = \frac{A^+_{i,1,k}}{x_{i,1,k} - x_{i-1,1,k}}$$

$$\mathbf{g}_{i,1,k} = \frac{C^+_{i,1,k}}{z_{i,1,k} - z_{i,1,k-1}}$$

$$\mathbf{a}_{i,1,k} = \frac{A^-_{i,1,k}}{x_{i+1,1,k} - x_{i,1,k}} - \frac{A^+_{i,1,k}}{x_{i,1,k} - x_{i-1,1,k}} + \frac{B^-_{i,1,k}}{y_{i,2,k} - y_{i,1,k}} + \frac{C^-_{i,1,k}}{z_{i,1,k+1} - z_{i,1,k}} - \frac{C^+_{i,1,k}}{z_{i,1,k} - z_{i,1,k-1}}$$

$$\mathbf{e}_{i,1,k} = \frac{-A^-_{i,1,k}}{x_{i+1,1,k} - x_{i,1,k}}$$

$$\mathbf{c}_{i,1,k} = \frac{-B^-_{i,1,k}}{y_{i,2,k} - y_{i,1,k}}$$

$$\mathbf{f}_{i,1,k} = \frac{-C^-_{i,1,k}}{z_{i,1,k+1} - z_{i,1,k}}$$

$$\frac{\partial \delta \overrightarrow{u}_{i,1,N_3}}{\partial t} = \mathbf{d}_{i,1,N_3}\delta \overrightarrow{u}_{i-1,1,N_3} + \mathbf{g}_{i,1,N_3}\delta \overrightarrow{u}_{i,1,N_3-1} + \mathbf{a}_{i,1,N_3}\delta \overrightarrow{u}_{i,1,N_3} + \mathbf{e}_{i,1,N_3}\delta \overrightarrow{u}_{i+1,1,N_3} + \mathbf{c}_{i,1,N_3}\delta \overrightarrow{u}_{i,2,N_3} \tag{3.13}$$

$$\mathbf{d}_{i,1,N_3} = \frac{A^+_{i,1,N_3}}{x_{i,1,N_3} - x_{i-1,1,N_3}}$$

$$\mathbf{g}_{i,1,N_3} = \frac{C^+_{i,1,N_3}}{z_{i,1,N_3} - z_{i,1,N_3-1}}$$

$$\mathbf{a}_{i,1,N_3} = \frac{A^-_{i,1,N_3}}{x_{i+1,1,N_3} - x_{i,1,N_3}} - \frac{A^+_{i,1,N_3}}{x_{i,1,N_3} - x_{i-1,1,N_3}} + \frac{B^-_{i,1,N_3}}{y_{i,2,N_3} - y_{i,1,N_3}} - \frac{C^+_{i,1,N_3}}{z_{i,1,N_3} - z_{i,1,N_3-1}}$$

$$\mathbf{e}_{i,1,N_3} = \frac{-A^-_{i,1,N_3}}{x_{i+1,1,N_3} - x_{i,1,N_3}}$$

$$\mathbf{c}_{i,1,N_3} = \frac{-B^-_{i,1,N_3}}{y_{i,2,N_3} - y_{i,1,N_3}}$$

$$\frac{\partial \delta \overrightarrow{u}_{i,j,1}}{\partial t} = \mathbf{d}_{i,j,1}\delta \overrightarrow{u}_{i-1,j,1} + \mathbf{b}_{i,j,1}\delta \overrightarrow{u}_{i,j-1,1} + \mathbf{a}_{i,j,1}\delta \overrightarrow{u}_{i,j,1} + \mathbf{e}_{i,j,1}\delta \overrightarrow{u}_{i+1,j,1} + \mathbf{c}_{i,j,1}\delta \overrightarrow{u}_{i,j+1,1} + \mathbf{f}_{i,j,1}\delta \overrightarrow{u}_{i,j,2},\ j = 2, \cdots, N_2 - 1 \tag{3.14}$$

$$\mathbf{d}_{i,j,1} = \frac{A^+_{i,j,1}}{x_{i,j,1} - x_{i-1,j,1}}$$

$$\mathbf{b}_{i,j,1} = \frac{B^+_{i,j,1}}{y_{i,j,1} - y_{i,j-1,1}}$$

$$\mathbf{a}_{i,j,1} = \frac{A^-_{i,j,1}}{x_{i+1,j,1} - x_{i,j,1}} - \frac{A^+_{i,j,1}}{x_{i,j,1} - x_{i-1,j,1}} + \frac{B^-_{i,j,1}}{y_{i,j+1,1} - y_{i,j,1}} - \frac{B^+_{i,j,1}}{y_{i,j,1} - y_{i,j-1,1}} + \frac{C^-_{i,j,1}}{z_{i,j,2} - z_{i,j,1}}$$

$$\mathbf{e}_{i,j,1} = \frac{-A^-_{i,j,1}}{x_{i+1,j,1} - x_{i,j,1}}$$

$$\mathbf{c}_{i,j,1} = \frac{-B^-_{i,j,1}}{y_{i,j+1,1} - y_{i,j,1}}$$

$$\mathbf{f}_{i,j,1} = \frac{-C^-_{i,j,1}}{z_{i,j,2} - z_{i,j,1}}$$

$$\frac{\partial \delta \overrightarrow{u}_{i,j,N_3}}{\partial t} = \mathbf{d}_{i,j,N_3}\delta \overrightarrow{u}_{i-1,j,N_3} + \mathbf{b}_{i,j,N_3}\delta \overrightarrow{u}_{i,j-1,N_3} + \mathbf{g}_{i,j,N_3}\delta \overrightarrow{u}_{i,j,N_3-1} + \mathbf{a}_{i,j,N_3}\delta \overrightarrow{u}_{i,j,N_3} + \mathbf{e}_{i,j,N_3}\delta \overrightarrow{u}_{i+1,j,N_3} + \mathbf{c}_{i,j,N_3}\delta \overrightarrow{u}_{i,j+1,N_3},\ j = 2, \cdots, N_2 - 1 \tag{3.15}$$

$$\mathbf{d}_{i,j,N_3} = \frac{A^+_{i,j,N_3}}{x_{i,j,N_3} - x_{i-1,j,N_3}}$$

$$\mathbf{b}_{i,j,N_3} = \frac{B^+_{i,j,N_3}}{y_{i,j,N_3} - y_{i,j-1,N_3}}$$

$$\mathbf{g}_{i,j,N_3} = \frac{C^+_{i,j,N_3}}{z_{i,j,N_3} - z_{i,j,N_3-1}}$$

$$\mathbf{a}_{i,j,N_3} = \frac{A^-_{i,j,N_3}}{x_{i+1,j,N_3} - x_{i,j,N_3}} - \frac{A^+_{i,j,N_3}}{x_{i,j,N_3} - x_{i-1,j,N_3}} + \frac{B^-_{i,j,N_3}}{y_{i,j+1,N_3} - y_{i,j,N_3}} - \frac{B^+_{i,j,N_3}}{y_{i,j,N_3} - y_{i,j-1,N_3}} - \frac{C^+_{i,j,N_3}}{z_{i,j,N_3} - z_{i,j,N_3-1}}$$

$$\mathbf{e}_{i,j,N_3} = \frac{-A^-_{i,j,N_3}}{x_{i+1,j,N_3} - x_{i,j,N_3}}$$

$$\mathbf{c}_{i,j,N_3} = \frac{-B^-_{i,j,N_3}}{y_{i,j+1,N_3} - y_{i,j,N_3}}$$

$$\frac{\partial \delta\overrightarrow{u}_{i,N_2,1}}{\partial t} = \mathbf{d}_{i,N_2,1}\delta\overrightarrow{u}_{i-1,N_2,1} + \mathbf{b}_{i,N_2,1}\delta\overrightarrow{u}_{i,N_2-1,1} + \mathbf{a}_{i,N_2,1}\delta\overrightarrow{u}_{i,N_2,1} + \mathbf{e}_{i,N_2,1}\delta\overrightarrow{u}_{i+1,N_2,1} + \mathbf{f}_{i,N_2,1}\delta\overrightarrow{u}_{i,N_2,2} \tag{3.16}$$

$$\mathbf{d}_{i,N_2,1} = \frac{A^+_{i,N_2,1}}{x_{i,N_2,1} - x_{i-1,N_2,1}}$$

$$\mathbf{b}_{i,N_2,1} = \frac{B^+_{i,N_2,1}}{y_{i,N_2,1} - y_{i,N_2-1,1}}$$

$$\mathbf{a}_{i,N_2,1} = \frac{A^-_{i,N_2,1}}{x_{i+1,N_2,1} - x_{i,N_2,1}} - \frac{A^+_{i,N_2,1}}{x_{i,N_2,1} - x_{i-1,N_2,1}} - \frac{B^+_{i,N_2,1}}{y_{i,N_2,1} - y_{i,N_2-1,1}} + \frac{C^-_{i,N_2,1}}{z_{i,N_2,2} - z_{i,N_2,1}}$$

$$\mathbf{e}_{i,N_2,1} = \frac{-A^-_{i,N_2,1}}{x_{i+1,N_2,1} - x_{i,N_2,1}}$$

$$\mathbf{f}_{i,N_2,1} = \frac{-C^-_{i,N_2,1}}{z_{i,N_2,2} - z_{i,N_2,1}}$$

$$\frac{\partial \delta\overrightarrow{u}_{i,N_2,k}}{\partial t} = \mathbf{d}_{i,N_2,k}\delta\overrightarrow{u}_{i-1,N_2,k} + \mathbf{b}_{i,N_2,k}\delta\overrightarrow{u}_{i,N_2-1,k} + \mathbf{g}_{i,N_2,k}\delta\overrightarrow{u}_{i,N_2,k-1} + \mathbf{a}_{i,N_2,k}\delta\overrightarrow{u}_{i,N_2,k} + \mathbf{e}_{i,N_2,k}\delta\overrightarrow{u}_{i+1,N_2,k} + \mathbf{f}_{i,N_2,k}\delta\overrightarrow{u}_{i,N_2,k+1},\ k = 2, \cdots, N_3 \tag{3.17}$$

$$\mathbf{d}_{i,N_2,k} = \frac{A^+_{i,N_2,k}}{x_{i,N_2,k} - x_{i-1,N_2,k}}$$

$$\mathbf{b}_{i,N_2,k} = \frac{B^+_{i,N_2,k}}{y_{i,N_2,k} - y_{i,N_2-1,k}}$$

$$\mathbf{g}_{i,N_2,k} = \frac{C^+_{i,N_2,k}}{z_{i,N_2,k} - z_{i,N_2,k-1}}$$

$$\mathbf{a}_{i,N_2,k} = \frac{A^-_{i,N_2,k}}{x_{i+1,N_2,k} - x_{i,N_2,k}} - \frac{A^+_{i,N_2,k}}{x_{i,N_2,k} - x_{i-1,N_2,k}} - \frac{B^+_{i,N_2,k}}{y_{i,N_2,k} - y_{i,N_2-1,k}} + \frac{C^-_{i,N_2,k}}{z_{i,N_2,k+1} - z_{i,N_2,k}} - \frac{C^+_{i,N_2,k}}{z_{i,N_2,k} - z_{i,N_2,k-1}}$$

$$\mathbf{e}_{i,N_2,k} = \frac{-A^-_{i,N_2,k}}{x_{i+1,N_2,k} - x_{i,N_2,k}}$$

$$\mathbf{f}_{i,N_2,k} = \frac{-C^-_{i,N_2,k}}{z_{i,N_2,k+1} - z_{i,N_2,k}}$$

$$\frac{\partial \delta\overrightarrow{u}_{i,N_2,N_3}}{\partial t} = \mathbf{d}_{i,N_2,N_3}\delta\overrightarrow{u}_{i-1,N_2,N_3} + \mathbf{b}_{i,N_2,N_3}\delta\overrightarrow{u}_{i,N_2-1,N_3} + \mathbf{g}_{i,N_2,N_3}\delta\overrightarrow{u}_{i,N_2,N_3-1} + \mathbf{a}_{i,N_2,N_3}\delta\overrightarrow{u}_{i,N_2,N_3} + \mathbf{e}_{i,N_2,N_3}\delta\overrightarrow{u}_{i+1,N_2,N_3} \tag{3.18}$$

$$\mathbf{d}_{i,N_2,N_3} = \frac{A^+_{i,N_2,N_3}}{x_{i,N_2,N_3} - x_{i-1,N_2,N_3}}$$

$$\mathbf{b}_{i,N_2,N_3} = \frac{B^+_{i,N_2,N_3}}{y_{i,N_2,N_3} - y_{i,N_2-1,N_3}}$$

$$\mathbf{g}_{i,N_2,N_3} = \frac{C^+_{i,N_2,N_3}}{z_{i,N_2,N_3} - z_{i,N_2,N_3-1}}$$

$$\mathbf{a}_{i,N_2,N_3} = \frac{A^-_{i,N_2,N_3}}{x_{i+1,N_2,N_3} - x_{i,N_2,N_3}} - \frac{A^+_{i,N_2,N_3}}{x_{i,N_2,N_3} - x_{i-1,N_2,N_3}} - \frac{B^+_{i,N_2,N_3}}{y_{i,N_2,N_3} - y_{i,N_2-1,N_3}} - \frac{C^+_{i,N_2,N_3}}{z_{i,N_2,N_3} - z_{i,N_2,N_3-1}}$$

$$\mathbf{e}_{i,N_2,N_3} = \frac{-A^-_{i,N_2,N_3}}{x_{i+1,N_2,N_3} - x_{i,N_2,N_3}}$$

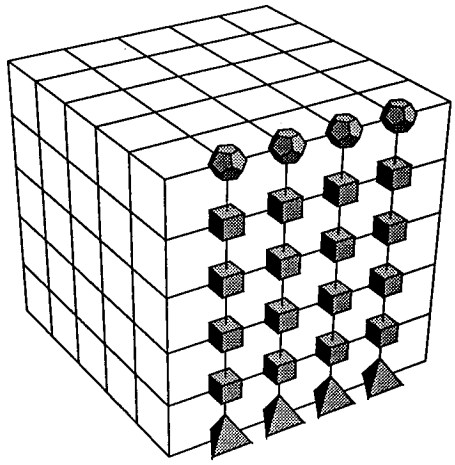

Wall Boundary Conditions

Equation 3.11

Equation 3.12

Equation 3.13

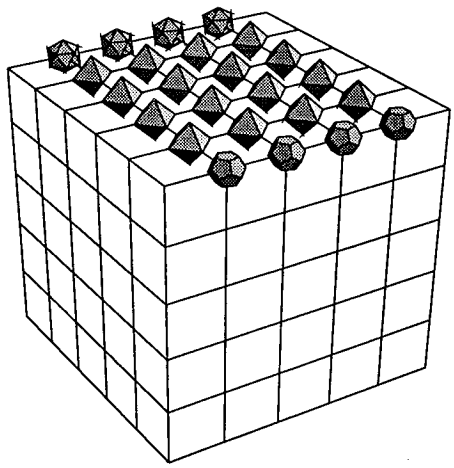

Wall Boundary Conditions

Equation 3.13

Equation 3.15

Equation 3.18

3.2.2 Inflow Boundary Conditions for the System Matrix

The inflow boundary conditions are implemented as modifications to the system matrix following the method developed in section 2.3.2. For this paper, the inflow boundary condition is assumed to be supersonic; therefore, there are five physical boundary conditions and zero numerical boundary conditions [10]. From equation (2.49), the matrices for the supersonic inflow boundary condition become:

$$\begin{aligned} L_1 &= \frac{\partial B_{bc}}{\partial \overrightarrow{u}} \\ L_2 &= 0 \end{aligned} \tag{3.19}$$

and

$$\begin{aligned} \frac{\partial \overrightarrow{u}}{\partial t} &= -L_1^{-1} B_{bc} \\ &= -\left[\frac{\partial B_{bc}}{\partial \overrightarrow{u}}\right]^{-1} B_{bc} \end{aligned} \tag{3.20}$$

with

$$B_{bc} = \begin{bmatrix} \rho \\ m_1 \\ m_2 \\ m_3 \\ \varepsilon \end{bmatrix} \tag{3.21}$$

Equation (3.20) becomes the following when it is linearized:

$$\frac{\partial \delta \overrightarrow{u}}{\partial t} = -\left[\frac{\partial B_{bc}}{\partial \overrightarrow{u}}\right]^{-1} \delta B_{bc} \tag{3.22}$$

If there are no upstream inputs δB_{bc} becomes:

$$\delta B_{bc} = \frac{\partial B_{bc}}{\partial \overrightarrow{u}} \delta \overrightarrow{u} \tag{3.23}$$

and the inflow boundary condition is represented by the following equation:

$$\frac{\partial \delta \overrightarrow{u}_{1,j,k}}{\partial t} = -\delta \overrightarrow{u}_{1,j,k} \tag{3.24}$$

with $j = 1, \cdots, N_2$ and $k = 1, \cdots, N_3$.

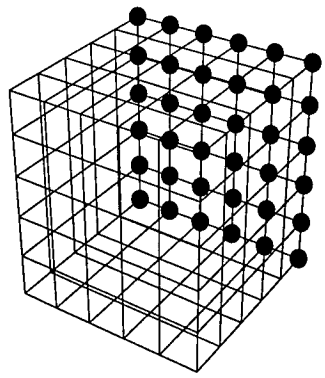

Inflow Boundary Conditions

These boundary conditions are included as modifications to the system matrix at the first grid point in the x-direction.

3.2.3 Outflow Boundary Conditions for the System Matrix

The outflow boundary conditions are also implemented as modifications to the system matrix following the method developed in section 2.3.2. In general, the outflow boundary condition is subsonic; therefore, there are four numerical boundary conditions and one physical boundary condition [10]. The equations for the subsonic outflow boundary condition are as follows:

$$\frac{\partial \delta\overrightarrow{u}_{N_1,1,1}}{\partial t} = \mathbf{d}_{N_1,1,1}\delta\overrightarrow{u}_{N_1-1,1,1} + \mathbf{a}_{N_1,1,1}\delta\overrightarrow{u}_{N_1,1,1} + \mathbf{c}_{N_1,1,1}\delta\overrightarrow{u}_{N_1,2,1} + \mathbf{f}_{N_1,1,1}\delta\overrightarrow{u}_{N_1,1,2} \tag{3.25a}$$

$$\begin{aligned}\frac{\partial \delta\overrightarrow{u}_{N_1,1,k}}{\partial t} &= \mathbf{d}_{N_1,1,k}\delta\overrightarrow{u}_{N_1-1,1,k} + \mathbf{g}_{N_1,1,k}\delta\overrightarrow{u}_{N_1,1,k-1} + \mathbf{a}_{N_1,1,k}\delta\overrightarrow{u}_{N_1,1,k} \\ &\quad + \mathbf{c}_{N_1,1,k}\delta\overrightarrow{u}_{N_1,2,k} + \mathbf{f}_{N_1,1,k}\delta\overrightarrow{u}_{N_1,1,k+1},\ k = 2,\cdots,N_3-1\end{aligned} \tag{3.25b}$$

$$\frac{\partial \delta\overrightarrow{u}_{N_1,1,N_3}}{\partial t} = \mathbf{d}_{N_1,1,N_3}\delta\overrightarrow{u}_{N_1-1,1,N_3} + \mathbf{g}_{N_1,1,N_3}\delta\overrightarrow{u}_{N_1,1,N_3-1} + \mathbf{a}_{N_1,1,N_3}\delta\overrightarrow{u}_{N_1,1,N_3} + \mathbf{c}_{N_1,1,N_3}\delta\overrightarrow{u}_{N_1,2,N_3} \tag{3.25c}$$

$$\begin{aligned}\frac{\partial \delta\overrightarrow{u}_{N_1,j,1}}{\partial t} &= \mathbf{d}_{N_1,j,1}\delta\overrightarrow{u}_{N_1-1,j,1} + \mathbf{b}_{N_1,j,1}\delta\overrightarrow{u}_{N_1,j-1,1} + \mathbf{a}_{N_1,j,1}\delta\overrightarrow{u}_{N_1,j,1} \\ &\quad + \mathbf{c}_{N_1,j,1}\delta\overrightarrow{u}_{N_1,j+1,1} + \mathbf{f}_{N_1,j,1}\delta\overrightarrow{u}_{N_1,j,2},\ j = 2,\cdots,N_2-1\end{aligned} \tag{3.25d}$$

$$\begin{aligned}\frac{\partial \delta\overrightarrow{u}_{N_1,j,k}}{\partial t} &= \mathbf{d}_{N_1,j,k}\delta\overrightarrow{u}_{N_1-1,j,k} + \mathbf{b}_{N_1,j,k}\delta\overrightarrow{u}_{N_1,j-1,k} + \mathbf{g}_{N_1,j,k}\delta\overrightarrow{u}_{N_1,j,k-1} \\ &\quad + \mathbf{a}_{N_1,j,k}\delta\overrightarrow{u}_{N_1,j,k} + \mathbf{c}_{N_1,j,k}\delta\overrightarrow{u}_{N_1,j+1,k} + \mathbf{f}_{N_1,j,k}\delta\overrightarrow{u}_{N_1,j,k+1} \\ &\quad j = 2,\cdots,N_2-1, k = 2,\cdots,N_3-1\end{aligned} \tag{3.25e}$$

$$\begin{aligned}\frac{\partial \delta\overrightarrow{u}_{N_1,j,N_3}}{\partial t} &= \mathbf{d}_{N_1,j,N_3}\delta\overrightarrow{u}_{N_1-1,j,N_3} + \mathbf{b}_{N_1,j,N_3}\delta\overrightarrow{u}_{N_1,j-1,N_3} + \mathbf{g}_{N_1,j,N_3}\delta\overrightarrow{u}_{N_1,j,N_3-1} \\ &\quad + \mathbf{a}_{N_1,j,N_3}\delta\overrightarrow{u}_{N_1,j,N_3} + \mathbf{c}_{N_1,j,N_3}\delta\overrightarrow{u}_{N_1,j+1,N_3},\ j = 2,\cdots,N_2-1\end{aligned} \tag{3.25f}$$

$$\frac{\partial \delta\overrightarrow{u}_{N_1,N_2,1}}{\partial t} = \mathbf{d}_{N_1,N_2,1}\delta\overrightarrow{u}_{N_1-1,N_2,1} + \mathbf{b}_{N_1,N_2,1}\delta\overrightarrow{u}_{N_1,N_2-1,1} + \mathbf{a}_{N_1,N_2,1}\delta\overrightarrow{u}_{N_1,N_2,1} + \mathbf{f}_{N_1,N_2,1}\delta\overrightarrow{u}_{N_1,N_2,2} \tag{3.25g}$$

$$\begin{aligned}\frac{\partial \delta\overrightarrow{u}_{N_1,N_2,k}}{\partial t} &= \mathbf{d}_{N_1,N_2,k}\delta\overrightarrow{u}_{N_1-1,N_2,k} + \mathbf{b}_{N_1,N_2,k}\delta\overrightarrow{u}_{N_1,N_2-1,k} + \mathbf{g}_{N_1,N_2,k}\delta\overrightarrow{u}_{N_1,N_2,k-1} \\ &\quad + \mathbf{a}_{N_1,N_2,k}\delta\overrightarrow{u}_{N_1,N_2,k} + \mathbf{f}_{N_1,N_2,k}\delta\overrightarrow{u}_{N_1,N_2,k+1},\ k = 2,\cdots,N_3-1\end{aligned} \tag{3.25h}$$

$$\begin{aligned}\frac{\partial \delta\overrightarrow{u}_{N_1,N_2,N_3}}{\partial t} &= \mathbf{d}_{N_1,N_2,N_3}\delta\overrightarrow{u}_{N_1-1,N_2,N_3} + \mathbf{b}_{N_1,N_2,N_3}\delta\overrightarrow{u}_{N_1,N_2-1,N_3} + \mathbf{g}_{N_1,N_2,N_3}\delta\overrightarrow{u}_{N_1,N_2,N_3-1} \\ &\quad + \mathbf{a}_{N_1,N_2,N_3}\delta\overrightarrow{u}_{N_1,N_2,N_3}\end{aligned} \tag{3.25i}$$

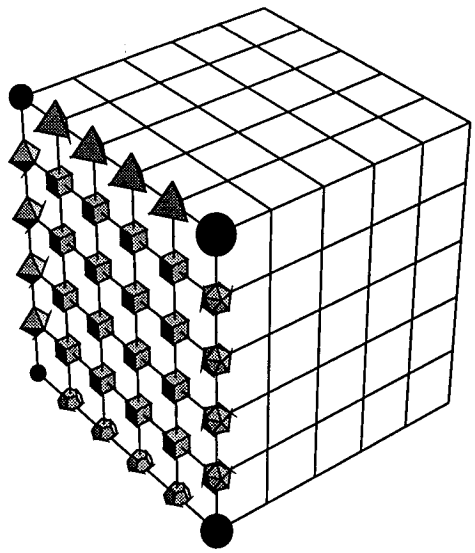

Outflow Boundary Conditions

Equation 3.25a

Equation 3.25b

Equation 3.25c

Equation 3.25d

Equation 3.25e

Equation 3.25f

Equation 3.25g

Equation 3.25h

Equation 3.25i

These boundary conditions are included as modifications to the system matrix at the last grid point in the x-direction. They will be discussed at length in section 3.3 where the coefficients of the equations are defined, and the input matrix, **B**, is derived.

3.3 Input Matrix for Downstream Mach Number

When the flow at the compressor face is subsonic, there are four numerical boundary conditions and one physical boundary condition [10]. The numerical boundary conditions are associated with the positive characteristics, and the physical boundary condition is associated with the negative characteristic. The implementation of the downstream Mach number as a boundary condition input is derived below.

To begin with, take the inverse of (2.25), and then partition the matrix following the procedure from section 2.3.2.

$$K_1^{-1} = \begin{bmatrix} \left(K_1^{-1}\right)^N \\ ---- \\ \left(K_1^{-1}\right)^P \end{bmatrix}^{-1} \tag{3.26}$$

Here, $\left(K_1^{-1}\right)^N$ is the first four rows of K_1^{-1} , and $\left(K_1^{-1}\right)^P$ is the last row of K_1^{-1}. The physical boundary condition equation is:

$$B_{bc} = M - M_{input} \tag{3.27}$$

where M_{input} is the prescribed boundary condition input or set point, and M is defined as:

$$M = \frac{\sqrt{u^2 + v^2 + w^2}}{c} \tag{3.28}$$

If M is rewritten in terms of the state variables ρ, m_1, m_2, m_3, and ε, equation (3.28) becomes the following:

$$M = \frac{\sqrt{2}\sqrt{m_1^2 + m_2^2 + m_3^2}}{\sqrt{\gamma\left(2\varepsilon\rho\left(\gamma - 1\right) - \gamma\left(m_1^2 + m_2^2 + m_3^2\right) + m_1^2 + m_2^2 + m_3^2\right)}} \tag{3.29}$$

Taking the partial derivative of $B_{bc}(\overrightarrow{u})$ with respect to $\overrightarrow{u}$ yields,

$$\frac{\partial B_{bc}}{\partial \overrightarrow{u}} = \begin{bmatrix} \frac{\partial M}{\partial \rho} & \frac{\partial M}{\partial m_1} & \frac{\partial M}{\partial m_2} & \frac{\partial M}{\partial m_3} & \frac{\partial M}{\partial \varepsilon} \end{bmatrix} \tag{3.30}$$

where $\frac{\partial M}{\partial \rho}$, $\frac{\partial M}{\partial m_1}$, $\frac{\partial M}{\partial m_2}$, $\frac{\partial M}{\partial m_3}$, and $\frac{\partial M}{\partial \varepsilon}$ are shown below.

$$\begin{aligned}
\frac{\partial M}{\partial \rho} &= \frac{\sqrt{2}\sqrt{m_1^2 + m_2^2 + m_3^2}\left(\varepsilon - \rho\overrightarrow{v}^2\right)\sqrt{\frac{\gamma\left(2\varepsilon\left(\gamma - 1\right) - \gamma\rho\overrightarrow{v}^2\right) + \rho\overrightarrow{v}^2}{\rho}}}{\gamma\left(2\varepsilon - \rho\overrightarrow{v}^2\right)^2\left(1 - \gamma\right)|\rho|} \\
\frac{\partial M}{\partial m_1} &= \frac{\sqrt{2}m_1\sqrt{\frac{\gamma\left(2\varepsilon\left(\gamma - 1\right) - \gamma\rho\overrightarrow{v}^2\right) + \rho\overrightarrow{v}^2}{\rho}}\operatorname{sgn}\left(\rho\right)}{\gamma\left(2\varepsilon - \rho\overrightarrow{v}^2\right)\left(\gamma - 1\right)\sqrt{m_1^2 + m_2^2 + m_3^2}} \\
\frac{\partial M}{\partial m_2} &= \frac{\sqrt{2}m_2\sqrt{\frac{\gamma\left(2\varepsilon\left(\gamma - 1\right) - \gamma\rho\overrightarrow{v}^2\right) + \rho\overrightarrow{v}^2}{\rho}}\operatorname{sgn}\left(\rho\right)}{\gamma\left(2\varepsilon - \rho\overrightarrow{v}^2\right)\left(\gamma - 1\right)\sqrt{m_1^2 + m_2^2 + m_3^2}} \\
\frac{\partial M}{\partial m_3} &= \frac{\sqrt{2}m_3\sqrt{\frac{\gamma\left(2\varepsilon\left(\gamma - 1\right) - \gamma\rho\overrightarrow{v}^2\right) + \rho\overrightarrow{v}^2}{\rho}}\operatorname{sgn}\left(\rho\right)}{\gamma\left(2\varepsilon - \rho\overrightarrow{v}^2\right)\left(\gamma - 1\right)\sqrt{m_1^2 + m_2^2 + m_3^2}} \\
\frac{\partial M}{\partial \varepsilon} &= \frac{\sqrt{2}\sqrt{m_1^2 + m_2^2 + m_3^2}\sqrt{\frac{\gamma\left(2\varepsilon\left(\gamma - 1\right) - \gamma\rho\overrightarrow{v}^2\right) + \rho\overrightarrow{v}^2}{\rho}}\operatorname{sgn}\left(\rho\right)}{\gamma\left(2\varepsilon - \rho\overrightarrow{v}^2\right)^2\left(1 - \gamma\right)}
\end{aligned} \tag{3.31}$$

Therefore, for the downstream Mach number boundary condition, L_1 is defined as:

$$L_1 = \begin{bmatrix} \left(K_1^{-1}\right)^N \\ ---- \\ \frac{\partial B_{bc}}{\partial \overrightarrow{u}} \end{bmatrix} \tag{3.32}$$

and L_2 is defined as:

$$L_2 = \begin{bmatrix} \left(K_1^{-1}\right)^N \\ ---- \\ 0 \end{bmatrix} \tag{3.33}$$

From equation (2.48), the compressor face boundary condition may be written as follows.

$$\frac{\partial \overrightarrow{u}_{N_1,j,k}}{\partial t} + L_1^{-1} L_2 \left(A_{N_1,j,k} \frac{\partial \overrightarrow{u}_{N_1,j,k}}{\partial x} + B_{N_1,j,k} \frac{\partial \overrightarrow{u}_{N_1,j,k}}{\partial y} + C_{N_1,j,k} \frac{\partial \overrightarrow{u}_{N_1,j,k}}{\partial z} \right) = L_1^{-1} \begin{bmatrix} 0 \\ -B_{bc} \end{bmatrix} \tag{3.34}$$

For this boundary condition to be implemented in the small perturbation model, it must be linearized as shown below.

$$\frac{\partial \delta\overrightarrow{u}_{N_1,j,k}}{\partial t} + L_1^{-1} L_2 \left(A_{N_1,j,k} \frac{\partial \delta\overrightarrow{u}_{N_1,j,k}}{\partial x} + B_{N_1,j,k} \frac{\partial \delta\overrightarrow{u}_{N_1,j,k}}{\partial y} + C_{N_1,j,k} \frac{\partial \delta\overrightarrow{u}_{N_1,j,k}}{\partial z} \right) = L_1^{-1} \begin{bmatrix} 0 \\ -\delta B_{bc} \end{bmatrix} \tag{3.35}$$

δB_{bc} is calculated as:

$$\delta B_{bc} = \frac{\partial B_{bc}}{\partial \overrightarrow{u}} \delta\overrightarrow{u} + \frac{\partial B_{bc}}{\partial M_{input}} \delta M_{input} \tag{3.36}$$

and can be rewritten as:

$$\delta B_{bc} = \begin{bmatrix} \frac{\partial M}{\partial \rho} & \frac{\partial M}{\partial m_1} & \frac{\partial M}{\partial m_2} & \frac{\partial M}{\partial m_3} & \frac{\partial M}{\partial \varepsilon} \end{bmatrix} \delta\overrightarrow{u} - \delta M_{input} \tag{3.37}$$

Now substituting equation (3.37) into equation (3.35) and replacing $\frac{\partial \delta\overrightarrow{u}_{N_1,j,k}}{\partial x}$ with equation (2.31) yields:

$$\begin{aligned} \frac{\partial \delta\overrightarrow{u}_{N_1,j,k}}{\partial t} \quad = \quad & -L_1^{-1} L_2 A_{N_1,j,k} \left(\frac{\delta\overrightarrow{u}_{N_1,j,k} - \delta\overrightarrow{u}_{N_1-1,j,k}}{x_{N_1,j,k} - x_{N_1-1,j,k}} \right) \\ & -L_1^{-1} L_2 B_{N_1,j,k} \frac{\partial \delta\overrightarrow{u}_{N_1,j,k}}{\partial y} - L_1^{-1} L_2 C_{N_1,j,k} \frac{\partial \delta\overrightarrow{u}_{N_1,j,k}}{\partial z} \\ & -L_1^{-1} \begin{bmatrix} & 0_{4\times 5} & \\ \frac{\partial M}{\partial \rho} & \frac{\partial M}{\partial m_1} & \frac{\partial M}{\partial m_2} & \frac{\partial M}{\partial m_3} & \frac{\partial M}{\partial \varepsilon} \end{bmatrix} \delta\overrightarrow{u}_{N_1,j,k} \\ & +L_1^{-1} \begin{bmatrix} 0 & 0 & 0 & 0 & 1 \end{bmatrix}^T \delta M_{input} \end{aligned} \tag{3.38}$$

this can be rewritten as the following:

$$\begin{aligned}
\frac{\partial \delta\overrightarrow{u}_{N_1,j,k}}{\partial t} &= L_1^{-1}L_2\left(-\frac{A_{N_1,j,k}}{x_{N_1,j,k}-x_{N_1-1,j,k}}\delta\overrightarrow{u}_{N_1,j,k}+\frac{A_{N_1,j,k}}{x_{N_1,j,k}-x_{N_1-1,j,k}}\delta\overrightarrow{u}_{N_1-1,j,k}\right.\\
&+\frac{B^+_{N_1,j,k}}{y_{N_1,j,k}-y_{N_1,j-1,k}}\delta\overrightarrow{u}_{N_1,j-1,k}-\left(\frac{B^+_{N_1,j,k}}{y_{N_1,j,k}-y_{N_1,j-1,k}}-\frac{B^-_{N_1,j,k}}{y_{N_1,j+1,k}-y_{N_1,j,k}}\right)\delta\overrightarrow{u}_{N_1,j,k}\\
&-\frac{B^-_{N_1,j,k}}{y_{N_1,j+1,k}-y_{N_1,j,k}}\delta\overrightarrow{u}_{N_1,j+1,k}+\frac{C^+_{N_1,j,k}}{z_{N_1,j,k}-z_{N_1,j,k-1}}\delta\overrightarrow{u}_{N_1,j,k-1} \qquad (3.39)\\
&\left.-\left(\frac{C^+_{N_1,j,k}}{z_{N_1,j,k}-z_{N_1,j,k-1}}-\frac{C^-_{N_1,j,k}}{z_{N_1,j,k+1}-z_{N_1,j,k}}\right)\delta\overrightarrow{u}_{N_1,j,k}-\frac{C^-_{N_1,j,k}}{z_{N_1,j,k+1}-z_{N_1,j,k}}\delta\overrightarrow{u}_{N_1,j,k+1}\right)\\
&-L_1^{-1}\begin{bmatrix}0_{4\times5}\\ \dfrac{\partial B_{bc}}{\partial\overrightarrow{u}}\end{bmatrix}\delta\overrightarrow{u}_{N_1,j,k}+L_1^{-1}\begin{bmatrix}0&0&0&0&1\end{bmatrix}^T\delta M_{input}
\end{aligned}$$

The terms for the input matrix, $\mathbf{B}$, are obtained from the coefficient on δM_{input}. Equations (3.40) through (3.48) are used to modify the system matrix, (3.10).

$$\frac{\partial \delta\overrightarrow{u}_{N_1,1,1}}{\partial t} = \mathbf{d}_{N_1,1,1}\delta\overrightarrow{u}_{N_1-1,1,1}+\mathbf{a}_{N_1,1,1}\delta\overrightarrow{u}_{N_1,1,1}+\mathbf{c}_{N_1,1,1}\delta\overrightarrow{u}_{N_1,2,1}+\mathbf{f}_{N_1,1,1}\delta\overrightarrow{u}_{N_1,1,2} \qquad (3.40)$$

$$\mathbf{d}_{N_1,1,1} = L_1^{-1}L_2\left(\frac{A_{N_1,1,1}}{x_{N_1,1,1}-x_{N_1-1,1,1}}\right)$$

$$\mathbf{a}_{N_1,1,1} = L_1^{-1}L_2\left(-\frac{A_{N_1,1,1}}{x_{N_1,1,1}-x_{N_1-1,1,1}}+\frac{B^-_{N_1,1,1}}{y_{N_1,2,1}-y_{N_1,1,1}}+\frac{C^-_{N_1,1,1}}{z_{N_1,1,2}-z_{N_1,1,1}}\right)-L_1^{-1}\begin{bmatrix}0_{4\times5}\\ \dfrac{\partial B_{bc}}{\partial\overrightarrow{u}}\end{bmatrix}$$

$$\mathbf{c}_{N_1,1,1} = -L_1^{-1}L_2\left(\frac{B^-_{N_1,1,1}}{y_{N_1,2,1}-y_{N_1,1,1}}\right)$$

$$\mathbf{f}_{N_1,1,1} = -L_1^{-1}L_2\left(\frac{C^-_{N_1,1,1}}{z_{N_1,1,2}-z_{N_1,1,1}}\right)$$

$$\begin{aligned}
\frac{\partial \delta\overrightarrow{u}_{N_1,1,k}}{\partial t} &= \mathbf{d}_{N_1,1,k}\delta\overrightarrow{u}_{N_1-1,1,k}+\mathbf{g}_{N_1,1,k}\delta\overrightarrow{u}_{N_1,1,k-1}+\mathbf{a}_{N_1,1,k}\delta\overrightarrow{u}_{N_1,1,k} \qquad (3.41)\\
&+\mathbf{c}_{N_1,1,k}\delta\overrightarrow{u}_{N_1,2,k}+\mathbf{f}_{N_1,1,k}\delta\overrightarrow{u}_{N_1,1,k+1},\ k=2,\cdots,N_3-1
\end{aligned}$$

$$\mathbf{d}_{N_1,1,k} = L_1^{-1}L_2\left(\frac{A_{N_1,1,k}}{x_{N_1,1,k}-x_{N_1-1,1,k}}\right)$$

$$\mathbf{g}_{N_1,1,k} = L_1^{-1}L_2\left(\frac{C^+_{N_1,1,k}}{z_{N_1,1,k}-z_{N_1,1,k-1}}\right)$$

$$
\begin{aligned}
\mathbf{a}_{N_1,1,k} &= L_1^{-1}L_2\left(-\frac{A_{N_1,1,k}}{x_{N_1,1,k}-x_{N_1-1,1,k}}+\frac{B^-_{N_1,1,k}}{y_{N_1,2,k}-y_{N_1,1,k}}\right.\\
&\quad\left.-\frac{C^+_{N_1,1,k}}{z_{N_1,1,k}-z_{N_1,1,k-1}}+\frac{C^-_{N_1,1,k}}{z_{N_1,1,k+1}-z_{N_1,1,k}}\right)-L_1^{-1}\begin{bmatrix}0_{4\times5}\\ \dfrac{\partial B_{bc}}{\partial\overrightarrow{u}}\end{bmatrix}\\
\mathbf{c}_{N_1,1,k} &= -L_1^{-1}L_2\left(\frac{B^-_{N_1,1,k}}{y_{N_1,2,k}-y_{N_1,1,k}}\right)\\
\mathbf{f}_{N_1,1,k} &= -L_1^{-1}L_2\left(\frac{C^-_{N_1,1,k}}{z_{N_1,1,k+1}-z_{N_1,1,k}}\right)
\end{aligned}
$$

$$
\begin{aligned}
\frac{\partial\delta\overrightarrow{u}_{N_1,1,N_3}}{\partial t} &= \mathbf{d}_{N_1,1,N_3}\delta\overrightarrow{u}_{N_1-1,1,N_3}+\mathbf{g}_{N_1,1,N_3}\delta\overrightarrow{u}_{N_1,1,N_3-1}\\
&\quad+\mathbf{a}_{N_1,1,N_3}\delta\overrightarrow{u}_{N_1,1,N_3}+\mathbf{c}_{N_1,1,N_3}\delta\overrightarrow{u}_{N_1,2,N_3}
\end{aligned}
\tag{3.42}
$$

$$
\begin{aligned}
\mathbf{d}_{N_1,1,N_3} &= L_1^{-1}L_2\left(\frac{A_{N_1,1,N_3}}{x_{N_1,1,N_3}-x_{N_1-1,1,N_3}}\right)\\
\mathbf{g}_{N_1,1,N_3} &= L_1^{-1}L_2\left(\frac{C^+_{N_1,1,N_3}}{z_{N_1,1,N_3}-z_{N_1,1,N_3-1}}\right)\\
\mathbf{a}_{N_1,1,N_3} &= L_1^{-1}L_2\left(-\frac{A_{N_1,1,N_3}}{x_{N_1,1,N_3}-x_{N_1-1,1,N_3}}+\frac{B^-_{N_1,1,N_3}}{y_{N_1,2,N_3}-y_{N_1,1,N_3}}\right.\\
&\quad\left.-\frac{C^+_{N_1,1,N_3}}{z_{N_1,1,N_3}-z_{N_1,1,N_3-1}}\right)-L_1^{-1}\begin{bmatrix}0_{4\times5}\\ \dfrac{\partial B_{bc}}{\partial\overrightarrow{u}}\end{bmatrix}\\
\mathbf{c}_{N_1,1,N_3} &= -L_1^{-1}L_2\left(\frac{B^-_{N_1,1,N_3}}{y_{N_1,2,N_3}-y_{N_1,1,N_3}}\right)
\end{aligned}
$$

$$
\begin{aligned}
\frac{\partial\delta\overrightarrow{u}_{N_1,j,1}}{\partial t} &= \mathbf{d}_{N_1,j,1}\delta\overrightarrow{u}_{N_1-1,j,1}+\mathbf{b}_{N_1,j,1}\delta\overrightarrow{u}_{N_1,j-1,1}+\mathbf{a}_{N_1,j,1}\delta\overrightarrow{u}_{N_1,j,1}\\
&\quad+\mathbf{c}_{N_1,j,1}\delta\overrightarrow{u}_{N_1,j+1,1}+\mathbf{f}_{N_1,j,1}\delta\overrightarrow{u}_{N_1,j,2},\ j=2,\cdots,N_2-1
\end{aligned}
\tag{3.43}
$$

$$
\begin{aligned}
\mathbf{d}_{N_1,j,1} &= L_1^{-1}L_2\left(\frac{A_{N_1,j,1}}{x_{N_1,j,1}-x_{N_1-1,j,1}}\right)\\
\mathbf{b}_{N_1,j,1} &= L_1^{-1}L_2\left(\frac{B^+_{N_1,j,1}}{y_{N_1,j,1}-y_{N_1,j-1,1}}\right)\\
\mathbf{a}_{N_1,j,1} &= L_1^{-1}L_2\left(-\frac{A_{N_1,j,1}}{x_{N_1,j,1}-x_{N_1-1,j,1}}-\frac{B^+_{N_1,j,1}}{y_{N_1,j,1}-y_{N_1,j-1,1}}\right.\\
&\quad\left.-\frac{B^-_{N_1,j,1}}{y_{N_1,j+1,1}-y_{N_1,j,1}}+\frac{C^-_{N_1,j,1}}{z_{N_1,j,2}-z_{N_1,j,1}}\right)-L_1^{-1}\begin{bmatrix}0_{4\times5}\\ \dfrac{\partial B_{bc}}{\partial\overrightarrow{u}}\end{bmatrix}
\end{aligned}
$$

$$\mathbf{c}_{N_1,j,1} = -L_1^{-1}L_2\left(\frac{B^-_{N_1,j,1}}{y_{N_1,j+1,1}-y_{N_1,j,1}}\right)$$

$$\mathbf{f}_{N_1,j,1} = -L_1^{-1}L_2\left(\frac{C^-_{N_1,j,1}}{z_{N_1,j,2}-z_{N_1,j,1}}\right)$$

$$\frac{\partial \delta\overrightarrow{u}_{N_1,j,k}}{\partial t} = \mathbf{d}_{N_1,j,k}\overrightarrow{u}_{N_1-1,j,k} + \mathbf{b}_{N_1,j,k}\overrightarrow{u}_{N_1,j-1,k} + \mathbf{g}_{N_1,j,k}\overrightarrow{u}_{N_1,j,k-1} + \mathbf{a}_{N_1,j,k}\overrightarrow{u}_{N_1,j,k} \quad (3.44)$$
$$+\mathbf{c}_{N_1,j,k}\overrightarrow{u}_{N_1,j+1,k} + \mathbf{f}_{N_1,j,k}\overrightarrow{u}_{N_1,j,k+1},\ j=2,\cdots,N_2-1, k=2,\cdots,N_3-1$$

$$\mathbf{d}_{N_1,j,k} = L_1^{-1}L_2\left(\frac{A_{N_1,j,k}}{x_{N_1,j,k}-x_{N_1-1,j,k}}\right)$$

$$\mathbf{b}_{N_1,j,k} = L_1^{-1}L_2\left(\frac{B^+_{N_1,j,k}}{y_{N_1,j,k}-y_{N_1,j-1,k}}\right)$$

$$\mathbf{g}_{N_1,j,k} = L_1^{-1}L_2\left(\frac{C^+_{N_1,j,k}}{z_{N_1,j,k}-z_{N_1,j,k-1}}\right)$$

$$\mathbf{a}_{N_1,j,k} = L_1^{-1}L_2\left(-\frac{A_{N_1,j,k}}{x_{N_1,j,k}-x_{N_1-1,j,k}} - \frac{B^+_{N_1,j,k}}{y_{N_1,j,k}-y_{N_1,j-1,k}} + \frac{B^-_{N_1,j,k}}{y_{N_1,j+1,k}-y_{N_1,j,k}}\right.$$
$$\left. - \frac{C^+_{N_1,j,k}}{z_{N_1,j,k}-z_{N_1,j,k-1}} + \frac{C^-_{N_1,j,k}}{z_{N_1,j,k+1}-z_{N_1,j,k}}\right) - L_1^{-1}\begin{bmatrix} 0_{4\times 5} \\ \dfrac{\partial B_{bc}}{\partial \overrightarrow{u}} \end{bmatrix}$$

$$\mathbf{c}_{N_1,j,k} = -L_1^{-1}L_2\left(\frac{B^-_{N_1,j,k}}{y_{N_1,j+1,k}-y_{N_1,j,k}}\right)$$

$$\mathbf{f}_{N_1,j,k} = -L_1^{-1}L_2\left(\frac{C^-_{N_1,j,k}}{z_{N_1,j,k+1}-z_{N_1,j,k}}\right)$$

$$\frac{\partial \overrightarrow{u}_{N_1,j,N_3}}{\partial t} = \mathbf{d}_{N_1,j,N_3}\delta\overrightarrow{u}_{N_1-1,j,N_3} + \mathbf{b}_{N_1,j,N_3}\delta\overrightarrow{u}_{N_1,j-1,N_3} + \mathbf{g}_{N_1,j,N_3}\delta\overrightarrow{u}_{N_1,j,N_3-1} \quad (3.45)$$
$$+\mathbf{a}_{N_1,j,N_3}\delta\overrightarrow{u}_{N_1,j,N_3} + \mathbf{c}_{N_1,j,N_3}\delta\overrightarrow{u}_{N_1,j+1,N_3},\ j=2,\cdots,N_2-1$$

$$\mathbf{d}_{N_1,j,N_3} = L_1^{-1}L_2\left(\frac{A_{N_1,j,N_3}}{x_{N_1,j,N_3}-x_{N_1-1,j,N_3}}\right)$$

$$\mathbf{b}_{N_1,j,N_3} = L_1^{-1}L_2\left(\frac{B^+_{N_1,j,N_3}}{y_{N_1,j,N_3}-y_{N_1,j-1,N_3}}\right)$$

$$\mathbf{g}_{N_1,j,N_3} = L_1^{-1}L_2\left(\frac{C^+_{N_1,j,N_3}}{z_{N_1,j,N_3}-z_{N_1,j,N_3-1}}\right)$$

$$\mathbf{a}_{N_1,j,N_3} = L_1^{-1}L_2\left(-\frac{A_{N_1,j,N_3}}{x_{N_1,j,N_3}-x_{N_1-1,j,N_3}} - \frac{B^+_{N_1,j,N_3}}{y_{N_1,j,N_3}-y_{N_1,j-1,N_3}}\right.$$
$$\left. + \frac{B^-_{N_1,j,N_3}}{y_{N_1,j+1,N_3}-y_{N_1,j,N_3}} - \frac{C^+_{N_1,j,N_3}}{z_{N_1,j,N_3}-z_{N_1,j,N_3-1}}\right) - L_1^{-1}\begin{bmatrix} 0_{4\times 5} \\ \dfrac{\partial B_{bc}}{\partial \overrightarrow{u}} \end{bmatrix}$$

$$\mathbf{c}_{N_1,j,N_3} = -L_1^{-1}L_2\left(\frac{B^-_{N_1,j,N_3}}{y_{N_1,j+1,N_3}-y_{N_1,j,N_3}}\right)$$

$$\begin{aligned}\frac{\partial \delta\overrightarrow{u}_{N_1,N_2,1}}{\partial t} &= \mathbf{d}_{N_1,N_2,1}\delta\overrightarrow{u}_{N_1-1,N_2,1}+\mathbf{b}_{N_1,N_2,1}\delta\overrightarrow{u}_{N_1,N_2-1,1} \\ &\quad +\mathbf{a}_{N_1,N_2,1}\delta\overrightarrow{u}_{N_1,N_2,1}+\mathbf{f}_{N_1,N_2,1}\delta\overrightarrow{u}_{N_1,N_2,2}\end{aligned} \tag{3.46}$$

$$\mathbf{d}_{N_1,N_2,1} = L_1^{-1}L_2\left(\frac{A_{N_1,N_2,1}}{x_{N_1,N_2,1}-x_{N_1-1,N_2,1}}\right)$$

$$\mathbf{b}_{N_1,N_2,1} = L_1^{-1}L_2\left(\frac{B^+_{N_1,N_2,1}}{y_{N_1,N_2,1}-y_{N_1,N_2-1,1}}\right)$$

$$\begin{aligned}\mathbf{a}_{N_1,N_2,1} &= L_1^{-1}L_2\left(-\frac{A_{N_1,N_2,1}}{x_{N_1,N_2,1}-x_{N_1-1,N_2,1}}-\frac{B^+_{N_1,N_2,1}}{y_{N_1,N_2,1}-y_{N_1,N_2-1,1}}\right. \\ &\quad \left.+\frac{C^-_{N_1,N_2,1}}{z_{N_1,N_2,2}-z_{N_1,N_2,1}}\right)-L_1^{-1}\begin{bmatrix}0_{4\times 5}\\ \dfrac{\partial B_{bc}}{\partial \overrightarrow{u}}\end{bmatrix}\end{aligned}$$

$$\mathbf{f}_{N_1,N_2,1} = -L_1^{-1}L_2\left(\frac{C^-_{N_1,N_2,1}}{z_{N_1,N_2,2}-z_{N_1,N_2,1}}\right)$$

$$\begin{aligned}\frac{\partial \delta\overrightarrow{u}_{N_1,N_2,k}}{\partial t} &= \mathbf{d}_{N_1,N_2,k}\delta\overrightarrow{u}_{N_1-1,N_2,k}+\mathbf{b}_{N_1,N_2,k}\delta\overrightarrow{u}_{N_1,N_2-1,k}+\mathbf{g}_{N_1,N_2,k}\delta\overrightarrow{u}_{N_1,N_2,k-1} \\ &\quad +\mathbf{a}_{N_1,N_2,k}\delta\overrightarrow{u}_{N_1,N_2,k}+\mathbf{f}_{N_1,N_2,k}\delta\overrightarrow{u}_{N_1,N_2,k+1},\ k=2,\cdots,N_3-1\end{aligned} \tag{3.47}$$

$$\mathbf{d}_{N_1,N_2,k} = L_1^{-1}L_2\left(\frac{A_{N_1,N_2,k}}{x_{N_1,N_2,k}-x_{N_1-1,N_2,k}}\right)$$

$$\mathbf{b}_{N_1,N_2,k} = L_1^{-1}L_2\left(\frac{B^+_{N_1,N_2,k}}{y_{N_1,N_2,k}-y_{N_1,N_2-1,k}}\right)$$

$$\mathbf{g}_{N_1,N_2,k} = L_1^{-1}L_2\left(\frac{C^+_{N_1,N_2,k}}{z_{N_1,N_2,k}-z_{N_1,N_2,k-1}}\right)$$

$$\begin{aligned}\mathbf{a}_{N_1,N_2,k} &= L_1^{-1}L_2\left(-\frac{A_{N_1,N_2,k}}{x_{N_1,N_2,k}-x_{N_1-1,N_2,k}}-\frac{B^+_{N_1,N_2,k}}{y_{N_1,N_2,k}-y_{N_1,N_2-1,k}}\right. \\ &\quad \left.-\frac{C^+_{N_1,N_2,k}}{z_{N_1,N_2,k}-z_{N_1,N_2,k-1}}+\frac{C^-_{N_1,N_2,k}}{z_{N_1,N_2,k+1}-z_{N_1,N_2,k}}\right)-L_1^{-1}\begin{bmatrix}0_{4\times 5}\\ \dfrac{\partial B_{bc}}{\partial \overrightarrow{u}}\end{bmatrix}\end{aligned}$$

$$\mathbf{f}_{N_1,N_2,k} = -L_1^{-1}L_2\left(\frac{C^-_{N_1,N_2,k}}{z_{N_1,N_2,k+1}-z_{N_1,N_2,k}}\right)$$

$$
\begin{aligned}
\frac{\partial \delta \overrightarrow{u}_{N_1,N_2,N_3}}{\partial t} &= \mathbf{d}_{N_1,N_2,N_3}\delta \overrightarrow{u}_{N_1-1,N_2,N_3} + \mathbf{b}_{N_1,N_2,N_3}\delta \overrightarrow{u}_{N_1,N_2-1,N_3} \\
&\quad + \mathbf{g}_{N_1,N_2,N_3}\delta \overrightarrow{u}_{N_1,N_2,N_3-1} + \mathbf{a}_{N_1,N_2,N_3}\delta \overrightarrow{u}_{N_1,N_2,N_3} \qquad (3.48)
\end{aligned}
$$

$$
\begin{aligned}
\mathbf{d}_{N_1,N_2,N_3} &= L_1^{-1} L_2 \left(\frac{A_{N_1,N_2,N_3}}{x_{N_1,N_2,N_3} - x_{N_1-1,N_2,N_3}} \right) \\
\mathbf{b}_{N_1,N_2,N_3} &= L_1^{-1} L_2 \left(\frac{B^+_{N_1,N_2,N_3}}{y_{N_1,N_2,N_3} - y_{N_1,N_2-1,N_3}} \right) \\
\mathbf{g}_{N_1,N_2,N_3} &= L_1^{-1} L_2 \left(\frac{C^+_{N_1,N_2,N_3}}{z_{N_1,N_2,N_3} - z_{N_1,N_2,N_3-1}} \right) \\
\mathbf{a}_{N_1,N_2,N_3} &= L_1^{-1} L_2 \left(-\frac{A_{N_1,N_2,N_3}}{x_{N_1,N_2,N_3} - x_{N_1-1,N_2,N_3}} - \frac{B^+_{N_1,N_2,N_3}}{y_{N_1,N_2,N_3} - y_{N_1,N_2-1,N_3}} \right. \\
&\quad \left. - \frac{C^+_{N_1,N_2,N_3}}{z_{N_1,N_2,N_3} - z_{N_1,N_2,N_3-1}} \right) - L_1^{-1} \begin{bmatrix} 0_{4\times 5} \\ \dfrac{\partial B_{bc}}{\partial \overrightarrow{u}} \end{bmatrix}
\end{aligned}
$$

3.4 Output Matrix

The outputs for the linearized inlet model are static pressure, total pressure, and Mach number. For an input located at the compressor face, these outputs are located downstream of the normal shock. Outputs upstream of the normal shock remain unaffected by a downstream disturbance, therefore they do not need to be considered.

3.4.1 Static Pressure

The components of the output matrix, $\mathbf{C}$, for the static pressure response are obtained by linearizing the static pressure equation:

$$
\begin{aligned}
p &= (\gamma - 1)\left(\varepsilon - \frac{m_1^2 + m_2^2 + m_3^2}{2\rho} \right) \\
\delta p &= \frac{\partial p}{\partial \rho}\delta\rho + \frac{\partial p}{\partial m_1}\delta m_1 + \frac{\partial p}{\partial m_2}\delta m_2 + \frac{\partial p}{\partial m_3}\delta m_3 + \frac{\partial p}{\partial \varepsilon}\delta\varepsilon \qquad (3.49) \\
\delta p &= \frac{1}{2}(\gamma - 1)\left(\frac{m_1^2 + m_2^2 + m_3^2}{\rho^2} \right)\delta\rho - (\gamma - 1)\left(\frac{m_1}{\rho^2} \right)\delta m_1 - (\gamma - 1)\left(\frac{m_2}{\rho^2} \right)\delta m_2 \\
&\quad - (\gamma - 1)\left(\frac{m_3}{\rho^2} \right)\delta m_3 + (\gamma - 1)\,\delta\varepsilon
\end{aligned}
$$

Each coefficient of the small perturbation terms is an entry in the output matrix.

3.4.2 Total Pressure

The output equation for the total pressure is determined in the same manner as for the static pressure. The components of the output matrix for the total pressure response are obtained from the linearization of

the total pressure equation:

$$p_t = p\left(1 + \frac{\gamma - 1}{2} M^2\right)^{\frac{\gamma}{\gamma - 1}} \tag{3.50}$$

The pressure and Mach number terms are replaced with expressions in terms of ρ, m_1, m_2, m_3, and ε,

$$p_t = \frac{(\gamma - 1)\left(2\varepsilon\gamma\rho + \left(m_1^2 + m_2^2 + m_3^2\right)(1 - \gamma)\right)\left(\frac{2\varepsilon\gamma\rho + \left(m_1^2 + m_2^2 + m_3^2\right)(1 - \gamma)}{\gamma\left(2\varepsilon\rho - m_1^2 - m_2^2 - m_3^2\right)}\right)^{\frac{1}{\gamma - 1}}}{2\gamma\rho} \tag{3.51}$$

Then the total pressure differential is calculated as shown below.

$$\delta p_t = \frac{\partial p_t}{\partial \rho}\delta\rho + \frac{\partial p_t}{\partial m_1}\delta m_1 + \frac{\partial p_t}{\partial m_2}\delta m_2 + \frac{\partial p_t}{\partial m_3}\delta m_3 + \frac{\partial p_t}{\partial \varepsilon}\delta\varepsilon \tag{3.52}$$

Each one of the coefficients in the small perturbation terms of the above equation is an entry in the output matrix for the total pressure.

$$\begin{aligned}
\frac{\partial p_t}{\partial \rho} &= \frac{\overrightarrow{v}^2\left(2\varepsilon\gamma(\gamma - 2) - \rho\overrightarrow{v}^2\left(\gamma^2 - 4\gamma + 1\right)\right)\left(\frac{2\varepsilon\gamma + \rho\overrightarrow{v}^2(1 - \gamma)}{\gamma(2\varepsilon - \rho\overrightarrow{v}^2)}\right)^{\frac{1}{\gamma - 1}}}{2\gamma(2\varepsilon - \rho\overrightarrow{v}^2)} \\
\frac{\partial p_t}{\partial m_1} &= \frac{u\left(\rho\overrightarrow{v}^2\left(\gamma^2 - 3\gamma + 1\right) - 2\varepsilon\gamma(\gamma - 2)\right)\left(\frac{2\varepsilon\gamma + \rho\overrightarrow{v}^2(1 - \gamma)}{\gamma(2\varepsilon - \rho\overrightarrow{v}^2)}\right)^{\frac{1}{\gamma - 1}}}{\gamma(2\varepsilon - \rho\overrightarrow{v}^2)} \\
\frac{\partial p_t}{\partial m_2} &= \frac{v\left(\rho\overrightarrow{v}^2\left(\gamma^2 - 3\gamma + 1\right) - 2\varepsilon\gamma(\gamma - 2)\right)\left(\frac{2\varepsilon\gamma + \rho\overrightarrow{v}^2(1 - \gamma)}{\gamma(2\varepsilon - \rho\overrightarrow{v}^2)}\right)^{\frac{1}{\gamma - 1}}}{\gamma(2\varepsilon - \rho\overrightarrow{v}^2)} \\
\frac{\partial p_t}{\partial m_3} &= \frac{w\left(\rho\overrightarrow{v}^2\left(\gamma^2 - 3\gamma + 1\right) - 2\varepsilon\gamma(\gamma - 2)\right)\left(\frac{2\varepsilon\gamma + \rho\overrightarrow{v}^2(1 - \gamma)}{\gamma(2\varepsilon - \rho\overrightarrow{v}^2)}\right)^{\frac{1}{\gamma - 1}}}{\gamma(2\varepsilon - \rho\overrightarrow{v}^2)} \\
\frac{\partial p_t}{\partial \varepsilon} &= \frac{\left(2\varepsilon\gamma(\gamma - 1) - \rho\overrightarrow{v}^2\left(\gamma^2 - \gamma + 1\right)\right)\left(\frac{2\varepsilon\gamma + \rho\overrightarrow{v}^2(1 - \gamma)}{\gamma(2\varepsilon - \rho\overrightarrow{v}^2)}\right)^{\frac{1}{\gamma - 1}}}{\gamma(2\varepsilon - \rho\overrightarrow{v}^2)}
\end{aligned} \tag{3.53}$$

3.4.3 Mach Number

Likewise, the output equation for the Mach number is determined in the same manner. The components of the output matrix for the Mach number response are obtained from the linearization of the Mach number equation,

$$M = \frac{\sqrt{u^2 + v^2 + w^2}}{c} \tag{3.54}$$

The velocity and speed of sound terms are replaced with expressions in terms of ρ, m_1, m_2, m_3, and ε (as shown in section 3.3). Again, the total differential of the Mach number is calculated,

$$\delta M = \frac{\partial M}{\partial \rho}\delta\rho + \frac{\partial M}{\partial m_1}\delta m_1 + \frac{\partial M}{\partial m_2}\delta m_2 + \frac{\partial M}{\partial m_3}\delta m_3 + \frac{\partial M}{\partial \varepsilon}\delta\varepsilon \tag{3.55}$$

and each coefficient on the small perturbation terms is an entry in the output matrix for the Mach number.

$$\frac{\partial M}{\partial \rho} = \frac{\sqrt{2}\sqrt{m_1^2+m_2^2+m_3^2}\left(\varepsilon-\rho\overrightarrow{v}^2\right)\sqrt{\frac{\gamma\left(2\varepsilon\left(\gamma-1\right)-\gamma\rho\overrightarrow{v}^2\right)+\rho\overrightarrow{v}^2}{\rho}}}{\gamma\left(2\varepsilon-\rho\overrightarrow{v}^2\right)^2\left(1-\gamma\right)|\rho|}$$

$$\frac{\partial M}{\partial m_1} = \frac{\sqrt{2}m_1\sqrt{\frac{\gamma\left(2\varepsilon\left(\gamma-1\right)-\gamma\rho\overrightarrow{v}^2\right)+\rho\overrightarrow{v}^2}{\rho}}\operatorname{sgn}\left(\rho\right)}{\gamma\left(2\varepsilon-\rho\overrightarrow{v}^2\right)\left(\gamma-1\right)\sqrt{m_1^2+m_2^2+m_3^2}}$$

$$\frac{\partial M}{\partial m_2} = \frac{\sqrt{2}m_2\sqrt{\frac{\gamma\left(2\varepsilon\left(\gamma-1\right)-\gamma\rho\overrightarrow{v}^2\right)+\rho\overrightarrow{v}^2}{\rho}}\operatorname{sgn}\left(\rho\right)}{\gamma\left(2\varepsilon-\rho\overrightarrow{v}^2\right)\left(\gamma-1\right)\sqrt{m_1^2+m_2^2+m_3^2}} \tag{3.56}$$

$$\frac{\partial M}{\partial m_3} = \frac{\sqrt{2}m_3\sqrt{\frac{\gamma\left(2\varepsilon\left(\gamma-1\right)-\gamma\rho\overrightarrow{v}^2\right)+\rho\overrightarrow{v}^2}{\rho}}\operatorname{sgn}\left(\rho\right)}{\gamma\left(2\varepsilon-\rho\overrightarrow{v}^2\right)\left(\gamma-1\right)\sqrt{m_1^2+m_2^2+m_3^2}}$$

$$\frac{\partial M}{\partial \varepsilon} = \frac{\sqrt{2}\sqrt{m_1^2+m_2^2+m_3^2}\sqrt{\frac{\gamma\left(2\varepsilon\left(\gamma-1\right)-\gamma\rho\overrightarrow{v}^2\right)+\rho\overrightarrow{v}^2}{\rho}}\operatorname{sgn}\left(\rho\right)}{\gamma\left(2\varepsilon-\rho\overrightarrow{v}^2\right)^2\left(1-\gamma\right)}$$

4 Model Reduction

The models developed from the linearized split flux method are usually too large to be used effectively in the design of a control system; therefore, model reduction is necessary so that the linear model can be transformed into one that is of manageable size. In addition, a reduced order model (ROM) is needed when a transfer function of the system is desired, because the calculation of the transfer function from the full order model (FOM) becomes a numerically ill-conditioned problem. In general, the linear reduced order model is expected to perform like the linear full order model. There are many different methods that can be used for model reduction; those considered here take advantage of the state space format of the linear model.

One of the most common model reduction methods is singular perturbation [13]. This method requires a linear model that can be partitioned into slow and fast subsystems so that a reduced order model can be obtained by neglecting the fast subsystem. The ability to partition the model into subsystems indicates that the model possesses a two-time scale property; that is, there is a large gap in the spread of the eigenvalues of the linear model. There is little contribution to the dynamics of the system from the fast eigenvalues; therefore they can be discarded and a reduced order model obtained. But as was shown in [14] this method does not provide the smallest reduced order model that can be achieved, since in general the linear systems do not possess a two-time scale property.

Another popular method is balancing [15] [16] [17]. This method requires a linear model that can be partitioned into a strongly controllable/observable subsystem and a least controllable/observable subsystem. A reduced order model is then be obtained by discarding the least controllable/observable subsystem.

However, the ability to partition the system into these subsystems indicates that the model is minimal; that is, it is both controllable and observable. In general, linear models developed from the linearized CFD method are not minimal. Therefore this method does not work well because of the many uncontrollable and unobservable states in the linear model.

Two model reduction methods that are successfully applied to the linear model are the Schur and square root methods [18]. Both of these methods take into account the controllability and observability of the linear system, but they do not depend on the linear model being minimal. Although the Schur method is more numerically robust than the square root method, the square root method is preferred over the Schur method because it is computationally less expensive. In addition, since the reduced order model is balanced from the square root method, smaller reduced order models can be extracted from the original reduced order model without any more computations. The same is not true for the Schur method. The square root method is described in the next section and will be applied to the linear models developed later in the paper.

4.1 Square Root Model Reduction

The square root method of model reduction detailed in [18] is summarized here for the readers convenience. This model reduction method reduces the full order model by a balancing transformation that requires only the first $\mathbf{k}$ (size of reduced order model) columns of the balancing transformation matrix. The reduced order model $(\mathbf{A_k}, \mathbf{B_k}, \mathbf{C_k}, \mathbf{D_k})$ for the state space system $(\mathbf{A}, \mathbf{B}, \mathbf{C}, \mathbf{D})$ is calculated from:

$$\begin{aligned} \mathbf{A_k} &= S_{L,big}^T \mathbf{A} S_{R,big} \\ \mathbf{B_k} &= S_{L,big}^T \mathbf{B} \\ \mathbf{C_k} &= \mathbf{C} S_{R,big} \\ \mathbf{D_k} &= \mathbf{D} \end{aligned} \tag{4.1}$$

Computation of the transformation matrices $S_{L,big}^T$ and $S_{R,big}$ is shown below.

To begin with, the controllability and observability Grammians, P and Q, are calculated from the following Liapunov equations.

$$\begin{aligned} \mathbf{A}P + P\mathbf{A}^T &= -\mathbf{B}\mathbf{B}^T \\ \mathbf{A}^T Q + Q\mathbf{A} &= -\mathbf{C}^T\mathbf{C} \end{aligned} \tag{4.2}$$

Once the Liapunov equations are solved for the Grammians, the square roots of P and Q,

$$\begin{aligned} P &= L_c L_c^T \\ Q &= L_o L_o^T \end{aligned} \tag{4.3}$$

are calculated from the following:

$$\begin{aligned} [U_p, S_p, V_p] &= SVD\,(P) \\ L_c &= U_p diag\left(\sqrt{diag\,(S_p)}\right) \\ [U_q, S_q, V_q] &= SVD\,(Q) \\ L_o &= U_q diag\left(\sqrt{diag\,(S_q)}\right) \end{aligned} \tag{4.4}$$

A singular value decomposition (SVD) of $L_o^T L_c$ produces the matrices needed to compute $S_{L,big}^T$ and $S_{R,big}$.

$$[U, \textstyle\sum_1, V] = SVD\left(L_o^T L_c\right) \tag{4.5}$$

$\sum_1$ is defined as:

$$\sum_1 = diag(\sigma_1, \sigma_2, \cdots, \sigma_m) \tag{4.6}$$

where m is the number of nonzero Hankel singular values represented by σ. The σ are defined as the square roots of the eigenvalues of the PQ matrix.

$$\sigma = (\lambda(PQ))^{\frac{1}{2}} \tag{4.7}$$

From $\sum_1$, $\sum_{bal}$ is defined as:

$$\sum_{bal} = diag(\sigma_1, \sigma_2, \cdots, \sigma_{\mathbf{k}}) \tag{4.8}$$

Note that the σ are in descending order according to their magnitude. Now $S_{L,big}$ and $S_{R,big}$ can be calculated from the following equations,

$$\begin{aligned} S_{L,big} &= L_o U \begin{bmatrix} \sum_{bal}^{-\frac{1}{2}} \\ 0 \end{bmatrix} \\ S_{R,big} &= L_c V \begin{bmatrix} \sum_{bal}^{-\frac{1}{2}} \\ 0 \end{bmatrix} \end{aligned} \tag{4.9}$$

and the reduced order model can be determined using equation (4.1). While this method works well for the linearized one dimensional CFD models, it must be modified before it can be used for the linearized multidimensional CFD models; because due to their large size and sparse structure, the multidimensional CFD models are numerically ill-conditioned. These modifications are described in the next section.

4.2 Modified Square Root Model Reduction

Unfortunately for the linearized multidimensional CFD models, the calculation of the Grammians that are needed for the square root model reduction is computationally prohibitive because of the large number of equations involved. However, low-rank approximate solutions to these large scale Liapunov equations are possible. The approximate solution for the large scale Liapunov equation is calculated using the Arnoldi method from [19]. In addition, further numerical savings are achieved if the SVD calculations are performed using the partial SVD method from [20]. The modifications that are needed to the square root model reduction method when using these approximations are detailed in this section.

Since the controllability and observability Grammians are approximations, the square root model reduction method has to be modified [21]. The approximate controllability and observability Grammians are equal to:

$$\begin{aligned} P_{approx} &= V_p X_p V_p^T \\ Q_{approx} &= V_q X_q V_q^T \end{aligned} \tag{4.10}$$

where the matrices V_p, X_p, V_q, and X_q are calculated using the Arnoldi approximation method from [19]. Then the matrices L_c and L_o from (4.3) are calculated using the following equations:

$$\begin{aligned} L_c &= V_p R_p \\ L_o &= V_q R_q \end{aligned} \tag{4.11}$$

where R_p is the square root of X_p, and R_q is the square root of X_q as shown below.

$$\begin{aligned} [U_{X_p}, S_{X_p}, V_{X_p}] &= SVD(X_p) \\ R_p &= U_{X_p} diag\left(\sqrt{diag\left(S_{X_p}\right)}\right) \end{aligned}$$

$$
\begin{aligned}
[U_{X_q}, S_{X_q}, V_{X_q}] &= SVD(X_q) \\
R_q &= U_{X_q} diag\left(\sqrt{diag\left(S_{X_q}\right)}\right)
\end{aligned}
\tag{4.12}
$$

The matrices needed to compute $S_{L,big}^T$ and $S_{R,big}$ for equation (4.9) are then calculated from:

$$
[U, \sum_1, V] = SVD\left(L_o^T L_c\right) \tag{4.13}
$$

where $\sum_1$ is defined (4.6) by and $\sum_{bal}$ is defined by (4.8). Finally $S_{L,big}$ and $S_{R,big}$ are determined from the following equations,

$$
\begin{aligned}
S_{L,big} &= L_o U \begin{bmatrix} \sum_{bal}^{-\frac{1}{2}} \\ 0 \end{bmatrix} \\
S_{R,big} &= L_c V \begin{bmatrix} \sum_{bal}^{-\frac{1}{2}} \\ 0 \end{bmatrix}
\end{aligned}
\tag{4.14}
$$

and the reduced order model is computed using equation (4.1). For this work, the singular value decompositions in the above equations were calculated using the subspace approximation method from [20]. Note that in the modified square root model reduction, the approximate Grammians are never calculated; this results in a significant savings in computation time and in storage requirements. The errors associated with the model reduction and linearization processes are described in the next section.

5 Uncertainty

There is a certain amount of error associated with the linear models developed using the linearized split flux method; in particular, there is error due to the linearization process and the model reduction process. These errors can be characterized as modeling uncertainties which are represented by error bounds and are derived below.

5.1 Linearization Error

The major source of error incurred in developing linear control models lies in the linearization process. As long as all the expected perturbations from steady-state are "small", the error bounds will be small. Here, small depends upon which variables are being considered and how sensitive the system dynamics are to steady-state changes. Clearly this must be determined by trial and error for each system considered. Normalizing the data allows all the variables to be weighted similarly. While many approaches can be considered for determining error bounds, the one described below uses infinity norm bounds and is probably the most useful for the control system designer. In addition, it is also a convenient form for the numerical experiments considered. It should be noted that this error bound holds exactly only for linear systems; as such, it only serves as an approximation of the true bound. Its accuracy will certainly be degraded for larger perturbations.

The modeling error due to the linearization process is based on the fact that the infinity norm of the transfer function error is less than or equal to the one norm of the unit impulse response error (B. Veillette, University of Akron, Akron, OH., private communication).

$$
\left\|\mathbf{G}_{true}(j\omega) - \mathbf{G}(j\omega)\right\|_\infty \leqslant \left\|\mathbf{g}_{true}(t) - \mathbf{g}(t)\right\|_1 \tag{5.1}
$$

$\mathbf{G}_{true}(j\omega)$ represents the transfer function of an exact linear model, if it were available, and $\mathbf{G}(j\omega)$ represents the transfer function from the split flux linearization process. The infinity norm of the transfer function error

is defined as:

$$\|\mathbf{G}_{true}(j\omega) - \mathbf{G}(j\omega)\|_\infty = \sigma_{\max}\{\mathbf{G}_{true}(j\omega) - \mathbf{G}(j\omega)\} \tag{5.2}$$

and the one norm of the impulse response error is defined as:

$$\|\mathbf{g}_{true}(t) - \mathbf{g}(t)\|_1 = \int_0^\infty |\mathbf{g}_{true}(t) - \mathbf{g}(t)|\, dt \tag{5.3}$$

$\int_0^\infty |\mathbf{g}_{true}(t) - \mathbf{g}(t)|\, dt$ can be approximated by:

$$\int_0^\infty |\mathbf{g}_{true}(t) - \mathbf{g}(t)|\, dt \simeq \sum_{n=0}^{\mathbf{N}} |\mathbf{g}_{true}^n - \mathbf{g}^n|\, \Delta T \tag{5.4}$$

Therefore, the error bound on the infinity norm of the transfer function can be represented by the following:

$$\|\mathbf{G}_{true}(j\omega) - \mathbf{G}(j\omega)\|_\infty \lesssim \sum_{n=0}^{\mathbf{N}} |\mathbf{g}_{true}^n - \mathbf{g}^n|\, \Delta T \tag{5.5}$$

The notation can be simplified by expressing $\mathbf{G}_{true}(j\omega) - \mathbf{G}(j\omega)$ as $\mathbf{E}(j\omega)$ and $\mathbf{g}_{true}^n - \mathbf{g}^n$ as $\mathbf{e}^n$. Therefore, the linearization error bound is represented as:

$$\|\mathbf{E}(j\omega)\|_\infty \lesssim \sum_{n=0}^{\mathbf{N}} |\mathbf{e}^n|\, \Delta T \tag{5.6}$$

For multi-input/multi-output systems (MIMO), the transfer functions and impulse responses are represented in matrix form, and the linearization error bound can be determined from the following:

$$\|\mathbf{E}(j\omega)\|_\infty \lesssim \sigma_{\max}\left\{\begin{bmatrix} \|\mathbf{e}_{11}(t)\|_1 & \|\mathbf{e}_{12}(t)\|_1 & \cdots & \|\mathbf{e}_{1p}(t)\|_1 \\ \|\mathbf{e}_{21}(t)\|_1 & \|\mathbf{e}_{22}(t)\|_1 & \cdots & \|\mathbf{e}_{2p}(t)\|_1 \\ \vdots & \vdots & \ddots & \vdots \\ \|\mathbf{e}_{r1}(t)\|_1 & \|\mathbf{e}_{r2}(t)\|_1 & \cdots & \|\mathbf{e}_{rp}(t)\|_1 \end{bmatrix}\right\} \tag{5.7}$$

The maximum singular value of a matrix is defined as:

$$\sigma_{\max} = \left(\lambda_{\max}\left(matrix^T matrix\right)\right)^{\frac{1}{2}} \tag{5.8}$$

For a MIMO system with p number of inputs and r number of outputs, the transfer function error matrix is written as:

$$\mathbf{E} = \begin{bmatrix} \mathbf{E}_{11}(j\omega) & \mathbf{E}_{12}(j\omega) & \cdots & \mathbf{E}_{1p}(j\omega) \\ \mathbf{E}_{21}(j\omega) & \mathbf{E}_{22}(j\omega) & \cdots & \mathbf{E}_{2p}(j\omega) \\ \vdots & \vdots & \ddots & \vdots \\ \mathbf{E}_{r1}(j\omega) & \mathbf{E}_{r2}(j\omega) & \cdots & \mathbf{E}_{rp}(j\omega) \end{bmatrix} \tag{5.9}$$

and the impulse error matrix is written as:

$$\mathbf{e} = \begin{bmatrix} \mathbf{e}_{11}(t) & \mathbf{e}_{12}(t) & \cdots & \mathbf{e}_{1p}(t) \\ \mathbf{e}_{21}(t) & \mathbf{e}_{22}(t) & \cdots & \mathbf{e}_{2p}(t) \\ \vdots & \vdots & \ddots & \vdots \\ \mathbf{e}_{r1}(t) & \mathbf{e}_{r2}(t) & \cdots & \mathbf{e}_{rp}(t) \end{bmatrix} \tag{5.10}$$

In the preceding definition, the one norm of each element is:

$$\int_0^\infty |\mathbf{e}|\, dt = \begin{bmatrix} \|\mathbf{e}_{11}(t)\|_1 & \|\mathbf{e}_{12}(t)\|_1 & \cdots & \|\mathbf{e}_{1p}(t)\|_1 \\ \|\mathbf{e}_{21}(t)\|_1 & \|\mathbf{e}_{22}(t)\|_1 & \cdots & \|\mathbf{e}_{2p}(t)\|_1 \\ \vdots & \vdots & \ddots & \vdots \\ \|\mathbf{e}_{r1}(t)\|_1 & \|\mathbf{e}_{r2}(t)\|_1 & \cdots & \|\mathbf{e}_{rp}(t)\|_1 \end{bmatrix} \tag{5.11}$$

and the approximation for (5.11) is:

$$\int_0^\infty |\mathbf{e}|\, dt \simeq \begin{bmatrix} \sum_{n=0}^{\mathbf{N}} |\mathbf{e}_{11}^n| \Delta T & \sum_{n=0}^{\mathbf{N}} |\mathbf{e}_{12}^n| \Delta T & \cdots & \sum_{n=0}^{\mathbf{N}} |\mathbf{e}_{1p}^n| \Delta T \\ \sum_{n=0}^{\mathbf{N}} |\mathbf{e}_{21}^n| \Delta T & \sum_{n=0}^{\mathbf{N}} |\mathbf{e}_{22}^n| \Delta T & \cdots & \sum_{n=0}^{\mathbf{N}} |\mathbf{e}_{2p}^n| \Delta T \\ \vdots & \vdots & \ddots & \vdots \\ \sum_{n=0}^{\mathbf{N}} |\mathbf{e}_{r1}^n| \Delta T & \sum_{n=0}^{\mathbf{N}} |\mathbf{e}_{r2}^n| \Delta T & \cdots & \sum_{n=0}^{\mathbf{N}} |\mathbf{e}_{rp}^n| \Delta T \end{bmatrix} \tag{5.12}$$

Therefore the infinity norm of the error transfer function matrix is bounded by:

$$\|\mathbf{E}(j\omega)\|_\infty \lesssim \sigma_{\max} \left\{ \begin{bmatrix} \sum_{n=0}^{\mathbf{N}} |\mathbf{e}_{11}^n| \Delta T & \sum_{n=0}^{\mathbf{N}} |\mathbf{e}_{12}^n| \Delta T & \cdots & \sum_{n=0}^{\mathbf{N}} |\mathbf{e}_{1p}^n| \Delta T \\ \sum_{n=0}^{\mathbf{N}} |\mathbf{e}_{21}^n| \Delta T & \sum_{n=0}^{\mathbf{N}} |\mathbf{e}_{22}^n| \Delta T & \cdots & \sum_{n=0}^{\mathbf{N}} |\mathbf{e}_{2p}^n| \Delta T \\ \vdots & \vdots & \ddots & \vdots \\ \sum_{n=0}^{\mathbf{N}} |\mathbf{e}_{r1}^n| \Delta T & \sum_{n=0}^{\mathbf{N}} |\mathbf{e}_{r2}^n| \Delta T & \cdots & \sum_{n=0}^{\mathbf{N}} |\mathbf{e}_{rp}^n| \Delta T \end{bmatrix} \right\} \tag{5.13}$$

and (5.13) is used to calculate the linearization error bound for a MIMO system.

The error analysis described above is based on the error in the unit impulse response. However, in general, the input for the nonlinear model is a step not an impulse; therefore, the impulse error must be derived from step response data. In the block diagram shown below, the setup for the error analysis is illustrated.

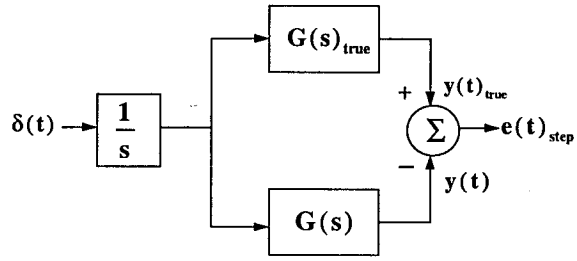

This block diagram can be rearranged so that the outputs of the transfer functions are the impulse responses.

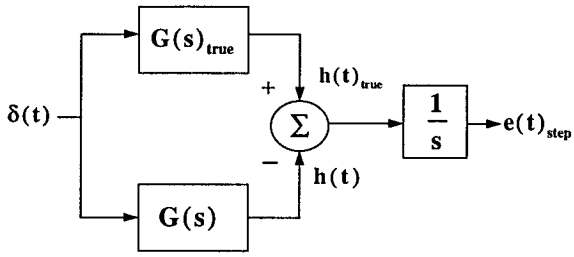

Now, the step error is represented as the integration of the impulse error. Therefore, the impulse response error can be determined from the step response data by taking the derivative of the step response error.

$$\mathbf{e}(t) = \frac{d}{dt}\left(y(t)_{true} - y(t)\right) \tag{5.14}$$

If the time derivative in the previous expression is approximated by a finite difference expression, then equation (5.14) can be rewritten as:

$$\mathbf{e}^n \simeq \left(\frac{\left(y^n_{true} - y^{n-1}_{true}\right) - \left(y^n - y^{n-1}\right)}{\Delta T}\right) \tag{5.15}$$

and the linearization error bound can be calculated using (5.13).

5.2 Model Reduction Error

When using the modified square root model reduction described in the previous section, the bound on the error between the linear full order model and the linear reduced order model can be calculated using the method of the previous section.

$$\left\|\mathbf{G}(j\omega) - \mathbf{G_k}(j\omega)\right\|_\infty \leqslant \left\|\mathbf{g}(t) - \mathbf{g_k}(t)\right\|_1 \tag{5.16}$$

$\mathbf{G}(j\omega)$ represents the transfer function from the split flux linearization process, and $\mathbf{G_k}(j\omega)$ represents the transfer function from the model reduction process. Following the procedure outlined above, the error bound is calculated from:

$$\left\|\mathbf{E}(j\omega)\right\|_\infty \lesssim \sigma_{\max}\left\{\begin{bmatrix} \sum_{n=0}^{N}\left|\mathbf{e}^n_{11}\right|\Delta T & \sum_{n=0}^{N}\left|\mathbf{e}^n_{12}\right|\Delta T & \cdots & \sum_{n=0}^{N}\left|\mathbf{e}^n_{1p}\right|\Delta T \\ \sum_{n=0}^{N}\left|\mathbf{e}^n_{21}\right|\Delta T & \sum_{n=0}^{N}\left|\mathbf{e}^n_{22}\right|\Delta T & \cdots & \sum_{n=0}^{N}\left|\mathbf{e}^n_{2p}\right|\Delta T \\ \vdots & \vdots & \ddots & \vdots \\ \sum_{n=0}^{N}\left|\mathbf{e}^n_{r1}\right|\Delta T & \sum_{n=0}^{N}\left|\mathbf{e}^n_{r2}\right|\Delta T & \cdots & \sum_{n=0}^{N}\left|\mathbf{e}^n_{rp}\right|\Delta T \end{bmatrix}\right\} \tag{5.17}$$

and $\mathbf{e}^n$ is defined as:

$$\mathbf{e}^n \simeq \left(\frac{\left(y^n - y^{n-1}\right) - \left(y^n_{\mathbf{k}} - y^{n-1}_{\mathbf{k}}\right)}{\Delta T}\right) \tag{5.18}$$

5.3 Total Error Bound

As the infinity norm bound of a system is a Nyquist plane bound, the bounds serve as magnitudes of error incurred in each step in the modeling process. Thus, the total infinity norm bound is determined as the sum of the individual bounds from linearization and model reduction. This is represented as:

$$\|\mathbf{G}_{true}(j\omega) - \mathbf{G_k}(j\omega)\|_\infty \leqslant \|\mathbf{G}_{true}(j\omega) - \mathbf{G}(j\omega)\|_\infty + \|\mathbf{G}(j\omega) - \mathbf{G_k}(j\omega)\|_\infty \tag{5.19}$$

where $\mathbf{G}_{true}(j\omega)$represents the transfer function of an exact linear model, $\mathbf{G}(j\omega)$ is the transfer function from the linearization process, and $\mathbf{G_k}(j\omega)$ is the transfer function from the model reduction process.

6 Example Application

In this section, two dimensional and three dimensional models of the variable diameter centerbody (VDC) inlet are used to illustrate the CFD-based linear modeling technique discussed in this paper. The VDC inlet is an axisymmetric inlet with a collapsible centerbody [22] and is typical of inlets being investigated for use on aircraft being developed under NASA's High Speed Civil Transport program. The inlet is designed to operate at the following conditions: $altitude = 65,000\ ft$, $p_\infty = 117.8\ \frac{lb}{ft^2}$, $T_\infty = 395\ ^\circ R$, $M_\infty = 2.5$, $M_{compressor\ face} = .33$, and $\gamma = 1.4$, and simulation data for the nonlinear model was obtained from the CFD code PARC [7]. The steady-state PARC data before the perturbation occurs is used to generate the linear model, and the linear model is validated from the transient PARC data that is generated by the perturbation. In general, the perturbation is a step input that is not too large so that the small perturbation analysis remains valid. Because the CFD model has so many equations (7,896 for the 2D model and 61,800 for the 3D model) it is not numerically feasible to use the entire grid to derive a linear model at this time. Therefore, the linear models are calculated based on reduced grids obtained from the original CFD grid. These reduced grids are obtained by selecting grid points that approximate the entire grid. Once the linear models are generated, the reduced order models are obtained using the modified square root method. The nondimensional results for these examples are discussed in the next section, and the data for these matrices are listed in section 8.3 of the appendix.

6.1 Results

6.1.1 2D VDC Inlet Model: Downstream Mach Number Perturbation

The two dimensional nonlinear CFD model from cowl lip to compressor face is represented by a 94×21 grid which has 1974 grid points (7896 states). The system has one input and two outputs. The inlet is perturbed at 0.01 seconds with a -3% step in compressor face Mach number, and the system outputs for static pressure are located downstream of the normal shock at $X/R_c = 4.08$ and $X/R_c = 5.01$. The -3% change in the compressor face Mach number produces a 4.24% change in steady-state for the static pressure output at $X/R_c = 4.08$ and a 3.05% change in the steady-state for the static pressure output at $X/R_c = 5.01$. The overall error bounds for various linear models based on reduced grids of the CFD model are listed below,

Grid	# FOM States	# ROM States	Error Bound
26×3	312	13	0.43461
26×5	520	13	0.43382
26×7	728	13	0.43342
48×3	576	13	0.41472
48×5	960	13	0.41449
48×7	1344	13	0.41424

and the nondimensional results for the above models are shown in Figures $1 - 12$.

In Figure 1, the PARC transient data from the 94×21 grid is compared to a ROM of the linearized CFD model developed from a 26×3 grid. In Figure 2, the locations of the FOM eigenvalues are compared with those of the ROM. The FOM has 312 states and the ROM has 13 states; this represents a reduction of 95.8% in the size of the linear model. The minimum eigenvalue for the FOM is located at -8.9721×10^1 and at -8.9724×10^1 for the ROM. The maximum eigenvalue for the FOM is located at -4.6705×10^4 and at $-6.7659 \times 10^3 \pm j7.3296 \times 10^3$ for the ROM. Note the minimum eigenvalue for the FOM and ROM are approximately equal, but the maximum eigenvalue for the FOM is further to the left of the imaginary axis than for the ROM. This is evident in all of the examples.

In Figure 3, the PARC transient data from the 94×21 grid is compared to a ROM of the linearized CFD model developed from a 26×5 grid. In Figure 4, the locations of the FOM eigenvalues are compared with those of the ROM. The FOM has 520 states and the ROM has 13 states; this represents a reduction of 97.5% in the size of the linear model. The minimum eigenvalue for the FOM is located at -8.8813×10^1 and at -8.8783×10^1 for the ROM. The maximum eigenvalue for the FOM is located at -87577×10^4 and at -3.1972×10^4 for the ROM.

In Figure 5, the PARC transient data from the 94×21 grid is compared to a ROM of the linearized CFD model developed from a 26×7 grid. In Figure 6, the locations of the FOM eigenvalues are compared with those of the ROM. The FOM has 728 states and the ROM has 13 states; this represents a reduction of 98.2% in the size of the linear model. The minimum eigenvalue for the FOM is located at -8.8463×10^1 and at -8.8442×10^1 for the ROM. The maximum eigenvalue for the FOM is located at -1.2967×10^5 and at -2.9908×10^4 for the ROM.

In Figure 7, the PARC transient data from the 94×21 grid is compared to a ROM of the linearized CFD model developed from a 48×3 grid. In Figure 8, the locations of the FOM eigenvalues are compared with those of the ROM. The FOM has 576 states and the ROM has 13 states; this represents a reduction of 97.7% in the size of the linear model. The minimum eigenvalue for the FOM is located at -1.0385×10^2 and at -1.0398×10^2 for the ROM. The maximum eigenvalue for the FOM is located at -8.6676×10^4 and at $-3.9629 \times 10^3 \pm j8.4573 \times 10^3$ for the ROM.

In Figure 9, the PARC transient data from the 94×21 grid is compared to a ROM of the linearized CFD model developed from a 48×5 grid. In Figure 10, the locations of the FOM eigenvalues are compared with those of the ROM. The FOM has 960 states and the ROM has 13 states; this represents a reduction of 98.6% in the size of the linear model. The minimum eigenvalue for the FOM is located at -1.0399×10^2 and at -1.0424×10^2 for the ROM. The maximum eigenvalue for the FOM is located at -1.1310×10^5 and at $-3.4176 \times 10^3 \pm j8.3316 \times 10^3$ for the ROM.

In Figure 11, the PARC transient data from the 94×21 grid is compared to a ROM of the linearized CFD model developed from a 48×7 grid. In Figure 12, the locations of the FOM eigenvalues are compared with those of the ROM. The FOM has 1344 states and the ROM has 13 states; this represents a reduction of 99% in the size of the linear model. The minimum eigenvalue for the FOM is located at -1.0414×10^2 and at -1.0463×10^2 for the ROM. The maximum eigenvalue for the FOM is located at -1.5374×10^5 and at $-3.2790 \times 10^3 \pm j8.2064 \times 10^3$ for the ROM.

6.1.2 3D VDC Inlet Model: Downstream Mach Number Perturbation

The three dimensional nonlinear CFD model from cowl lip to compressor face is represented by a $103 \times 15 \times 8$ grid which has $12,360$ grid points ($61,800$ states). The system has one input and two outputs. The inlet is perturbed at 0.01 seconds with a -3% step in compressor face Mach number, and the system outputs

for static pressure are located at $X/R_c = 3.9448$ and $X/R_c = 4.9262$. The -3% change in the compressor face Mach number produces a 3.988% change in steady-state for the static pressure output at $X/R_c = 3.9448$ and a 3.3362% change in the steady-state for the static pressure output at $X/R_c = 4.9262$. The overall error bounds are listed below for two linear models based on reduced grids of the CFD model,

Grid	# FOM States	# ROM States	Error Bound
$15 \times 3 \times 3$	675	17	0.69196
$20 \times 3 \times 3$	900	17	0.67617

and the nondimensional results for the above models are shown in Figures $13 - 16$.

In Figure 13, the PARC transient data from the $103 \times 15 \times 8$ grid is compared to a ROM of the linearized CFD model developed from a $15 \times 3 \times 3$ grid. In Figure 14, the locations of the FOM eigenvalues are compared with those of the ROM. The FOM has 675 states and the ROM has 17 states; this represents a reduction of 97.5% in the size of the linear model. The minimum eigenvalue for the FOM is located at -1.4375×10^2 and at -1.1705×10^2 for the ROM. The maximum eigenvalue for the FOM is located at -5.4626×10^4 and at $-8.3988 \times 10^3 \pm j3.6576 \times 10^3$ for the ROM.

In Figure 15, the PARC transient data from the $103 \times 15 \times 8$ grid is compared to a ROM of the linearized CFD model developed from a $20 \times 3 \times 3$ grid. In Figure 16, the locations of the FOM eigenvalues are compared with those of the ROM. The FOM has 900 states and the ROM has 17 states; this represents a reduction of 98.1% in the size of the linear model. The minimum eigenvalue for the FOM is located at -1.1268×10^2 and at -1.1268×10^2 for the ROM. The maximum eigenvalue for the FOM is located at -5.4626×10^4 and at $-8.4927 \times 10^3 \pm j3.3323 \times 10^3$ for the ROM.

6.2 Discussion

The CFD steady-state data from the reduced CFD grids seem to provide enough information to calculate reasonable linear models that represent the original CFD model. Note that in the two dimensional results, an increase in the number of nodes in the y-direction did not have as much effect on lowering the linearization error bound as did an increase in the number of nodes in the x-direction. This result is shown in Figure 17 and illustrates that the inlet model is not strongly two dimensional. In general as the number of grid points is increased in the reduced CFD grid, the better the linear model; in other words, linear models obtained from larger reduced CFD grids have lower linearization error bounds. For the three dimensional model, increasing the number of nodes in the x-direction lowered the linearization error bound but not by very much. This is probably due to the fact that so little of the original CFD grid is being used in the development of the linear model. The three dimensional example is included mainly as an application of the linear modeling concept and model reduction process.

Linear results based on one dimensional data obtained from averaged two dimensional data are shown in Figures 18 and 19. As was noted above, the inlet model is not strongly two dimensional; therefore, the dynamic behavior of the inlet can be represented by a one dimensional linear model. The linear model based on the averaged steady-state data has 282 states. The linear results based on one dimensional data obtained from averaged three dimensional data are shown in Figures 20 and 21. The linear model based on the averaged steady-state data has 309 states. Again, the three dimensional inlet model is adequately represented by a one dimensional linear model based on the averaged steady-state data.

As was noted in the one dimensional modeling paper [9], the full order model eigenvalues closest to the origin are reproduced in the reduced order model, but the eigenvalues farther away from the origin

are approximated by just a few eigenvalues in the reduced order model. The model reduction for the linearized models based on the multidimensional CFD data is not as straight forward as it is for the one dimensional models. In the one dimensional case, the model reduction process for the linear models used established methods. For the multidimensional linear models, the model reduction process had to be modified by implementing approximation methods for the Grammian and SVD calculations. These approximation methods require that the user declare error tolerances for the algorithms and approximation sizes for the matrices. The smaller the error tolerance used, the longer the approximation method takes to converge; so there is a trade-off between computation speed and accuracy. In addition, as the full order linear models become larger, the approximation sizes need to be made larger; this also increases the amount of time needed to compute the reduced order model. Unfortunately, there are no proven guidelines that can be used when choosing the approximation sizes and error tolerances for the model reduction method; improvement in this process needs to be addressed.

7 Conclusion

Linear dynamic models of multidimensional mixed compression inlets have been developed from steady-state CFD results. As was the case for the one dimensional CFD models, it is possible to obtain a linear model from the spatial information and steady-state operating conditions of a multidimensional CFD simulation. The linearization process for the multidimensional models was more difficult due to the different types of boundary conditions. The small perturbation models that result are useful for control applications, real-time simulations, and model reduction. Additional types of inputs need to be developed as was done for the linear models based on quasi-one dimensional CFD results [9].

Model reduction proved to be a more difficult problem than for the one dimensional case due to the size of the computational grids of the multidimensional CFD models. Modifications to the existing model reduction method were made which produced viable reduced order models. Furthermore, model reduction for systems on the order of a thousand states is possible. Work remains to be completed on more efficient model reduction algorithms for these large scale systems.

8 Appendices

8.1 Symbols

A	Jacobian for $\frac{\partial \vec{f}}{\partial x}$
$\mathbf{A}$	system matrix
B	Jacobian for $\frac{\partial \vec{g}}{\partial y}$
$\mathbf{B}$	input matrix
B_{bc}	physical boundary condition
C	Jacobian for $\frac{\partial \vec{h}}{\partial z}$
$\mathbf{C}$	output matrix
$\mathbf{D}$	input/output matrix
c	speed of sound $\left(\frac{ft}{\text{sec}}\right)$
E	total energy per unit mass $\left(\frac{lb\,ft}{slug}\right)$
$\mathbf{E}$	error transfer function matrix
e	internal energy per unit mass $\left(\frac{ft^2}{\text{sec}^2}\right)$
$e(t)$	error response
$\mathbf{e}$	error impulse matrix
$\vec{f}$	flux vector for the x-direction
$\mathbf{G}$	transfer function
$\vec{g}$	flux vector for the y-direction
$\mathbf{g}(t)$	impulse response
$\vec{h}$	flux vector for the z-direction
K	matrix of right eigenvectors
j	$\sqrt{-1}$
M	Mach number
m	massflow per unit area $\left(\frac{slug}{\text{sec}\ ft^2}\right)$
N_1	number of grid points in the x-direction
N_2	number of grid points in the y-direction
N_3	number of grid points in the z-direction
p	pressure $\left(\frac{lb}{ft^2}\right)$
P	controllability Grammian
Q	observability Grammian
R_c	cowl radius (ft)
s	entropy
t	time (sec)
u	velocity $\left(\frac{ft}{\text{sec}}\right)$ in the x-direction
v	velocity $\left(\frac{ft}{\text{sec}}\right)$ in the y-direction
w	velocity $\left(\frac{ft}{\text{sec}}\right)$ in the z-direction
$\vec{u}$	vector of conservative variables
$\vec{v}$	velocity vector
$\vec{w}$	vector of characteristic variables
x	distance (ft)
y	distance (ft)
$y(t)$	output reponse
z	distance (ft)

8.1.1 Greek Symbols

ΔT	sampling time (sec)
ε	$\varepsilon = \rho E$, total energy per unit volume $\left(\frac{lb\,ft}{ft^3}\right)$
δ	small perturbation variable
$\delta(t)$	unit impulse
γ	ratio of specific heats
Λ	diagonal matrix of local characteristics
λ	eigenvalue
ρ	density $\left(\frac{slug}{ft^3}\right)$
σ	singular value
ω	frequency $\left(\frac{rad}{\text{sec}}\right)$

8.1.2 Subscripts

bc	boundary condition
i	grid point in the x-direction
j	grid point in the y-direction
k	grid point in the z-direction
$\mathbf{k}$	size of reduced order model
L	left
p	number of outputs
R	right
r	number of inputs
t	total conditions

8.1.3 Superscripts

N	numerical
n	time level
P	physical
T	transpose

8.2 Figures

8.2.1 2D VDC Inlet Model: Downstream Mach Number Perturbation

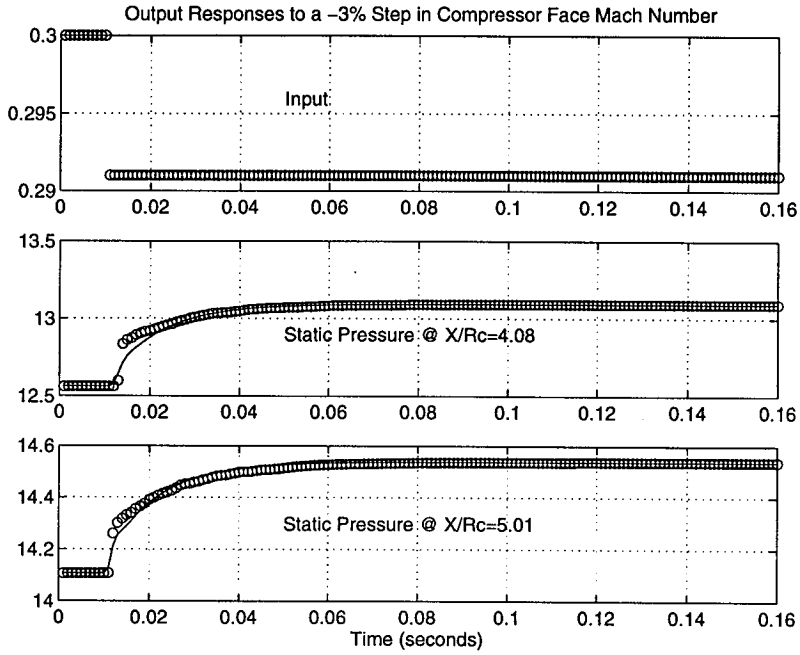

Figure 1: o PARC, 94×21 Grid/- Linear ROM, 26×3 Grid

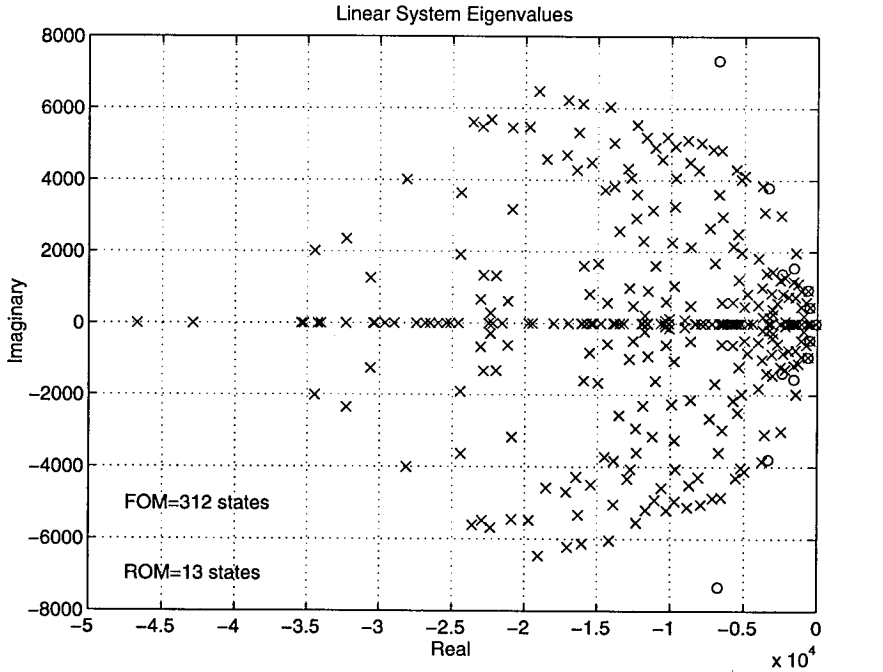

Figure 2: x FOM Eigenvalues/o ROM Eigenvalues

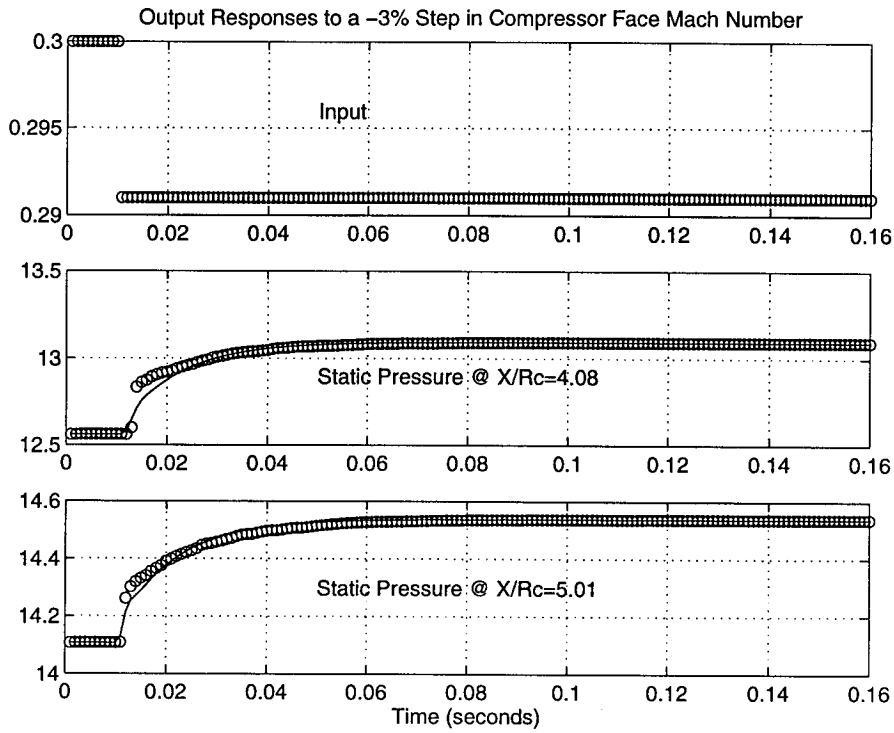

Figure 3: o PARC, 94× 21 Grid/- Linear ROM, 26 × 5 Grid

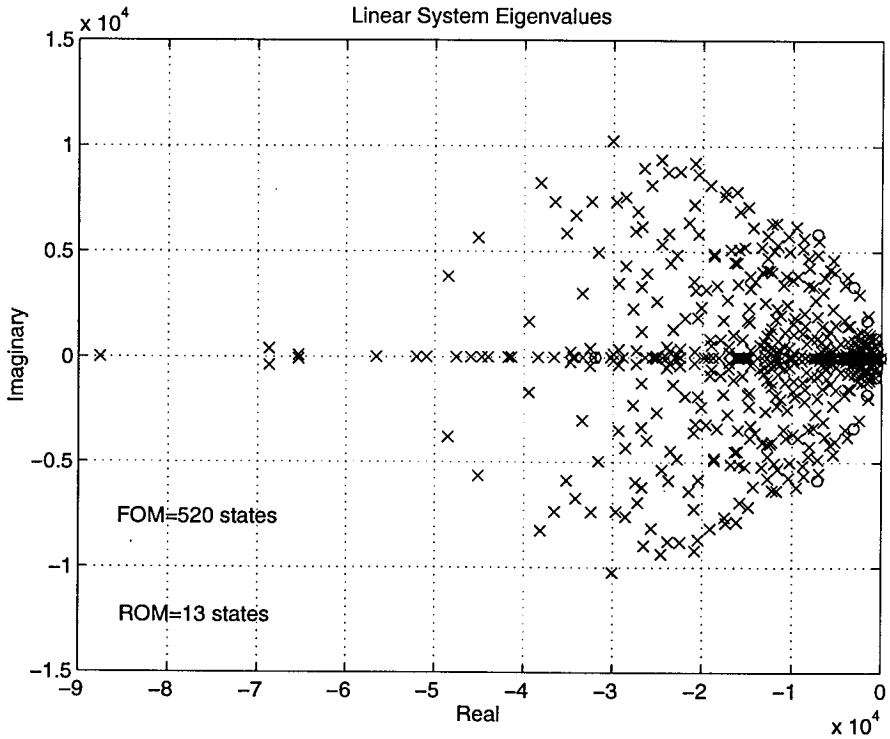

Figure 4: x FOM Eigenvalues/o ROM Eigenvalues

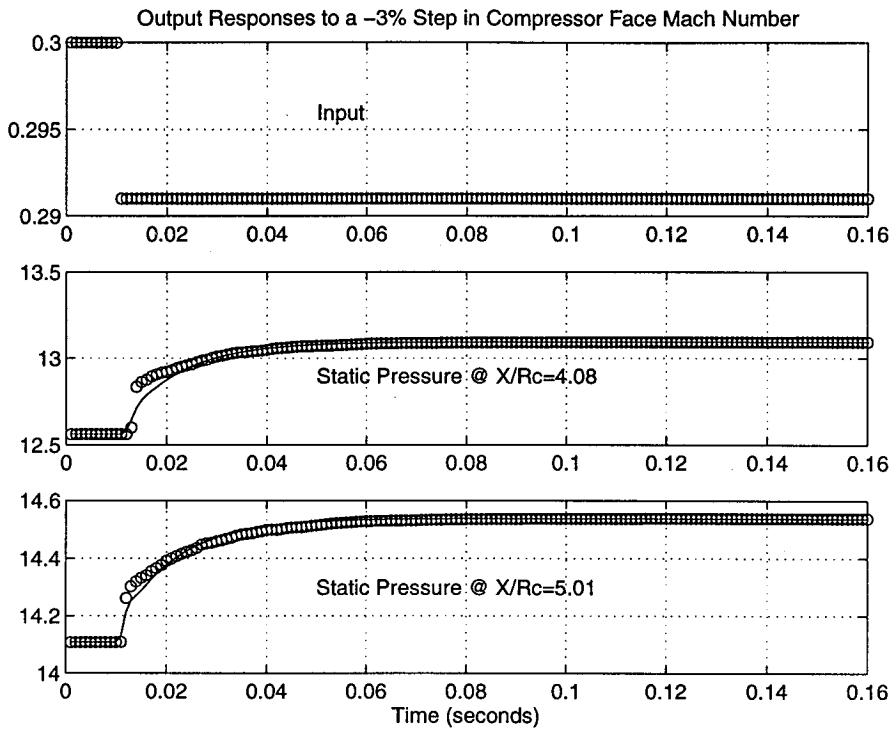

Figure 5: o PARC, 94 × 21 Grid/- Linear ROM, 26 × 7 Grid

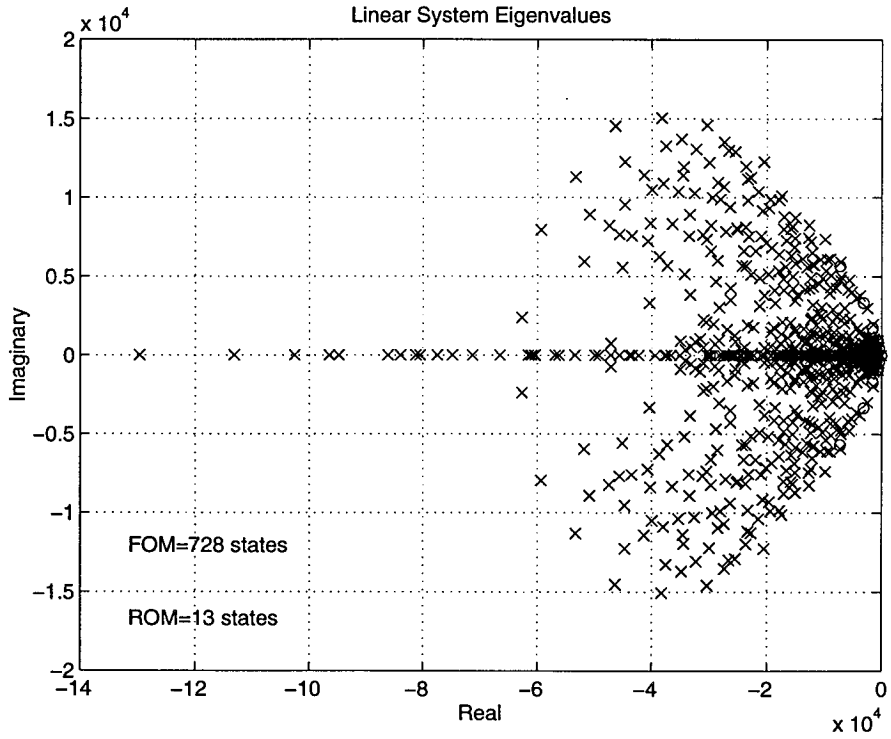

Figure 6: x FOM Eigenvalues/o ROM Eigenvalues

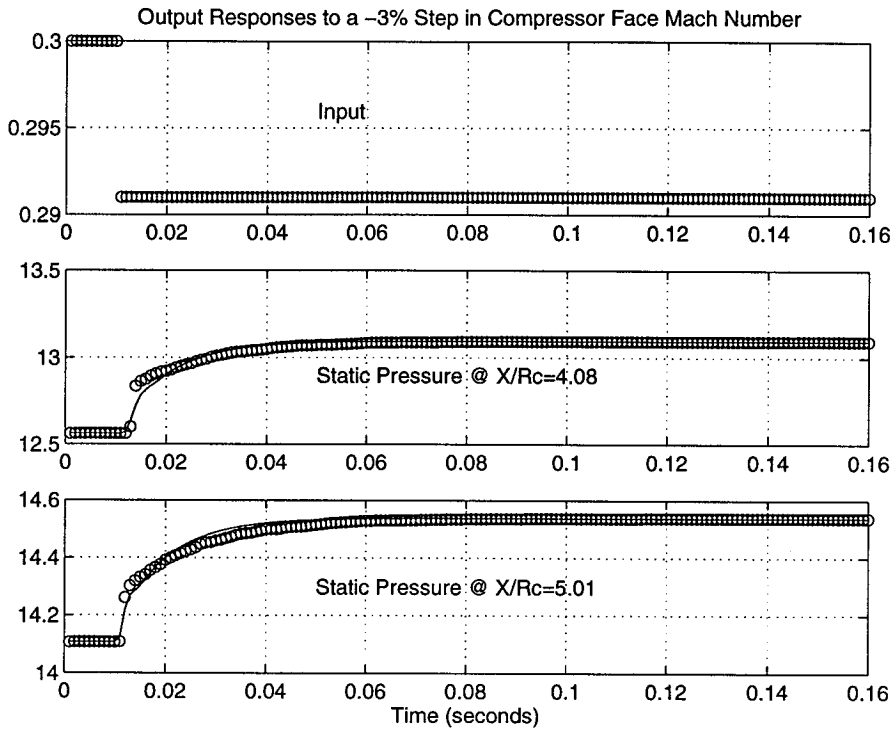

Figure 7: o PARC, 94 × 21 Grid/- Linear ROM, 48 ×3 Grid

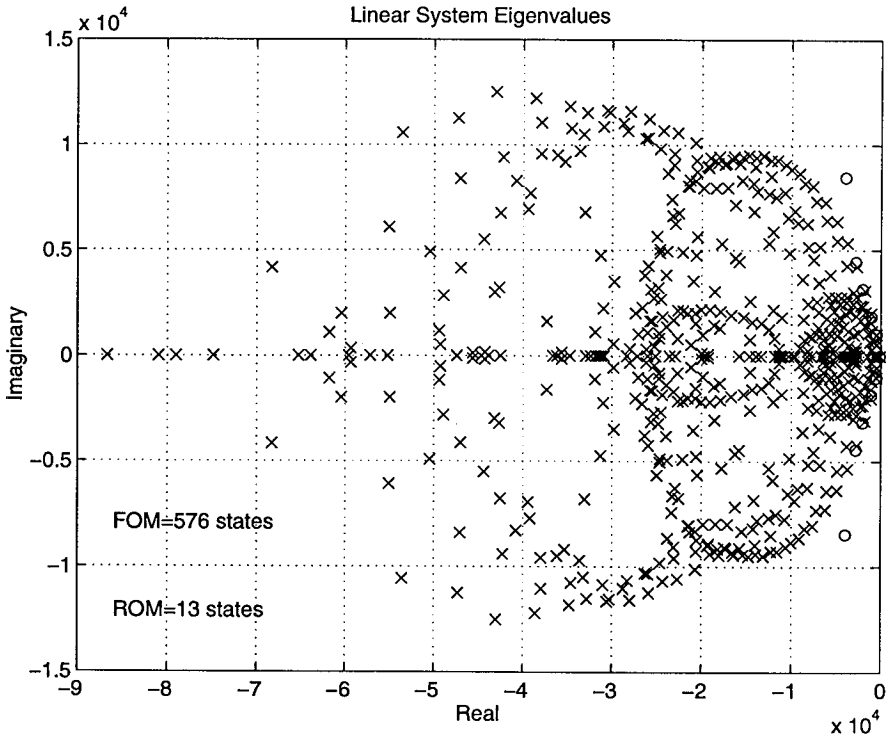

Figure 8: x FOM Eigenvalues/o ROM Eigenvalues

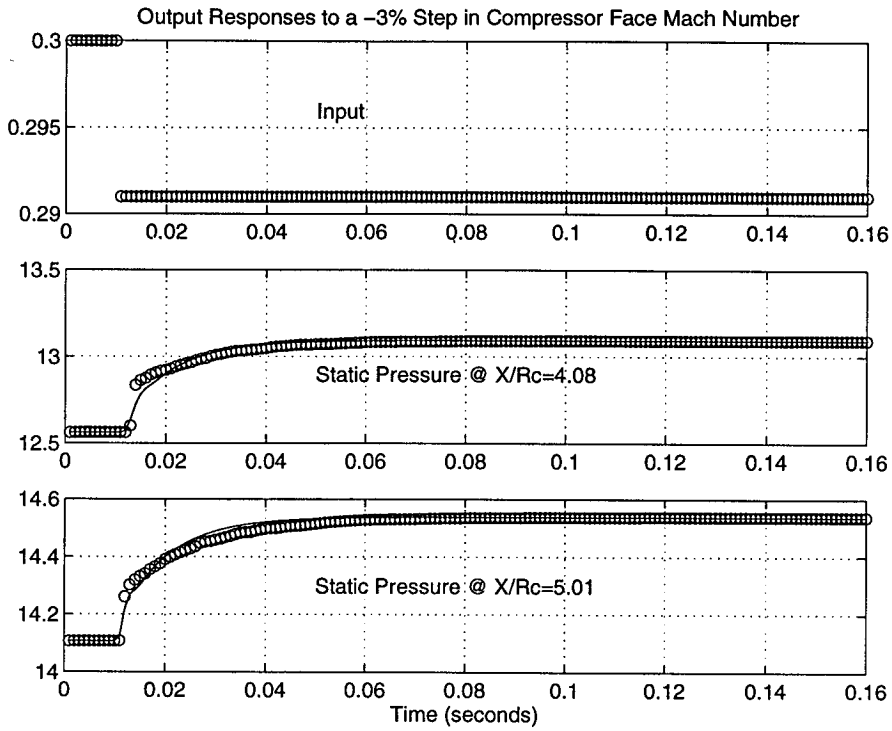

Figure 9: o PARC, 94×21 Grid/- Linear ROM, 48×5 Grid

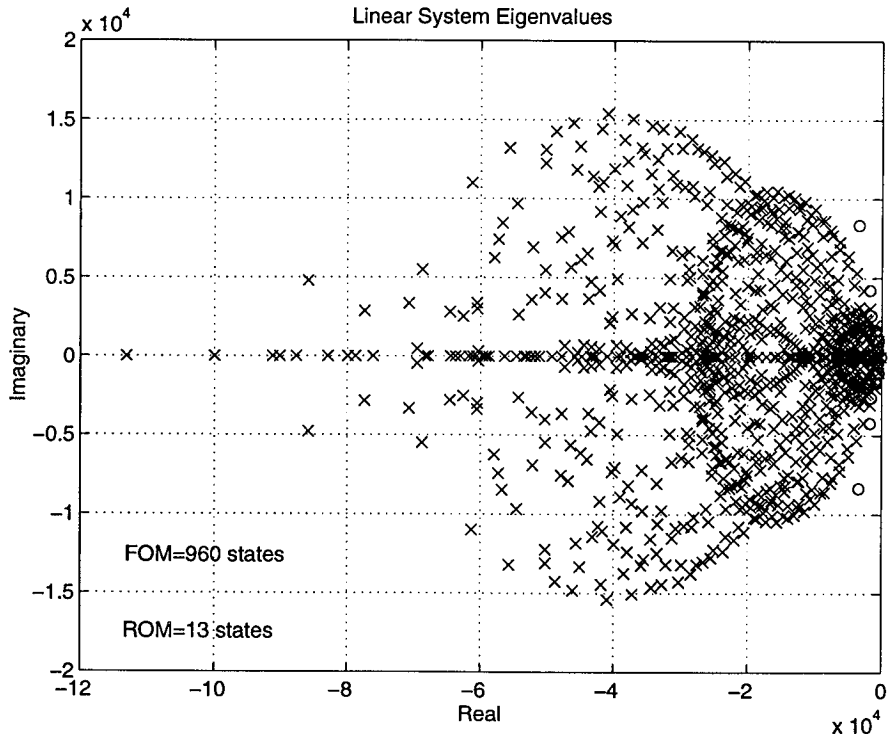

Figure 10: x FOM Eigenvalues/o ROM Eigenvalues

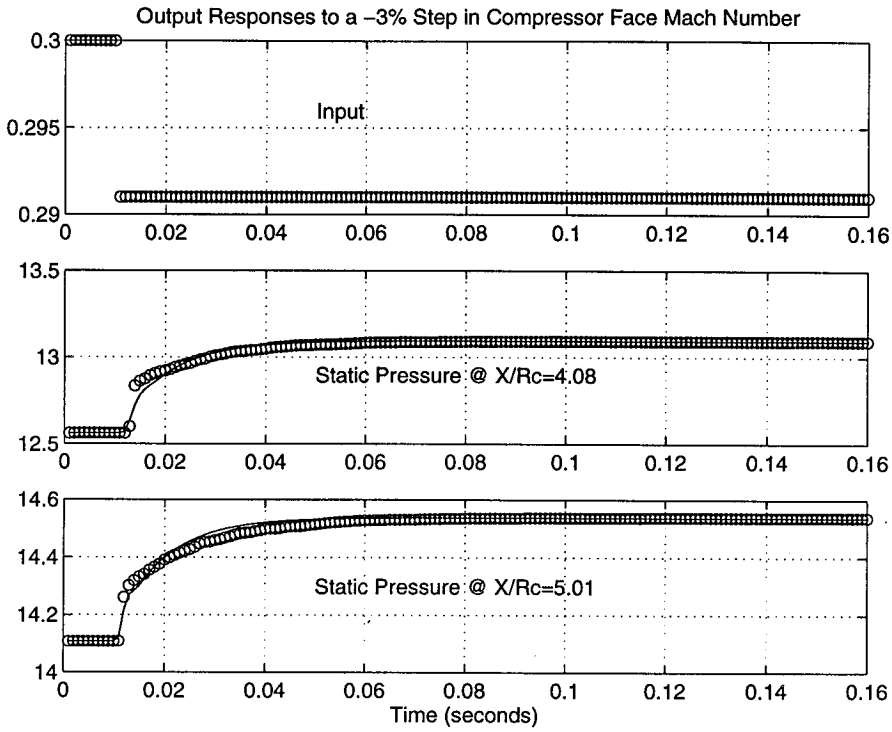

Figure 11: o PARC, 94 × 21 Grid/- Linear ROM, 48 × 7 Grid

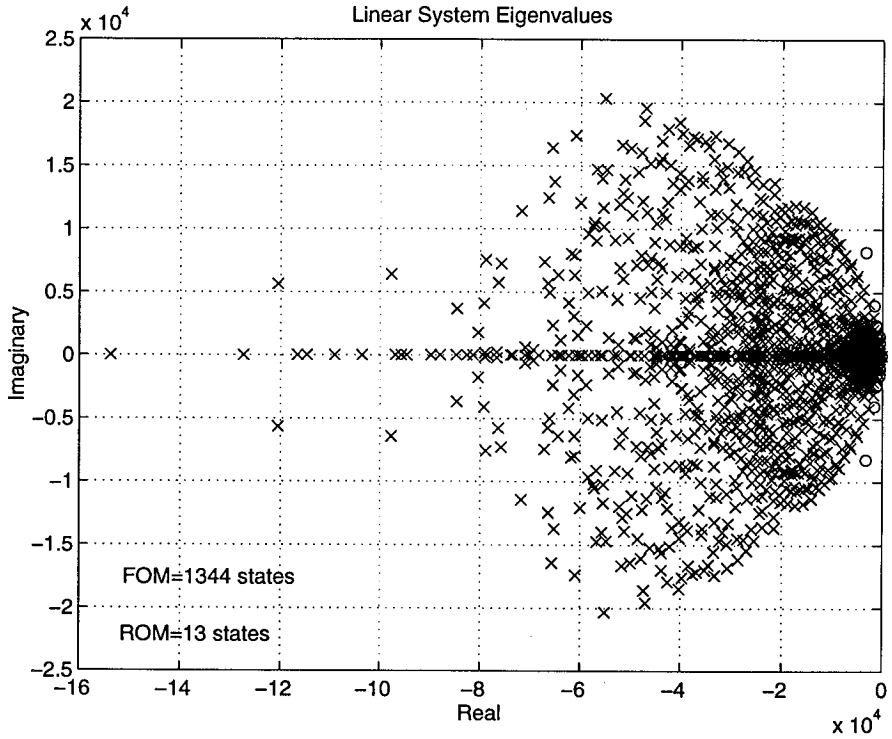

Figure 12: x FOM Eigenvalues/ o ROM Eigenvalues

8.2.2 3D VDC Inlet Model: Downstream Mach Number Perturbation

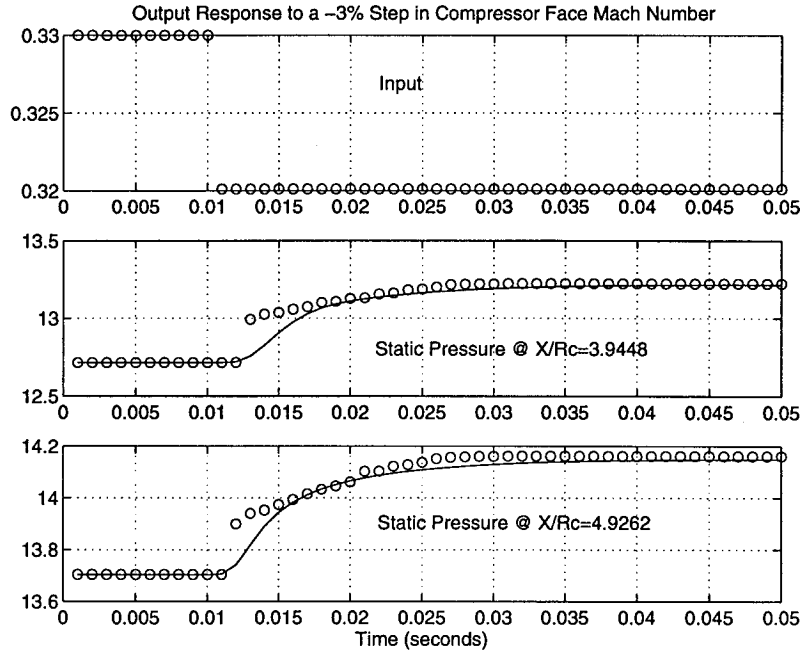

Figure 13: o PARC, $103 \times 15 \times 8$ Grid/- Linear ROM, $15 \times 3 \times 3$ Grid

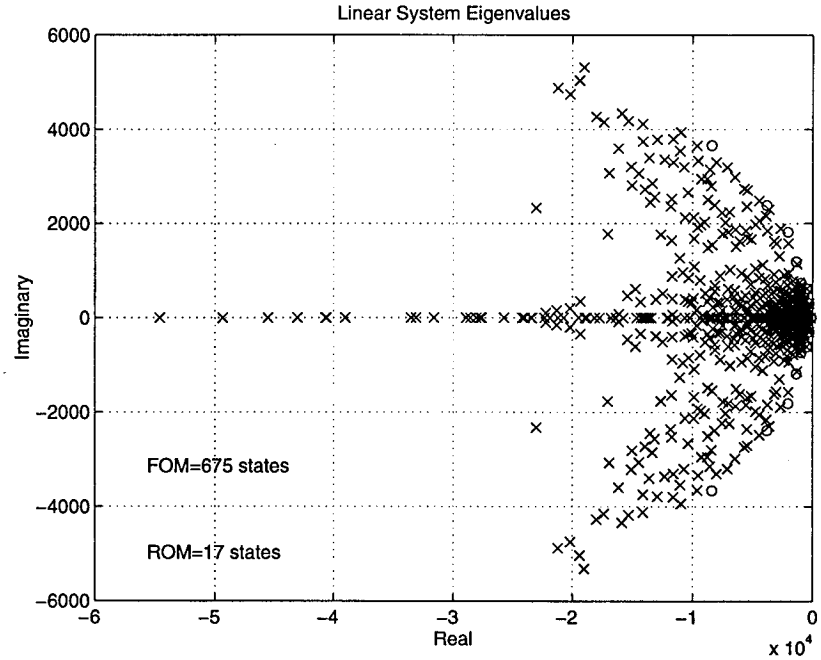

Figure 14: x FOM Eigenvalues/o ROM Eigenvalues

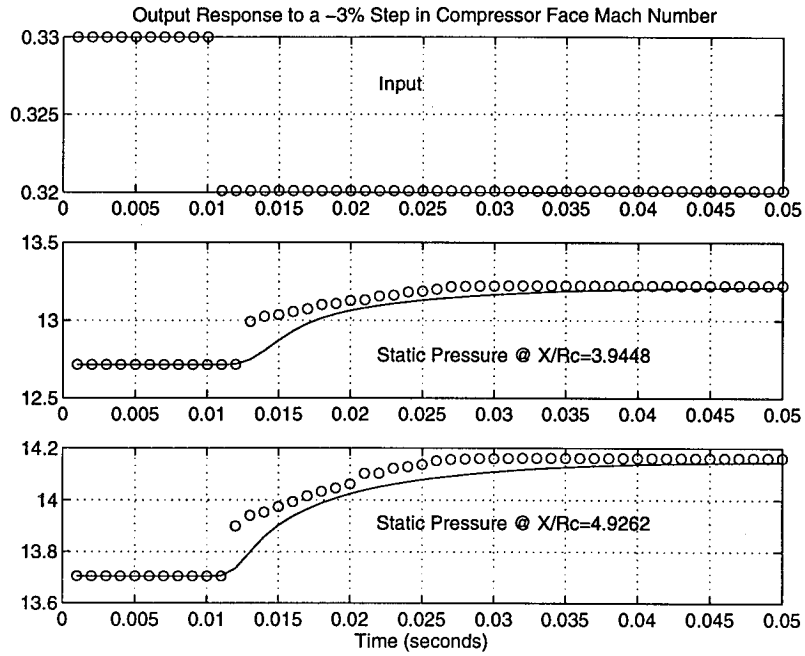

Figure 15: o PARC, $103 \times 15 \times 8$ Grid/- Linear ROM $20 \times 3 \times 3$ Grid

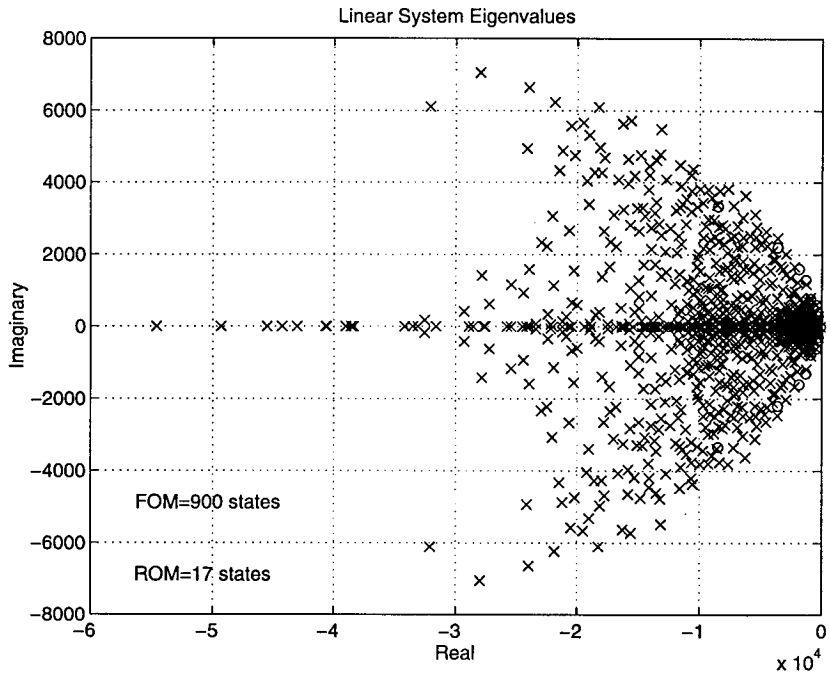

Figure 16: x FOM Eigenvalues/o ROM Eigenvalues

8.2.3 2D VDC Inlet Model: Data Comparison

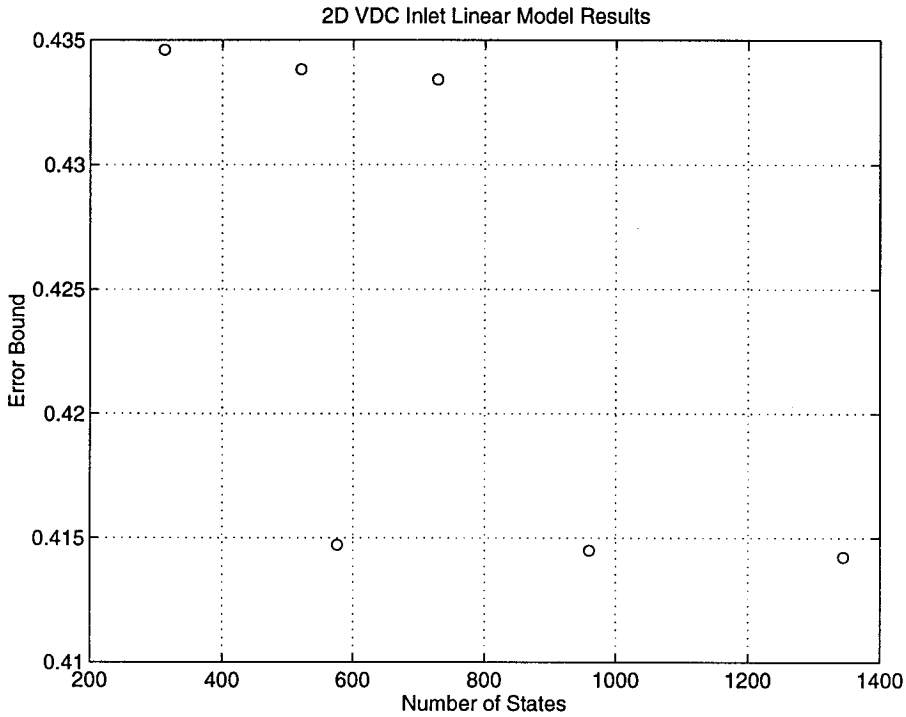

Figure 17: 2D VDC Inlet Linear Model Comparison

2D VDC Inlet Data

Grid	Number of States	Error Bound
26×3	312	0.43461
26×5	520	0.43382
26×7	728	0.43342
48×3	576	0.41472
48×5	960	0.41449
48×5	1344	0.41424

8.2.4 2D VDC Inlet Model: 1D Model from 2D Averaged Data

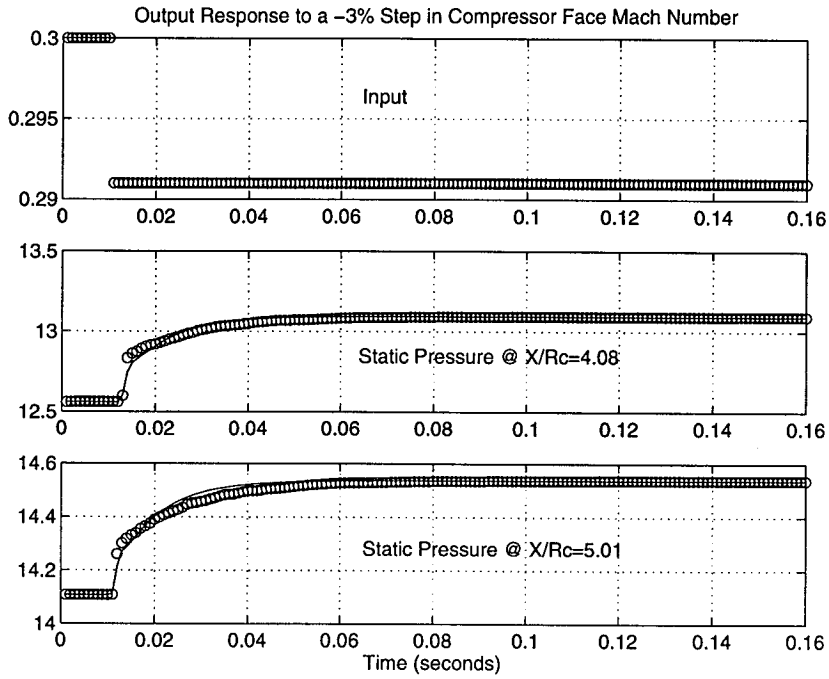

Figure 18: 1D Linear Model Based on 2D Averaged Data

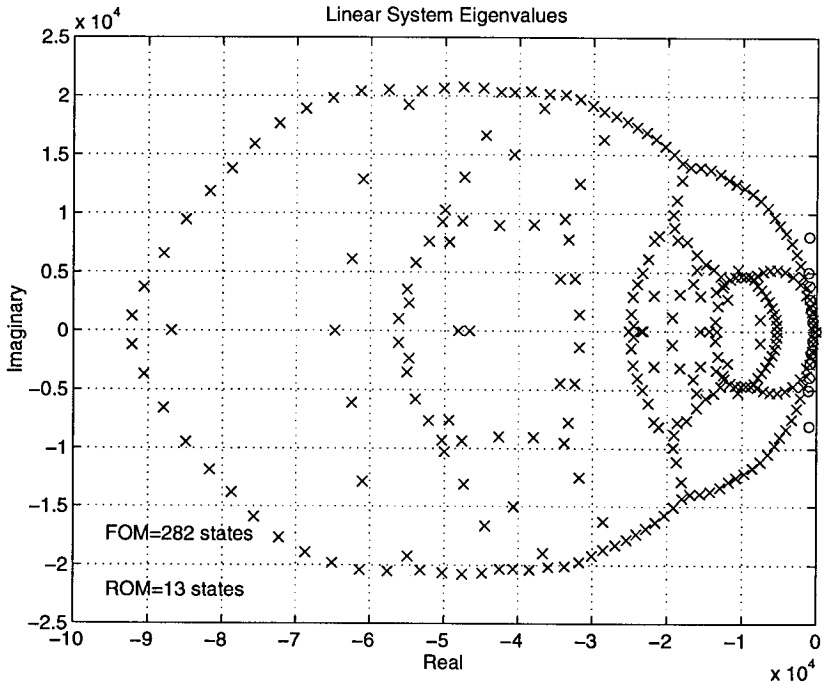

Figure 19: x FOM Eigenvalues/o ROM Eigenvalues

8.2.5 3D VDC Inlet Model: 1D Model from 3D Averaged Data

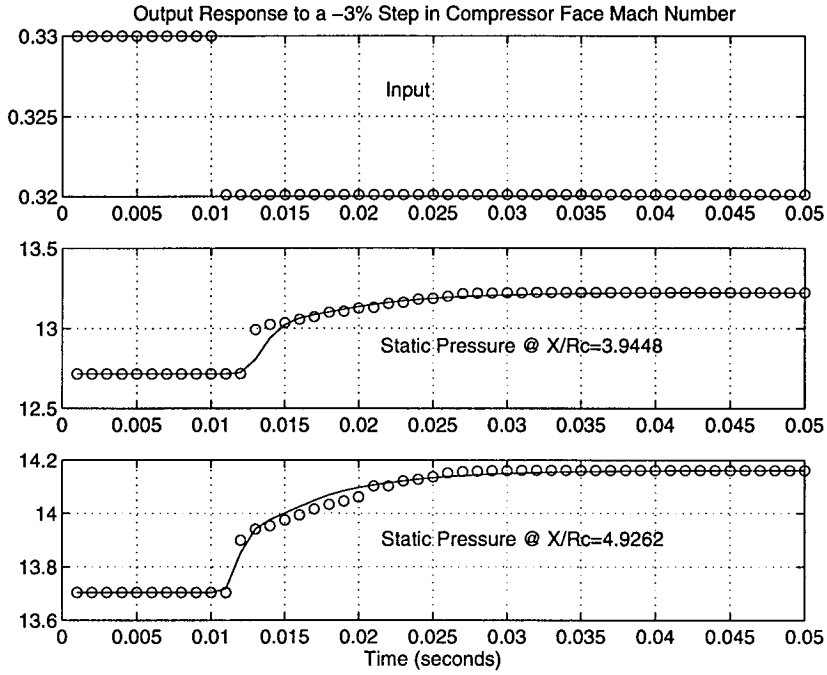

Figure 20: 1D Linear Model Based on 3D Averaged Data

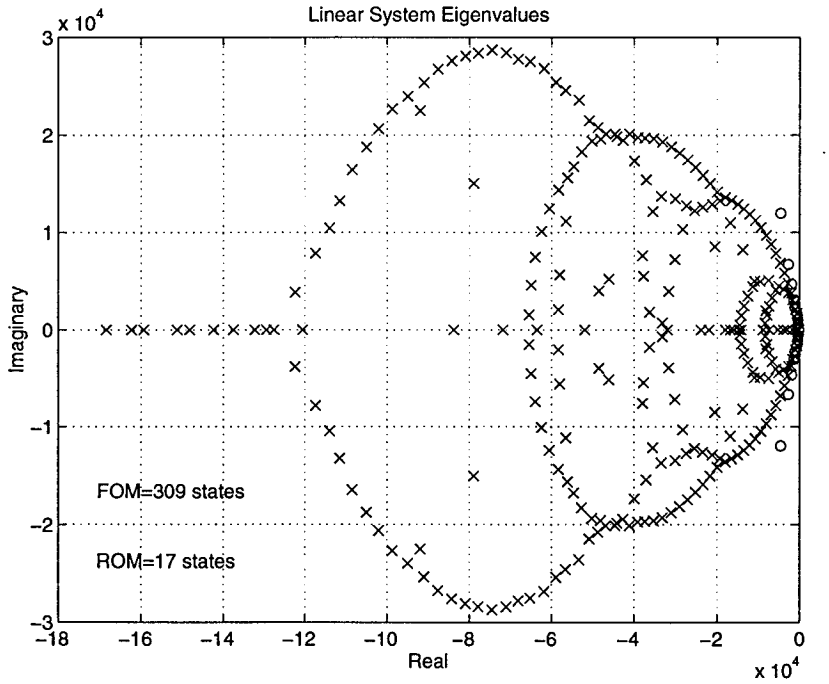

Figure 21: x FOM Eigenvalues/o ROM Eigenvalues

8.3 Matrices for Reduced Order Linear Models

8.3.1 2D VDC Inlet Model: Downstream Mach Number Perturbation

8.3.1.1 26×3 Grid

System Matrix [**A**]

```
 Columns 1 through 6
-1.0255e+002 -1.4033e+002  1.3501e+002 -8.3608e+001  3.4645e+001  1.0379e+002
 2.2093e+002 -3.7917e+002 -1.1727e+003  7.5097e+002  4.9048e+002  1.0045e+002
-1.8683e+002  1.4195e+003 -4.6557e+002  6.5513e+002  5.5007e+002 -5.5065e+002
 1.8411e+002 -9.2390e+002  7.1603e+002 -1.2450e+003 -2.3700e+003  1.2228e+003
-1.3245e+002  4.8332e+002 -8.1438e+002  2.6420e+003 -1.9782e+003 -9.0652e+002
 1.0913e+002 -4.4412e+002  6.3725e+002 -1.6596e+003  3.5833e+003 -4.3863e+003
 2.2540e+001 -9.1965e+001  1.2418e+002 -3.0009e+002  8.0327e+002 -2.1006e+003
-4.0438e+001  1.6202e+002 -2.2395e+002  5.5744e+002 -1.2103e+003  3.7847e+003
 2.1764e+001 -8.7417e+001  1.2041e+002 -2.9822e+002  6.6887e+002 -1.9898e+003
 2.2328e+001 -8.9731e+001  1.2412e+002 -3.0930e+002  6.7680e+002 -1.8642e+003
-1.5298e+001  6.1472e+001 -8.5217e+001  2.1272e+002 -4.6229e+002  1.2176e+003
 4.0977e+000 -1.6449e+001  2.2830e+001 -5.7033e+001  1.2324e+002 -3.2653e+002
-2.5383e+000  1.0197e+001 -1.4137e+001  3.5368e+001 -7.6172e+001  2.0254e+002

 Columns 7 through 12
 1.0069e+001  4.0819e+001 -1.9063e+001 -1.9510e+001 -7.4831e+000  3.6329e+000
 1.1725e+002  5.8929e+001  1.6378e+001  6.1803e+001 -6.7737e+001  5.8024e+000
 8.9505e+001 -1.7056e+002  1.4244e+002  1.6331e+002 -2.7573e+001 -1.3655e+001
-3.4241e+002  3.0550e+002 -3.4980e+002 -3.7484e+002  1.1328e+002  1.8785e+001
-1.0437e+003 -6.8509e+001 -4.0756e+002 -5.4782e+002  4.3561e+002 -3.0598e+001
 7.7816e+002 -3.7345e+003  2.0909e+003  2.2577e+003  2.3524e+002 -2.4656e+002
-4.8341e+002 -1.9894e+003  2.3277e+002 -5.6317e+002  8.7657e+002  1.5314e+001
 2.5063e+003 -3.9720e+003  1.5434e+002  3.2215e+003  1.2781e+003 -9.7361e+002
-1.0047e+003  4.1477e+003 -1.4139e+003 -4.1516e+003  4.1537e+002  5.7451e+002
-9.0363e+002  3.6098e+003 -1.6716e+003 -5.0254e+003 -2.6730e+003  2.2351e+003
 6.1240e+002 -3.1572e+003  1.8972e+003  8.1878e+003 -4.3154e+003  1.9289e+002
-1.7540e+002  8.1722e+002 -5.2263e+002 -1.9743e+003  2.0910e+003 -1.5182e+003
 1.0903e+002 -5.0426e+002  3.4477e+002  1.2017e+003 -1.6925e+003  3.5735e+003

 Column 13
 4.4124e-001
 7.9507e+000
 9.3206e+000
-2.8351e+001
-5.6142e+001
-8.3960e+000
-2.5088e+002
 1.6218e+002
-3.4820e+002
-1.9747e+003
 1.7715e+003
-1.9314e+003
-5.4131e+003
```

Input Matrix [**B**]

```
 9.6540e+002
-8.8858e+002
 7.8651e+002
-8.4196e+002
 6.1995e+002
-5.1694e+002
-1.0622e+002
 1.9015e+002
-1.0237e+002
-1.0507e+002
 7.2004e+001
-1.9283e+001
 1.1952e+001
```

Output Matrix [**C**]

```
 Columns 1 through 6
-6.7767e+002 -8.6623e+002 -7.4260e+001  3.2476e+002  5.3850e+002  2.3275e+002
-6.8859e+002  2.7100e+002  7.8304e+002 -7.8850e+002 -3.1708e+002  4.6508e+002

 Columns 7 through 12
 1.2966e+002  1.1676e+002 -7.9688e+000  1.3084e+001 -6.9400e+001  1.1069e+001
-6.2663e+001  1.5445e+002 -1.2043e+002 -1.3748e+002  1.6733e+001  1.2464e+001

 Column 13
 9.9737e+000
-6.7083e+000
```

Input/Output Matrix [**D**]

```
     0
     0
```

8.3.1.2 26×5 Grid

System Matrix [**A**]

```
 Columns 1 through 6
-1.0130e+002 -1.3867e+002  1.3372e+002 -8.4302e+001 -3.5668e+001 -1.0265e+002
 2.1620e+002 -3.7095e+002 -1.1746e+003  7.6559e+002 -4.9205e+002 -9.9622e+001
-1.8431e+002  1.4165e+003 -4.5959e+002  6.5398e+002 -5.3612e+002  5.5221e+002
 1.8193e+002 -9.1931e+002  7.0664e+002 -1.2391e+003  2.3686e+003 -1.2605e+003
 1.3075e+002 -4.7567e+002  8.0371e+002 -2.6390e+003 -1.9474e+003 -8.9620e+002
-1.0768e+002  4.3814e+002 -6.2956e+002  1.6548e+003  3.5253e+003 -4.3559e+003
 2.6730e+001 -1.0868e+002  1.4745e+002 -3.6009e+002 -9.2160e+002  2.5613e+003
-4.4093e+001  1.7667e+002 -2.4447e+002  6.1256e+002  1.3177e+003 -4.1251e+003
 9.7886e+000 -3.9404e+001  5.4141e+001 -1.3411e+002 -3.0788e+002  8.7511e+002
-2.1988e+001  8.8355e+001 -1.2237e+002  3.0707e+002  6.6459e+002 -1.8396e+003
-1.3105e+001  5.2636e+001 -7.3084e+001  1.8373e+002  3.9430e+002 -1.0467e+003
-1.7192e+000  6.9168e+000 -9.5971e+000  2.4089e+001  5.1498e+001 -1.3869e+002
 4.1066e+000 -1.6513e+001  2.2911e+001 -5.7641e+001 -1.2292e+002  3.3069e+002

 Columns 7 through 12
 7.2251e+000  4.3628e+001 -4.6580e+000  1.8437e+001 -9.0247e+000 -2.2976e+000
 1.1224e+002  6.0941e+001  3.2746e+001 -7.8357e+001 -5.4084e+001 -7.3942e-001
 1.0041e+002 -1.8714e+002  7.9812e+001 -1.6431e+002 -4.9668e+000  1.0593e+001
-3.7172e+002  3.4665e+002 -2.4685e+002  3.7983e+002  5.0626e+001 -8.9564e+000
 1.0192e+003  5.0733e+001  3.9817e+002 -5.9550e+002 -3.2707e+002 -1.0039e+001
-1.0833e+003  4.0840e+003 -7.5038e+002  2.2990e+003 -4.5683e+002 -1.6212e+002
-6.9951e+002 -1.3496e+003 -3.0139e+002  1.3548e+003  7.3993e+002 -8.9542e+001
 2.8122e+003 -5.0362e+003 -1.3600e+003 -4.1973e+003  1.8419e+003  7.1874e+002
-4.1704e+002  3.3567e+003 -2.9282e+002  3.7232e+003  7.4581e+002 -3.0943e+002
 1.0366e+003 -4.0932e+003  3.3911e+002 -5.6575e+003  3.2707e+003  1.2195e+003
 6.5647e+002 -3.1621e+003  6.7849e+002 -8.0595e+003 -4.2062e+003 -8.6596e+002
 9.0397e+001 -3.9964e+002  1.1878e+002 -9.1242e+002 -1.3702e+003 -1.6653e+003
-2.1633e+002  9.5083e+002 -2.8247e+002  2.2335e+003  3.5142e+003  4.6800e+003

 Column 13
 3.4407e+000
-1.9676e+001
-5.0931e+001
 1.0651e+002
-1.5241e+002
 2.8627e+002
 5.9106e+002
-1.7558e+003
 9.0314e+002
-9.9978e+003
-3.3404e+003
 7.7656e+003
-3.2657e+004
```

Input Matrix [B]

```
 9.5925e+002
-8.7457e+002
 7.8027e+002
-8.3652e+002
-6.1544e+002
 5.1305e+002
-1.2664e+002
 2.0856e+002
-4.6323e+001
 1.0408e+002
 6.2041e+001
 8.1399e+000
-1.9454e+001
```

Output Matrix [C]

```
 Columns 1 through 6
-6.7501e+002 -8.6288e+002 -6.8448e+001  3.2103e+002 -5.3706e+002 -2.3012e+002
-6.8408e+002  2.7743e+002  7.7683e+002 -7.8971e+002  3.0941e+002 -4.6601e+002

 Columns 7 through 12
 1.2159e+002  1.2135e+002  3.0474e+001 -2.4111e+001 -6.1034e+001 -5.1730e+000
-7.4744e+001  1.7143e+002 -6.4954e+001  1.3897e+002 -1.3402e+000 -9.1019e+000

 Column 13
-1.7028e+001
 3.8283e+001
```

Input/Output Matrix [D]

```
     0
     0
```

8.3.1.3 26×7 Grid

System Matrix [**A**]

```
 Columns 1 through 6
-1.0094e+002 -1.3798e+002  1.3332e+002 -8.4070e+001 -3.6817e+001 -1.0216e+002
 2.1573e+002 -3.7070e+002 -1.1756e+003  7.6819e+002 -4.8668e+002 -9.5743e+001
-1.8327e+002  1.4143e+003 -4.5510e+002  6.4886e+002 -5.2640e+002  5.5463e+002
 1.8062e+002 -9.1530e+002  6.9857e+002 -1.2265e+003  2.3685e+003 -1.2827e+003
 1.3007e+002 -4.7378e+002  7.9585e+002 -2.6273e+003 -1.9263e+003 -8.9618e+002
-1.0753e+002  4.3790e+002 -6.2659e+002  1.6508e+003  3.5024e+003 -4.3563e+003
 2.7303e+001 -1.1115e+002  1.4999e+002 -3.6590e+002 -9.3486e+002  2.6306e+003
-4.4105e+001  1.7693e+002 -2.4365e+002  6.1090e+002  1.3110e+003 -4.1186e+003
 5.5409e+000 -2.2388e+001  3.0435e+001 -7.4701e+001 -1.7837e+002  4.9365e+002
-2.3940e+001  9.6304e+001 -1.3274e+002  3.3332e+002  7.1945e+002 -2.0037e+003
-1.2842e+001  5.1639e+001 -7.1353e+001  1.7951e+002  3.8441e+002 -1.0273e+003
-1.3565e+000  5.4588e+000 -7.5427e+000  1.8946e+001  4.0374e+001 -1.0956e+002
 3.9972e+000 -1.6089e+001  2.2219e+001 -5.5950e+001 -1.1891e+002  3.2262e+002

 Columns 7 through 12
 7.3147e+000  4.3408e+001 -1.3041e+000  1.7895e+001 -8.8425e+000 -2.4964e+000
 1.1409e+002  5.8557e+001  3.3388e+001 -7.1789e+001 -5.3681e+001 -1.9640e+000
 1.0414e+002 -1.8876e+002  6.2528e+001 -1.6068e+002 -2.8642e+000  9.1749e+000
-3.9134e+002  3.5501e+002 -2.1222e+002  3.7902e+002  4.3260e+001 -2.8165e+000
 1.0075e+003  5.1882e+001  3.5019e+002 -5.5588e+002 -3.2941e+002 -5.1386e+000
-1.1153e+003  4.0569e+003 -3.9396e+002  2.2047e+003 -4.2147e+002 -2.0042e+002
-7.1866e+002 -1.2480e+003 -3.2944e+002  1.3015e+003  7.1261e+002 -6.5397e+001
 2.7725e+003 -5.1324e+003 -1.8005e+003 -3.9944e+003  1.7808e+003  7.9735e+002
-1.8722e+002  2.8397e+003 -8.9068e+001  2.8489e+003  8.6305e+002 -2.2395e+002
 1.1408e+003 -4.5755e+003 -2.1092e+001 -6.0759e+003  3.0742e+003  1.1337e+003
 6.4883e+002 -3.1493e+003  3.1203e+002 -7.6279e+003 -4.1982e+003 -9.4632e+002
 7.1734e+001 -3.2147e+002  4.9978e+001 -6.9491e+002 -9.2567e+002 -1.0687e+003
-2.1170e+002  9.4532e+002 -1.5810e+002  2.1186e+003  3.3551e+003  5.1491e+003

 Column 13
 3.7291e+000
-1.9685e+001
-4.8379e+001
 9.9238e+001
-2.0361e+002
 4.3820e+002
 5.2903e+002
-1.9198e+003
 6.2660e+002
-8.8375e+003
-3.7006e+003
 1.9702e+003
-3.1368e+004
```

Input Matrix [B]

```
 9.5738e+002
-8.7445e+002
 7.7681e+002
-8.3179e+002
-6.1311e+002
 5.1318e+002
-1.2957e+002
 2.0897e+002
-2.6269e+001
 1.1351e+002
 6.0896e+001
 6.4309e+000
-1.8967e+001
```

Output Matrix [C]

```
  Columns 1 through 6
-6.7403e+002 -8.6047e+002 -6.7453e+001  3.2312e+002 -5.3624e+002 -2.2718e+002
-6.8243e+002  2.7756e+002  7.7503e+002 -7.9089e+002  3.0228e+002 -4.6766e+002

  Columns 7 through 12
 1.2373e+002  1.1940e+002  3.6240e+001 -2.3144e+001 -5.9665e+001 -6.7813e+000
-7.7027e+001  1.7281e+002 -4.8324e+001  1.3570e+002 -1.8189e+000 -9.3922e+000

  Column 13
-1.5488e+001
 4.1400e+001
```

Input/Output Matrix [D]

```
     0
     0
```

8.3.1.4 48×3 Grid

System Matrix [**A**]

```
 Columns 1 through 6
-1.0483e+002 -1.9628e+002  1.2608e+002 -1.0084e+002  3.2454e+001  1.3399e+002
 2.5622e+002 -2.8724e+002 -1.2499e+003  2.7453e+002  4.4786e+002  2.3388e+002
-2.3583e+002  1.4265e+003 -5.2074e+002  4.7068e+002  9.9519e+002 -3.6918e+002
 1.5793e+002 -5.2051e+002  5.1647e+002 -5.5848e+002 -2.2011e+003  9.3637e+002
-1.6230e+002  4.0304e+002 -1.0421e+003  2.3818e+003 -1.2281e+003 -1.1625e+003
 1.3473e+002 -4.2055e+002  7.1668e+002 -1.2319e+003  2.5626e+003 -2.2635e+003
-5.8742e+000  1.8187e+001 -2.4751e+001  3.2393e+001 -1.4856e+002  4.2708e+002
-8.1706e+001  2.3803e+002 -3.9587e+002  5.8413e+002 -1.2593e+003  3.8865e+003
-5.0294e+001  1.4895e+002 -2.4552e+002  3.6853e+002 -8.0614e+002  1.8197e+003
-1.8189e+001  5.3657e+001 -9.0158e+001  1.3775e+002 -2.8291e+002  5.6571e+002
-2.2756e+001  6.7384e+001 -1.1268e+002  1.7121e+002 -3.4955e+002  6.9668e+002
 1.4650e+001 -4.3277e+001  7.2654e+001 -1.1063e+002  2.2303e+002 -4.8167e+002
 6.4721e+000 -1.9292e+001  3.2306e+001 -4.8944e+001  9.8268e+001 -2.1911e+002

 Columns 7 through 12
 9.6708e+000  8.8381e+001  2.8703e+001 -1.7045e+001 -3.6775e+001  1.7547e+001
-5.5568e+001  1.0082e+002 -1.0002e+002 -9.7755e+000 -9.4945e+001 -3.7994e+001
-1.4053e+002 -2.2539e+002 -2.9719e+002  5.8658e+001  1.9830e+001 -1.8108e+002
 1.8357e+002  4.4622e+002  3.9332e+002 -1.2578e+002 -5.6875e+001  2.7848e+002
 5.1149e+002  1.5517e+002  8.7505e+002  8.8372e+001  1.5213e+000  5.9753e+002
-7.9759e+002 -4.2275e+003 -1.5345e+003  4.5363e+002  1.2998e+003 -5.3892e+002
-1.4526e+001  1.8236e+003 -7.6998e+002  1.6516e+002  4.5397e+001 -1.5606e+003
-2.1361e+003 -2.7675e+003 -6.5346e+002  1.4433e+003  3.1795e+003 -2.7789e+003
 3.8276e+001 -3.1697e+003 -2.7704e+003  2.8469e+003  3.3216e+003 -7.1778e+003
-1.3928e+002 -1.5628e+003 -3.5625e+003 -2.8863e+002 -4.5229e+003  2.9258e+003
-1.2722e+002 -1.9778e+003 -3.6405e+003  1.5949e+003 -1.4218e+003 -1.5476e+003
 8.1512e+001  1.0234e+003  1.8274e+003  9.8400e+002  2.2969e+003 -9.1383e+003
 1.1508e+001  4.4335e+002  7.3170e+002  8.6116e+002  1.2048e+003 -8.5998e+003

 Column 13
-3.2506e+000
 1.0952e+001
 6.8427e+001
-1.2273e+002
-1.4504e+002
-1.1634e+001
 6.2712e+002
 8.9129e+002
 3.0751e+003
-1.3937e+003
 1.1527e+003
 5.3541e+003
-4.2265e+002
```

Input Matrix [**B**]

```
 9.9631e+002
-9.2447e+002
 9.9931e+002
-7.0536e+002
 7.6353e+002
-6.5291e+002
 2.7642e+001
 3.8592e+002
 2.3861e+002
 8.6305e+001
 1.0810e+002
-6.9656e+001
-3.0899e+001
```

Output Matrix [**C**]

```
 Columns 1 through 6
-6.8180e+002 -9.3312e+002 -4.1095e+002  1.1514e+002  6.9145e+002  3.9987e+002
-7.2794e+002  1.3294e+002  8.9597e+002 -6.7167e+002 -4.7058e+002  5.2363e+002

 Columns 7 through 12
-7.5019e+001  2.2344e+002 -1.0630e+002 -4.2305e+001 -1.4597e+002 -4.4552e+001
 1.3009e+002  3.5647e+002  2.7348e+002 -6.5985e+001 -1.0972e+002  1.6872e+002

 Column 13
 2.6625e+001
-5.1848e+001
```

Input/Output Matrix [**D**]

```
     0
     0
```

8.3.1.5 48 × 5 Grid

System Matrix [**A**]

```
 Columns 1 through 6
-1.0455e+002 -1.9623e+002  1.2796e+002 -1.0679e+002  2.8222e+001  1.3286e+002
 2.4939e+002 -2.7304e+002 -1.2457e+003  2.6547e+002  4.8648e+002  2.2737e+002
-2.3701e+002  1.4268e+003 -5.2322e+002  4.7425e+002  1.0004e+003 -3.2782e+002
 1.6106e+002 -5.1776e+002  5.3116e+002 -5.8328e+002 -2.1959e+003  9.0265e+002
-1.6248e+002  3.8723e+002 -1.0488e+003  2.4369e+003 -1.2197e+003 -1.1346e+003
 1.3445e+002 -4.1173e+002  7.1160e+002 -1.2488e+003  2.5172e+003 -2.2774e+003
-2.1338e+001  5.9735e+001 -1.0788e+002  1.6919e+002 -2.6683e+002  8.6235e+002
 7.5448e+001 -2.1514e+002  3.6488e+002 -5.4693e+002  1.1850e+003 -3.6783e+003
-4.6193e+001  1.3427e+002 -2.2532e+002  3.4517e+002 -7.3878e+002  1.7351e+003
 3.6405e+001 -1.0590e+002  1.8048e+002 -2.8175e+002  5.5866e+002 -1.1426e+003
-2.1556e+000  6.5082e+000 -1.0495e+001  1.6038e+001 -3.3701e+001  5.1640e+001
 1.3818e+001 -4.0038e+001  6.8588e+001 -1.0712e+002  2.0881e+002 -4.5851e+002
-7.3590e+000  2.1405e+001 -3.6831e+001  5.7324e+001 -1.1005e+002  2.5131e+002

 Columns 7 through 12
 1.8045e+001 -8.8483e+001  3.2974e+001  3.4044e+001 -1.0968e+001  1.5509e+001
 9.4530e+001 -1.2600e+002 -8.2547e+001  8.7920e+001 -1.1126e+002 -6.8768e+001
 8.5641e+001  2.6765e+002 -3.0785e+002 -7.4962e+000 -1.1002e+002 -1.7561e+002
-8.1814e+001 -5.5609e+002  4.4131e+002  8.6144e+001  9.9207e+001  2.5569e+002
-4.6196e+002 -4.6918e+002  9.0296e+002 -2.1406e+002  1.4286e+002  5.1793e+002
-5.0774e+002  4.3305e+003 -1.7812e+003 -1.1103e+003  6.5584e+002 -3.5196e+002
-1.8170e+002  2.7981e+003  1.6803e+002 -8.2331e+002  5.1974e+002  1.1448e+003
-1.2323e+003 -2.4868e+003  9.2563e+002  2.9132e+003  2.7243e+002  3.3454e+003
-8.3553e+002  2.6807e+003 -2.2497e+003 -3.4683e+003 -1.2280e+003 -7.4550e+003
 7.5695e+002 -3.0490e+003  5.2248e+003 -2.5891e+003  4.5829e+003 -2.7171e+002
-9.3351e+001  9.2561e+001  1.5412e+002 -2.2558e+003  7.2950e+001 -2.4987e+003
 2.2026e+002 -9.5159e+002  1.5415e+003 -2.2074e+003  4.2164e+002 -8.4456e+003
-1.3483e+002  4.5876e+002 -7.2494e+002  1.6582e+003  2.8144e+002  1.0547e+004

 Column 13
 5.5730e+000
-1.5162e+001
-6.1750e+001
 9.8114e+001
 1.0258e+002
-4.2661e+001
 4.0652e+002
 1.3328e+003
-3.0297e+003
-5.2930e+002
-1.5980e+003
-4.7722e+003
 3.4494e+003
```

Input Matrix [**B**]

```
 9.9516e+002
-8.9662e+002
 1.0041e+003
-7.1895e+002
 7.6645e+002
-6.5235e+002
 1.0104e+002
-3.5682e+002
 2.1942e+002
-1.7330e+002
 1.0295e+001
-6.5821e+001
 3.5145e+001
```

Output Matrix [**C**]

```
 Columns 1 through 6
-6.8178e+002 -9.4470e+002 -3.9999e+002  9.1059e+001  6.8014e+002  4.0995e+002
-7.2780e+002  1.4996e+002  8.9168e+002 -6.7764e+002 -4.7990e+002  5.1178e+002

 Columns 7 through 12
 1.5453e+002 -2.0383e+002 -8.8999e+001  1.5096e+002 -1.1461e+002 -5.8842e+001
-2.7551e+001 -3.8939e+002  2.8982e+002  8.4253e+001  1.0722e+001  1.6015e+002

 Column 13
-1.8861e+001
 5.3164e+001
```

Input/Output Matrix [**D**]

```
     0
     0
```

8.3.1.6 48×7 Grid

System Matrix [**A**]

```
 Columns 1 through 6
-1.0409e+002 -1.9907e+002  1.2492e+002 -1.1088e+002  2.9894e+001  1.3320e+002
 2.4836e+002 -2.6835e+002 -1.2575e+003  2.8630e+002  4.5674e+002  2.5421e+002
-2.3417e+002  1.4292e+003 -5.0954e+002  4.7450e+002  9.9335e+002 -3.3624e+002
 1.5853e+002 -5.1215e+002  5.0959e+002 -5.6875e+002 -2.1924e+003  9.5962e+002
-1.6412e+002  3.9156e+002 -1.0466e+003  2.4773e+003 -1.2193e+003 -1.0894e+003
 1.3282e+002 -4.0580e+002  6.9360e+002 -1.2409e+003  2.4404e+003 -2.2563e+003
-6.9811e+001  1.9870e+002 -3.3085e+002  4.9540e+002 -1.1131e+003  3.4127e+003
 5.7087e+001 -1.6083e+002  2.7634e+002 -4.2284e+002  8.3062e+002 -2.6048e+003
-4.7621e+001  1.3787e+002 -2.2965e+002  3.5650e+002 -7.5180e+002  1.7062e+003
-3.0830e+001  8.8913e+001 -1.5121e+002  2.3932e+002 -4.6115e+002  9.3352e+002
-1.2461e+001  3.6196e+001 -6.0560e+001  9.4811e+001 -1.9195e+002  4.0328e+002
-1.7659e+001  5.0840e+001 -8.6416e+001  1.3609e+002 -2.6390e+002  5.9107e+002
 3.8254e+000 -1.1058e+001  1.9034e+001 -2.9548e+001  5.6577e+001 -1.3604e+002

 Columns 7 through 12
 6.5031e+001 -5.7400e+001  1.5414e+001 -4.1640e+001 -1.1395e+001 -1.1287e+001
 5.3521e+001 -1.4669e+002 -1.2756e+002 -7.5931e+000 -1.2589e+002  2.5567e+001
-2.7061e+002  4.4545e+001 -2.7571e+002  1.4344e+002 -1.2242e+002  8.9461e+001
 5.4572e+002 -2.1265e+002  3.5902e+002 -2.6316e+002  7.4182e+001 -1.6091e+002
 5.9517e+002  1.9508e+002  9.1517e+002 -1.9123e+002  3.4736e+002 -3.0721e+002
-3.3884e+003  2.4739e+003 -1.1191e+003  1.6542e+003  3.6784e+002  3.9405e+002
-1.8312e+003 -3.2676e+002 -1.3111e+003  2.6818e+003 -6.1243e+002  1.0956e+003
 3.2844e+003 -1.3877e+003 -2.5450e+002 -2.4940e+003 -5.4361e+002 -9.1853e+001
-2.0740e+003  2.4228e+003 -2.5366e+003  3.7422e+003 -1.8956e+003  3.4725e+003
-2.0697e+003  1.9727e+003 -4.9978e+003 -1.9697e+003 -6.1339e+003 -4.3988e+003
-5.7788e+002  6.7734e+002 -6.3573e+002  2.8427e+003 -4.3431e+002  2.4845e+003
-9.4256e+002  8.6056e+002 -2.0691e+003 -2.5017e+003 -1.5847e+003 -9.2850e+003
 1.9036e+002 -1.8292e+002  4.4304e+002  1.0769e+003  1.0643e+002  4.8257e+003

 Column 13
-1.2417e+001
 2.1396e+001
 1.2171e+002
-1.9983e+002
-2.4419e+002
 2.0158e+002
 1.4490e+003
-1.3702e+002
 4.8391e+003
-7.6598e+003
 5.0499e+003
-1.4888e+004
 6.6320e+003
```

Input Matrix [B]

```
 9.9293e+002
-8.8926e+002
 9.9478e+002
-7.0708e+002
 7.7543e+002
-6.4590e+002
 3.3104e+002
-2.7082e+002
 2.2690e+002
 1.4710e+002
 5.9450e+001
 8.4334e+001
-1.8368e+001
```

Output Matrix [C]

```
 Columns 1 through 6
-6.8252e+002 -9.4337e+002 -4.1131e+002  8.2356e+001  6.7933e+002  4.0654e+002
-7.2855e+002  1.4783e+002  8.9199e+002 -6.8364e+002 -4.6891e+002  5.1561e+002

 Columns 7 through 12
 9.3072e+001 -2.3150e+002 -1.4495e+002 -7.8913e+001 -1.3905e+002  2.2953e+001
 3.4574e+002 -1.6555e+002  2.3060e+002 -1.8832e+002  3.4148e+001 -9.9862e+001

 Column 13
 3.6269e+001
-1.1410e+002
```

Input/Output Matrix [D]

```
     0
     0
```

8.3.2 3D VDC Inlet Model: Downstream Mach Number Perturbation

8.3.2.1 $15 \times 3 \times 3$ Grid

System Matrix [**A**]

```
 Columns 1 through 6
-8.9089e+001 -2.8477e+002 -3.1694e+001 -1.4626e+001 -1.5213e+001  3.9396e+001
 2.9149e+002 -4.0097e+002 -6.5305e+002 -7.6740e-001  2.1118e+001  1.4638e+002
-1.4482e+002  8.2662e+002 -5.4169e+002  9.9530e+001  8.6629e+002  3.6901e+001
 3.2395e+001 -1.2348e+002  1.9769e+002 -7.1802e+001 -1.0769e+003  1.4102e+002
-1.0587e+002  4.1102e+002 -9.4458e+002  1.0870e+003 -1.4188e+003 -1.0237e+002
 3.9694e+001 -1.5959e+002  2.8944e+002 -2.1048e+002  1.1077e+003 -5.3801e+002
 4.3595e+001 -1.6895e+002  3.1327e+002 -1.8525e+002  1.2994e+003 -1.4850e+003
-2.1687e+001  8.4185e+001 -1.5718e+002  9.5383e+001 -6.0640e+002  6.2848e+002
 1.3773e+001 -5.3478e+001  1.0076e+002 -6.2517e+001  3.6381e+002 -3.7131e+002
-1.1264e+001  4.3730e+001 -8.2295e+001  5.0883e+001 -2.9995e+002  3.0688e+002
 5.3664e+000 -2.0851e+001  3.9162e+001 -2.4234e+001  1.4336e+002 -1.4346e+002
-6.7474e+000  2.6213e+001 -4.9248e+001  3.0470e+001 -1.8017e+002  1.8097e+002
 1.6037e+000 -6.2298e+000  1.1705e+001 -7.2391e+000  4.2844e+001 -4.3122e+001
-1.2031e+000  4.6735e+000 -8.7810e+000  5.4311e+000 -3.2139e+001  3.2343e+001
-4.0208e-001  1.5620e+000 -2.9351e+000  1.8147e+000 -1.0739e+001  1.0804e+001
-3.3726e-001  1.3101e+000 -2.4603e+000  1.5216e+000 -9.0137e+000  9.0699e+000
 3.0765e-001 -1.1951e+000  2.2452e+000 -1.3885e+000  8.2194e+000 -8.2703e+000

 Columns 7 through 12
-1.9546e+001  8.4557e+000 -2.6019e+000  9.0706e+000  5.3139e+000 -6.1248e+000
-2.7240e+001  8.5437e+000 -2.4834e+001  4.1180e+001  2.0660e+001 -1.9513e+001
 2.1635e+002 -1.1723e+002 -9.9812e+001  6.7762e+001  1.8274e+001  5.5233e+000
-1.8545e+002  9.5964e+001  5.0899e+001 -1.0573e+001  6.5951e+000 -2.3554e+001
-1.2541e+003  5.9512e+002  3.4117e+002 -1.3407e+002  1.5380e+000 -1.0364e+002
 1.0853e+003 -3.7373e+002  3.3420e+001 -2.2376e+002 -1.3792e+002  1.7364e+002
-2.1997e+003  1.5421e+003  1.2776e+003 -2.6957e+002  1.7595e+002 -5.4335e+002
 1.5388e+003 -1.2908e+003 -1.9337e+003  5.3048e+002 -1.8416e+002  6.1092e+002
-1.5335e+003  2.1500e+003 -1.9758e+003  8.0054e+002  8.2780e+002  3.4747e+002
 1.1549e+003 -1.4212e+003  2.7745e+003 -2.3123e+003 -2.9372e+003  1.7109e+003
-5.4566e+002  6.4794e+002 -1.6890e+003  3.1305e+003 -1.6625e+003  2.1396e+003
 6.8607e+002 -8.1534e+002  1.9103e+003 -2.9995e+003  3.3137e+003 -6.3908e+003
-1.6192e+002  1.9075e+002 -4.6009e+002  6.5408e+002 -1.0364e+003  3.3619e+003
 1.2151e+002 -1.4326e+002  3.4526e+002 -4.9150e+002  7.5270e+002 -2.3743e+003
 4.0631e+001 -4.7967e+001  1.1557e+002 -1.6386e+002  2.4338e+002 -7.6408e+002
 3.4040e+001 -3.9972e+001  9.6734e+001 -1.4433e+002  2.1839e+002 -6.0228e+002
-3.1072e+001  3.6597e+001 -8.8326e+001  1.2768e+002 -1.9278e+002  5.7996e+002

 Columns 13 through 17
-1.5649e+000  1.4593e+000 -5.5831e-001 -4.2748e-001 -1.4646e+000
-5.5232e+000  4.8371e+000 -2.3537e+000 -1.5652e+000 -4.0649e+000
-1.7775e+000 -3.6660e-001 -2.9280e+000 -7.8528e-001  5.3497e+000
-4.1420e+000  5.0086e+000 -9.2137e-002 -9.2730e-001 -7.9436e+000
-1.4186e+001  2.0580e+001  3.9183e+000 -2.5391e+000 -3.9295e+001
 4.2598e+001 -3.9931e+001  1.3587e+001  1.1078e+001  4.1809e+001
-9.5518e+001  1.1678e+002 -4.4895e+000 -2.2706e+001 -1.8336e+002
 1.0522e+002 -1.4183e+002  6.0799e+000  2.9167e+001  2.3211e+002
-3.0088e+000 -7.9331e+001 -9.5073e+001 -1.2709e+001  2.8491e+002
 4.4558e+002 -3.4288e+002  2.3974e+002  1.3096e+002  1.6351e+002
 9.7643e+002 -8.3997e+002  3.5764e+002  2.5426e+002  7.5737e+002
-3.2367e+003  3.2056e+003 -8.5378e+002 -8.5345e+002 -3.9281e+003
-3.6401e+003  5.9916e+003 -2.5077e+003 -1.9577e+003 -7.4874e+003
 4.0288e+003 -8.3056e+003  5.3972e+003  2.5718e+003  1.0405e+004
 2.0885e+003 -7.5987e+003 -1.8870e+003  2.6544e+003  1.1980e+004
 1.5413e+003 -5.7425e+003 -7.0291e+003  2.1499e+003  2.2744e+004
-1.3061e+003  4.0209e+003  2.5996e+003 -1.4804e+003 -1.1146e+004
```

Input Matrix [B]

```
 9.2761e+002
-1.0753e+003
 7.7323e+002
-1.6571e+002
 5.5326e+002
-2.0849e+002
-2.2685e+002
 1.1292e+002
-7.1737e+001
 5.8665e+001
-2.7953e+001
 3.5146e+001
-8.3533e+000
 6.2665e+000
 2.0943e+000
 1.7566e+000
-1.6024e+000
```

Output Matrix [C]

```
 Columns 1 through 6
-6.2033e+002 -9.1893e+002 -7.1167e+002  6.5604e+001  3.4451e+002  1.1812e+002
-6.8972e+002 -5.5828e+002  3.0226e+002 -1.5240e+002 -4.3299e+002  1.7196e+002

 Columns 7 through 12
 8.3295e+001 -4.8461e+001 -6.1499e+001  5.7470e+001  2.1684e+001 -1.0069e+001
-2.1101e+002  1.0260e+002  3.7078e+001  1.1810e+001  1.7691e+001 -3.3818e+001

 Columns 13 through 17
-4.3743e+000  2.9658e+000 -2.8631e+000 -1.3750e+000 -2.0617e-001
-7.0344e+000  7.5784e+000 -1.3482e+000 -1.7679e+000 -1.0116e+001
```

Input/Output Matrix [D]

```
     0
     0
```

8.3.2.2 $20 \times 3 \times 3$ Grid

System Matrix [**A**]

```
 Columns 1 through 6
-8.0831e+001 -2.3762e+002 -2.4279e+001 -1.1006e+001 -9.3918e+000  3.8519e+001
 2.4335e+002 -4.0768e+002 -6.5485e+002  6.5546e+001  3.0660e+001  1.4726e+002
-1.2008e+002  8.2492e+002 -4.3398e+002  1.9499e+002  7.2874e+002 -9.0741e+001
 4.9785e+001 -2.3172e+002  2.6493e+002 -1.6325e+002 -1.0878e+003  2.5794e+002
-8.9752e+001  3.9894e+002 -7.7778e+002  1.0881e+003 -1.2054e+003  1.9803e+002
 4.4009e+001 -2.0361e+002  3.2216e+002 -3.4777e+002  1.0986e+003 -6.3949e+002
 3.5981e+001 -1.6012e+002  2.5023e+002 -2.2643e+002  1.0898e+003 -1.3591e+003
-2.6242e+001  1.1707e+002 -1.8412e+002  1.6992e+002 -7.4159e+002  8.2990e+002
 7.8240e+000 -3.4927e+001  5.5503e+001 -5.2264e+001  2.0636e+002 -2.1880e+002
-1.3911e+001  6.2035e+001 -9.8554e+001  9.2402e+001 -3.7090e+002  4.0243e+002
 4.1429e+000 -1.8490e+001  2.9308e+001 -2.7469e+001  1.1095e+002 -1.1872e+002
-6.4412e+000  2.8742e+001 -4.5573e+001  4.2704e+001 -1.7250e+002  1.8520e+002
 1.5951e+000 -7.1165e+000  1.1284e+001 -1.0573e+001  4.2728e+001 -4.5956e+001
-1.1163e+000  4.9805e+000 -7.8977e+000  7.3986e+000 -2.9905e+001  3.2154e+001
 3.9209e-001 -1.7494e+000  2.7738e+000 -2.5990e+000  1.0505e+001 -1.1297e+001
-5.0634e-001  2.2591e+000 -3.5820e+000  3.3557e+000 -1.3564e+001  1.4585e+001
 9.4549e-002 -4.2184e-001  6.6911e-001 -6.2672e-001  2.5326e+000 -2.7223e+000

 Columns 7 through 12
-1.6391e+001  7.8957e+000  3.5453e+000  9.4518e+000  4.1806e+000 -6.0721e+000
-2.8012e+001  1.6930e+000  6.3881e+000  5.3172e+001  1.7608e+001 -2.3139e+001
 1.7546e+002 -1.5057e+002 -3.9959e+001  8.9316e+001  7.6169e+000  2.1882e+000
-2.1594e+002  1.6919e+002  5.0304e+001 -5.6047e+001  6.0994e+000 -2.1821e+001
-1.0392e+003  7.3341e+002  1.9522e+002 -2.3762e+002  1.8842e+001 -8.0148e+001
 1.2189e+003 -6.4558e+002 -1.7947e+002 -1.0137e+002 -1.0716e+002  1.8433e+002
-1.5809e+003  1.5800e+003  8.0407e+002 -5.0530e+002  1.8952e+002 -4.2139e+002
 1.6258e+003 -1.9511e+003 -1.7080e+003  1.3627e+003 -2.4338e+002  6.0204e+002
-8.0071e+002  1.7172e+003 -5.3548e+002 -2.2080e+002 -1.9028e+002  6.0454e+002
 1.2549e+003 -2.2654e+003  2.0025e+003 -3.7971e+003 -2.5941e+003  1.7795e+003
-3.6853e+002  6.2851e+002 -5.3716e+002  3.1795e+003 -9.5163e+002  2.0955e+003
 5.6952e+002 -9.6798e+002  8.4994e+002 -3.7259e+003  2.2666e+003 -6.9498e+003
-1.4027e+002  2.3737e+002 -2.1770e+002  8.5394e+002 -7.7236e+002  3.9212e+003
 9.8165e+001 -1.6595e+002  1.5333e+002 -6.0817e+002  5.1506e+002 -2.4785e+003
-3.4460e+001  5.8257e+001 -5.3606e+001  2.1403e+002 -1.8322e+002  8.8212e+002
 4.4519e+001 -7.5260e+001  6.9220e+001 -2.7722e+002  2.3313e+002 -1.0918e+003
-8.3254e+000  1.4078e+001 -1.3171e+001  5.0869e+001 -4.2669e+001  2.1244e+002

 Columns 13 through 17
-1.2932e+000  8.8110e-001 -1.4053e+000  2.3677e-001 -6.2074e-001
-6.6970e+000  2.9214e+000 -5.0179e+000  1.7242e-001 -2.0624e+000
-9.0156e+000 -2.7423e+000  2.6890e+000 -4.1457e+000  2.0549e+000
 4.5313e+000  5.4978e+000 -6.9861e+000  4.7291e+000 -3.9265e+000
 2.0322e+001  2.1075e+001 -2.6298e+001  1.8847e+001 -1.4973e+001
 1.9609e+001 -3.1577e+001  4.5523e+001 -1.5061e+001  2.1823e+001
 2.1608e+001  8.8711e+001 -1.2143e+002  6.3272e+001 -6.3606e+001
-7.5223e+001 -1.3838e+002  1.9599e+002 -1.1335e+002  1.0600e+002
-3.1195e+001 -1.4075e+002  2.0121e+002 -1.0326e+002  1.0581e+002
 8.3095e+002 -4.7256e+001  1.7463e+002  1.9110e+002  2.5657e+001
 6.2929e+002 -4.3347e+002  6.9859e+002 -1.3583e+002  3.1492e+002
-2.6414e+003  2.4026e+003 -3.7595e+003  1.0895e+003 -1.7664e+003
-2.3172e+003  4.1506e+002 -1.7694e+003 -6.6328e+002 -5.8216e+002
 3.2785e+003 -7.3598e+003  1.8380e+004 -6.2113e+003  8.9025e+003
-1.0364e+003 -5.7799e+002 -2.5993e+003 -4.3101e+002 -3.3418e+002
 1.4858e+003 -6.2448e+003  7.5030e+003 -1.1786e+004  8.6370e+003
-3.0408e+002 -5.2502e+001 -1.5795e+003 -2.6536e+003  2.8574e+002
```

Input Matrix [B]

```
 8.6027e+002
-9.7457e+002
 6.5451e+002
-2.6276e+002
 4.7994e+002
-2.3679e+002
-1.9174e+002
 1.3995e+002
-4.1738e+001
 7.4189e+001
-2.2095e+001
 3.4352e+001
-8.5060e+000
 5.9528e+000
-2.0909e+000
 2.7001e+000
-5.0419e-001
```

Output Matrix [C]

```
 Columns 1 through 6
-5.9238e+002 -8.4183e+002 -5.8859e+002  1.5571e+002  3.0401e+002  5.9407e+001
-6.2388e+002 -4.9035e+002  2.8578e+002 -2.1171e+002 -3.7135e+002  2.2936e+002

 Columns 7 through 12
 6.4280e+001 -6.8326e+001 -1.4187e+001  7.4199e+001  1.4560e+001 -1.3534e+001
-1.8064e+002  1.2258e+002  3.9477e+001 -1.0981e+000  1.6838e+001 -3.1703e+001

 Columns 13 through 17
-8.3285e+000  5.8599e-001 -1.9637e+000 -1.7740e+000 -3.7570e-001
-1.5866e+000  5.9150e+000 -8.4767e+000  3.4320e+000 -4.2146e+000
```

Input/Output Matrix [D]

```
     0
     0
```

8.3.3 1D Model from 2D Averaged Data

System Matrix [**A**]

```
 Columns 1 through 6
-9.8584e+001  2.4455e+002  1.6793e+002  2.0341e+002 -7.1015e+001  1.7131e+002
-2.8000e+002 -1.4186e+002  1.4511e+003 -2.4207e+002  1.2358e+002 -3.4936e+002
-3.0312e+002 -1.5407e+003 -3.9981e+002  1.2190e+003  5.6456e+002 -3.5812e+002
-2.4737e+002 -2.4315e+002 -1.3903e+003 -4.8376e+002  2.0570e+003 -1.6233e+003
-8.8897e+001 -2.2576e+002 -6.2326e+002 -2.2527e+003 -1.4243e+002  2.3804e+002
 1.5402e+002  3.8103e+002  6.8001e+002  1.6473e+003  3.4002e+002 -6.8877e+002
-1.6297e+002 -2.3407e+002 -5.9834e+002 -5.5400e+002 -5.3727e+002  3.2588e+003
 1.6455e+002  2.9834e+002  4.9248e+002  8.7442e+002  5.3415e+002 -1.5768e+003
-1.0043e+002 -1.6631e+002 -3.4549e+002 -4.4008e+002 -2.7518e+002  8.5709e+002
 1.6757e+001  2.6745e+001  5.4938e+001  6.8069e+001  4.7297e+001 -1.6234e+002
-8.3077e+001 -1.4773e+002 -2.7794e+002 -4.1020e+002 -2.3463e+002  6.1397e+002
-1.0901e+000 -5.9525e-001 -2.6441e+000 -3.7015e+000 -1.6848e-001  1.3009e+001
-4.8729e+001 -8.4991e+001 -1.6060e+002 -2.3313e+002 -1.2837e+002  3.8545e+002

 Columns 7 through 12
 1.2185e+002 -4.4489e+001  2.7052e+001 -2.8182e+001 -8.6517e+001  2.1196e+001
-2.3521e+002 -2.0590e+002 -1.5972e+002  4.8691e+001  1.0008e+002  1.7938e+001
 4.6027e+002  5.0430e+002  3.1377e+002 -4.2673e+001  2.7896e+001 -1.2451e+002
-5.6916e+002 -6.0448e+002 -4.0688e+002  1.4473e+002  3.0481e+002  7.1453e+001
 2.8608e+002 -4.4595e+002 -3.5490e+001 -5.1368e+001 -1.9536e+002  8.0668e+001
-3.2350e+003  8.7985e+002 -3.6715e+002  3.2932e+002  8.4099e+002 -2.5436e+002
-8.7731e+002 -3.0424e+003 -9.0788e+002  3.0846e+002  6.7582e+002  1.5670e+002
 3.4071e+003 -1.9011e+003 -4.4534e+003  6.5000e+002 -6.2777e+002  9.0295e+002
-8.9785e+002  4.5798e+003 -1.4257e+003  4.4204e+002  2.5041e+003  5.0311e+002
 1.3322e+002 -6.0813e+002  1.7031e+002 -3.4059e+001 -4.4839e+003 -2.3094e+002
-1.0200e+003  2.1877e+003 -3.3635e+003  3.9685e+003 -2.1793e+003  1.0737e+003
-1.2556e+001 -4.6541e+001 -1.4002e+002  1.7375e+002 -2.1985e+002 -1.4654e+002
-5.6226e+002  1.0281e+003 -1.7322e+003  7.3388e+002 -3.9973e+003  3.1347e+003

 Column 13
 4.9590e+001
-6.2108e+001
-1.1102e+002
-1.9024e+002
 1.3820e+002
-2.7672e+002
-5.0154e+002
 7.0727e+002
 3.5872e+002
 8.7032e+002
 4.3775e+003
-6.5665e+003
-2.0530e+003
```

Input Matrix [**B**]

```
 9.7210e+002
 8.0536e+002
 1.1889e+003
 1.0025e+003
 5.0362e+002
-8.5236e+002
 7.6198e+002
-8.0286e+002
 4.9182e+002
-8.0081e+001
 4.1501e+002
 3.5179e+000
 2.3900e+002
```

Output Matrix [**C**]

```
 Columns 1 through 6
-6.3659e+002  8.1445e+002 -7.0900e+002  1.0345e+003 -7.9062e+001  6.4761e+002
-7.3606e+002  6.3800e+000  9.6624e+002  6.2264e+001 -5.0451e+002  6.9652e+002

 Columns 7 through 12
 8.0468e+002  4.8980e+002  4.5218e+002 -1.6378e+002 -3.0209e+002 -6.4401e+001
-3.4003e-002 -6.5999e+002 -2.3037e+002 -3.8097e+001 -2.9737e+002  1.9047e+002

 Column 13
 1.2770e+002
 2.3890e+002
```

Input/Output Matrix [**D**]

```
     0
     0
```

REPORT DOCUMENTATION PAGE

Form Approved
OMB No. 0704-0188

1. AGENCY USE ONLY (*Leave blank*)	2. REPORT DATE	3. REPORT TYPE AND DATES COVERED
	May 1998	Final Contractor Report

4. TITLE AND SUBTITLE

A Method for Generating Reduced-Order Linear Models of Multidimensional Supersonic Inlets

5. FUNDING NUMBERS

WU–519–30–53–00
NCC3–508

6. AUTHOR(S)

Amy Chicatelli and Tom T. Hartley

7. PERFORMING ORGANIZATION NAME(S) AND ADDRESS(ES)

University of Akron
Department of Electrical Engineering
Akron, Ohio 44325–3904

8. PERFORMING ORGANIZATION REPORT NUMBER

E–11164

9. SPONSORING/MONITORING AGENCY NAME(S) AND ADDRESS(ES)

National Aeronautics and Space Administration
Lewis Research Center
Cleveland, Ohio 44135–3191

10. SPONSORING/MONITORING AGENCY REPORT NUMBER

NASA CR—1998-207405

11. SUPPLEMENTARY NOTES

Project Manager, Kevin J. Melcher, Instrumentation and Controls Division, NASA Lewis Research Center, organization code 5530, (216) 433–3743.

12a. DISTRIBUTION/AVAILABILITY STATEMENT

Unclassified - Unlimited
Subject Categories: 01 and 07 Distribution: Nonstandard

This publication is available from the NASA Center for AeroSpace Information, (301) 621–0390.

12b. DISTRIBUTION CODE

13. ABSTRACT (*Maximum 200 words*)

Simulation of high speed propulsion systems may be divided into two categories, nonlinear and linear. The nonlinear simulations are usually based on multidimensional computational fluid dynamics (CFD) methodologies and tend to provide high resolution results that show the fine detail of the flow. Consequently, these simulations are large, numerically intensive, and run much slower than real-time. The linear simulations are usually based on large lumping techniques that are linearized about a steady-state operating condition. These simplistic models often run at or near real-time but do not always capture the detailed dynamics of the plant. Under a grant sponsored by the NASA Lewis Research Center, Cleveland, Ohio, a new method has been developed that can be used to generate improved linear models for control design from multidimensional steady-state CFD results. This CFD-based linear modeling technique provides a small perturbation model that can be used for control applications and real-time simulations. It is important to note the utility of the modeling procedure; all that is needed to obtain a linear model of the propulsion system is the geometry and steady-state operating conditions from a multidimensional CFD simulation or experiment. This research represents a beginning step in establishing a bridge between the controls discipline and the CFD discipline so that the control engineer is able to effectively use multidimensional CFD results in control system design and analysis.

14. SUBJECT TERMS

Supersonic inlets; Dynamic models; Linearization; Linear systems; Nonlinear systems

15. NUMBER OF PAGES

86

16. PRICE CODE

A05

17. SECURITY CLASSIFICATION OF REPORT	18. SECURITY CLASSIFICATION OF THIS PAGE	19. SECURITY CLASSIFICATION OF ABSTRACT	20. LIMITATION OF ABSTRACT
Unclassified	Unclassified	Unclassified	